



Structural behaviour of masonry walls strengthened with mortar layers reinforced with FRP grids.

Angelo Garofano

Czech Republic | 2011



ADVANCED MASTERS IN STRUCTURAL ANALYSIS
OF MONUMENTS AND HISTORICAL CONSTRUCTIONS

Master's Thesis

Angelo Garofano

**Structural behaviour of
masonry walls strengthened
with mortar layers reinforced
with FRP grids.**



CZECH TECHNICAL UNIVERSITY
IN PRAGUE



UNIVERSITAT POLITÈCNICA
DE CATALUNYA



Education and Culture

Erasmus Mundus



ADVANCED MASTERS IN STRUCTURAL ANALYSIS
OF MONUMENTS AND HISTORICAL CONSTRUCTIONS



Master's Thesis

Angelo Garofano

Structural behaviour of masonry walls strengthened with mortar layers reinforced with FRP grids.

This Masters Course has been funded with support from the European Commission. This publication reflects the views only of the author, and the Commission cannot be held responsible for any use which may be made of the information contained therein.

DECLARATION

Name: Angelo Garofano

Email: angelogarofano@alice.it

Title of the Msc Dissertation: Structural Behaviour of Masonry Walls Strengthened with Mortar Layers Reinforced with FRP

Supervisor(s): Ing. Zuzana Slížková, Ph.D., Prof. Ing. Miloš Drdácý, DrSc.

Year: 2010/2011

I hereby declare that all information in this document has been obtained and presented in accordance with academic rules and ethical conduct. I also declare that, as required by these rules and conduct, I have fully cited and referenced all material and results that are not original to this work.

I hereby declare that the MSc Consortium responsible for the Advanced Masters in Structural Analysis of Monuments and Historical Constructions is allowed to store and make available electronically the present MSc Dissertation.

University: Czech Technical University in Prague

Date: July 19, 2011

Signature:

ACKNOWLEDGEMENTS

I would like to express my highest appreciation to my supervisors Prof. Ing. Miloš Drdäcký, DrSc. and Ing. Zuzana Slížková, Ph.D., who gave me the opportunity to work in this interesting field and for their advice and guidance during the thesis. Their feedback and effort in supporting me through the work was invaluable.

I greatly appreciate and thank the precious cooperation and frequent attention provided by Dr. Ing. Stanislav Pospíšil, Ph.D. I really appreciated all the interesting discussions we have had. I am also grateful to Ing. Shota Urushadze, Ph.D. for his help and advice throughout this thesis.

I also would like to express my gratitude to Prof. Ing. Petr Kabele, Ph.D. for his constant assistance. His precious guidance represented a constant source of help and encouragement throughout all the work. The constructive criticisms offered and his valuable suggestions have resulted in the completion of this thesis.

I would like to express special gratitude to my family for their persistent support during my stay abroad.

A special thank goes to all my friends and colleagues for the unforgettable moments we shared with open heart and sincere feelings and which will be remembered forever.

Finally, acknowledgment is due to the MSc SAHC Consortium and European Commission for having supported this study through Erasmus Mundus scholarship.

ABSTRACT

The seismic events recently occurred all over the world and, in particular, in Europe have shown the high vulnerability of particular classes of buildings against the horizontal actions. The damage of structural masonry walls is one of the most widespread harming injuries and cause of loss of serviceability and seismic capacity for a building. The damage experienced by these masonry elements has brought to light the necessity to strengthen them with appropriate reinforcing systems in order to achieve an upgrading to the necessary seismic and energy dissipation capacity. Different strengthening systems have been proposed and studied during the last decades, with particular reference to the type of materials, system configuration with respect to the element to be strengthened, difficulties in the application and effectiveness of the reinforcement. Even though in the last years different studies have been carried out in this field, many issues regarding the methods for the evaluation of the actual behaviour of these techniques, and their effectiveness in the improvement of seismic behaviour of structural members to which they are applied, are still open.

In the present study the structural behaviour of unreinforced masonry walls strengthened with composite grid reinforced mortar layers is studied. The characterization of the reinforcing system and the assessment of the overall increase of capacity of the strengthened masonry walls is performed.

First of all, the study is focused on the investigation of the mechanical characteristics of the strengthening system in itself. In fact, the structural behaviour of an externally applied strengthening system for masonry walls is examined. The reinforcing technique considered in the present research is composed by mortar layers incorporating a FRP reinforcement in form of grid. The FRP reinforced mortar layers are externally applied to the wall surfaces in a symmetric fashion, and can also be connected to the wall by means of an adequate connection system. The mechanical behaviour of the reinforced mortar under tensile, compression and shear loading is assessed through laboratory tests and constitutive laws can be proposed to characterize the reinforced mortar mechanical behaviour. The experimental characterization of the presented system is followed by and validated through numerical modelling and simulation of its mechanical behaviour.

In a second phase, the behaviour of masonry walls strengthened by means of the considered technique is studied. The in-plane shear behaviour is considered, in case of cyclic loading state. The performances of the global strengthened assemblage is thus examined with both experimental and numerical investigation criteria. Also, the overall ductility and energy dissipation capacity of the system, while subjected to horizontal in-plane actions, is studied. The actual mechanical behaviour of the proposed structural solution is investigated through an experimental program with prototypes. Furthermore, a finite element model is realized in order to replicate the structural features of the strengthened masonry wall. The finite element model can be also used for further validation of the panels performances.

SHRNUTÍ

(CHOVÁNÍ ZDIVA ZESÍLENÉHO OMÍTKOU VYZTUŽENOU KOMPOSITNÍMI MŘÍŽEMI)

Zemětřesení ohrožují nepřetržitě řadu oblastí na celém světě a v poslední době se zejména v Evropě ukazuje vysoká zranitelnost určité třídy budov při zatížení vodorovnými silami. Poškození zděných stěn je jedním z nejrozšířenějších typů poruch a způsobuje snížení či ztrátu použitelnosti a odolnosti budov proti zemětřesení. Poruchy, pozorované na těchto zděných prvcích, vyvolaly potřebu jejich zesílení vhodnými vyztužujícími systémy s cílem dosáhnout jejich potřebné seismické kapacity a schopnosti disipovat energii. V posledních desetiletích byly navrženy a studovány různé systémy zesilování s ohledem na typ materiálu, na systémové uspořádání vzhledem k prvkům, které mají být zesíleny, s uvážením obtíží při realizaci i dosažení efektivnosti vyztužení. Přestože v nedávných letech byly provedeny různé studie v této oblasti, stále ještě jsou otevřené mnohé otázky, týkající se metod vyhodnocení skutečného působení použitých technik a jejich efektivnosti při zlepšování seismického chování konstrukčních prvků, které byly zesíleny.

V předkládané práci je studován problém chování nevyztužených zděných stěn zesílených omítkovou vrstvou s vyztužující sítí. Je provedena studie popisu vyztužujícího systému a jsou navrženy způsoby odhadu zvýšení celkové únosnosti zesílených zdí.

Nejprve se studie zaměřuje na výzkum mechanických charakteristik vlastního zesilovacího systému. Zkoumá se konstrukční chování externě aplikovaného zesilovacího systému. Technika vyztužení používaná v této práci je tvořena vrstvou malty, obsahující vyztužení vláknovým plastovým kompozitem ve formě sítě. Tyto vyztužené omítky jsou externě aplikovány na zděné stěny symetricky na obou površích a mohou být navíc připevněny ke stěnám vhodným kotevním systémem. Mechanické chování vyztužené omítky při tahovém zatížení, tlaku a smyku je zjištěno laboratorními zkouškami a v práci jsou navrženy konstitutivní vztahy, použitelné pro popis chování vyztužených omítek. Experimentální charakterizace prezentovaného systému je dále studována a ověřena numerickým modelováním a simulací mechanického chování.

Ve druhé fázi je studováno chování zděných stěn vyztužených výše navrženým systémem. Zkoušky byly zaměřeny na smykové chování stěn, zatěžovaných cyklicky v rovině stěny. Chování globálně zesílených těles je tak zkoumáno experimentálně i numericky. Pozornost byla zaměřena i na stadium celkové duktility a schopnosti disipovat energii při zatěžování v rovině stěny. Skutečné mechanické chování navrženého konstrukčního řešení bylo zkoumáno experimentálně na prototypch. Kromě toho byl vytvořen model pomocí konečných prvků, aby mohly být studovány variance konstrukčního uspořádání. Numerický model je také použit pro validaci chování panelů.

ESTRATTO

(COMPORTAMENTO STRUTTURALE DI PARETI IN MURATURA RINFORZATE CON STRATI DI MALTA ARMATA CON GRIGLIE IN FRP)

Gli eventi sismici recentemente registrati nel mondo e, in particolare, in Europa hanno mostrato l'elevata vulnerabilità di particolari classi di edifici nei confronti delle azioni orizzontali. Il danneggiamento delle pareti in muratura è una delle maggiori cause di crisi e causa di perdita di fruibilità e di capacità sismica per un edificio. Il danno subito da tali elementi strutturali ha portato alla luce la necessità di rinforzarli con adeguati sistemi di rinforzo in modo tale da raggiungere un adeguamento alla necessaria capacità sismica e dissipativa. Durante gli ultimi decenni sono stati proposti e studiati diversi sistemi di rinforzo, con particolare riferimento al tipo di materiali impiegati, alla configurazione del sistema rispetto all'elemento da rinforzare, alle difficoltà nell'applicazione e all'efficacia del rinforzo. Anche se negli ultimi anni sono stati condotti diversi studi in tale campo, sono ancora aperte molte questioni riguardanti i metodi per la valutazione del reale comportamento di tali sistemi, e della loro efficacia nel miglioramento del comportamento sismico degli elementi strutturali a cui sono applicati.

Nel presente studio è stato studiato il comportamento strutturale di pareti in muratura rinforzate con strati di malta e griglie di rinforzo. È stata condotta la caratterizzazione del sistema di rinforzo e la valutazione dell'incremento della capacità globale delle pareti rinforzate.

Innanzitutto, lo studio è focalizzato ad investigare le caratteristiche meccaniche del sistema di rinforzo. Infatti, è stato esaminato il comportamento strutturale di un sistema di rinforzo per pareti in muratura. La tecnica di rinforzo considerata nella presente ricerca è composta da strati di malta che incorporano un rinforzo in FRP in forma di griglia. Gli strati di malta rinforzati con FRP sono applicati esternamente sulle superfici della parete in maniera simmetrica, e possono anche essere connesse ad esse attraverso un adeguato sistema di connessione. Il comportamento meccanico della malta rinforzata in condizioni di trazione, compressione e taglio, ed il legame costitutivo del sistema, sono stati valutati attraverso prove di laboratorio. La caratterizzazione sperimentale del sistema presentato è seguita e validata attraverso la modellazione numerica e la simulazione del relativo comportamento sperimentale.

In una seconda fase, è stato studiato il comportamento di pareti in muratura rinforzate attraverso la tecnica considerata. È stato considerato il comportamento nel piano, nel caso di condizione di carico ciclica. Le prestazioni del sistema globale sono state quindi esaminate attraverso criteri sperimentali e numerici. Inoltre, è stata studiata la capacità in termini di duttilità del sistema soggetto ad azioni orizzontali nel piano. Il reale comportamento meccanico della soluzione strutturale proposta è stata investigata attraverso un programma sperimentale con prototipi. Inoltre, è stato realizzato un modello agli elementi finiti realizzato in modo da riprodurre le caratteristiche strutturali del

pannello rinforzato. Il modello agli elementi finiti potrà essere impiegato per ulteriori validazioni delle prestazioni dei pannelli.

TABLE OF CONTENTS

1.	INTRODUCTION	pag.	1
1.1	MOTIVATION	»	1
1.2	AIMS, SCOPE AND LIMITATIONS	»	3
1.3	OBJECTIVES OF THE THESIS	»	4
1.4	THESIS OUTLINE	»	4
2.	BACKGROUND	pag.	7
2.1	TRADITIONAL STRENGTHENING TECHNIQUES FOR UNREINFORCED MASONRY PANELS	»	8
2.1.1	Surface treatments	»	8
2.1.2	Grout and epoxy injection	»	10
2.1.3	External reinforcement	»	11
2.1.4	Confinement of URM with R.C. tie columns	»	11
2.1.5	Post-tensioning	»	12
2.1.6	Center core technique	»	13
2.2	NUMERICAL MODELLING OF MASONRY	»	13
2.2.1	Macro-elements modelling technique	»	14
2.2.2	Continuous modelling and homogenization techniques	»	15
2.2.3	Discontinuous modelling	»	16
3.	STATE-OF-THE-ART	pag.	19
3.1	GENERAL ASPECTS	»	19
3.2	STRENGTHENING TECHNIQUES FOR IN-PLANE BEHAVIOUR	»	20
3.3	EXTERNALLY APPLIED FRP GRID REINFORCED MORTAR LAYERS	»	23
3.4	MODELLING OF THE BEHAVIOUR OF THE REINFORCED SYSTEM	»	31
4.	MECHANICAL TESTS ON UNREINFORCED AND REINFORCED MORTAR SPECIMENS	pag.	37
4.1	EXPERIMENTAL SPECIMENS PREPARATION	»	37
4.2	TENSILE TESTS	»	43
4.3	COMPRESSION TESTS	»	45
4.4	THREE-POINTS BENDING TESTS	»	46
4.5	SUMMARY OF RESULTS	»	48

5.	EXPERIMENTAL TESTS ON REINFORCED MASONRY WALLS	pag. 49
5.1	EXPERIMENTAL SPECIMENS	» 50
5.2	EXPERIMENTAL EQUIPMENT AND TEST SET-UP	» 53
5.3	EXPERIMENTAL RESULTS	» 57
5.3.1	Adobe brick walls	» 57
5.3.2	Damaged adobe brick wall retrofitted with reinforced mortar plaster	» 69
6.	NUMERICAL MODELLING OF REINFORCED MORTAR SPECIMENS AND MASONRY WALL	pag. 75
6.1	FINITE ELEMENT TECHNIQUES	» 75
6.1.1	General	» 75
6.1.2	Cracking models	» 76
6.1.2.1	Discrete crack concept	» 76
6.1.2.2	Smeared crack concept	» 77
6.1.2.3	Fixed single crack approach	» 77
6.1.2.4	Fixed multi-directional crack approach	» 78
6.1.2.5	Rotating crack approach	» 79
6.1.3	Solution procedures for non-linear systems	» 79
6.1.3.1	Iterative procedures	» 79
6.1.3.2	Convergence criteria	» 81
6.1.3.3	Incremental procedures	» 81
6.2	ADOPTED MATERIAL MODELS	» 83
6.3	MODELLING OF REINFORCED MORTAR SPECIMEN FOR TENSILE TEST	» 85
6.4	MODELLING OF REINFORCED MORTAR SPECIMEN FOR SHEAR TEST	» 89
6.5	MODELLING OF MASONRY WALL	» 92
7.	DISCUSSION AND CONCLUSIONS	pag. 95
	REFERENCES	pag. 99

LIST OF FIGURES

Figure 2.1. Surface treatments: samples of reinforcement used in ferrocement (a); typical layout of reinforced plaster (b); application of shotcrete (c) [1].	9
Figure 2.2. Overview of injection holes distribution.	10
Figure 2.3. External reinforcement using vertical and diagonal bracing (a) or creating infill panel (b) [1].	11
Figure 2.4. Modelling techniques for masonry: masonry element (a); micro-modelling (b); macro-modelling (c) [2].	14
Figure 2.5. Structural components modelling techniques for masonry wall system (a): lumped masses (b); equivalent frame (c); panel system (d) [2].	15
Figure 2.6. Masonry failure mechanism: joint cracking (a); joint sliding (b); unit vertical cracking (c); unit diagonal cracking (d); masonry crushing (e).	17
Figure 3.1. Different in-plane test configurations to investigate the shear response of FRP reinforced brick masonry elements: (a) (Valluzzi et al., 2002) [30], (b) (ElGawady et al., 2005) [31], (c) (Eshani and Saadatmanesh, 1997) [43], (d) (Triantafillou, 1998) [40]. [29].	21
Figure 3.2. Textile-reinforced mortar (TRM) strengthening of a masonry panel. Phases of application [51].	24
Figure 3.3. Carbon fiber reinforcement mesh texture (a) and application of the TRM layer [52].	25
Figure 3.4. Bi-directional alkali resistant AR glass coated open grid, SRG 45 [53].	27
Figure 3.5. CMG system: reinforcing grid installation (a) and troweling of final mortar layer (b) [53].	28
Figure 3.6. Coated AR-glass grid employed by (Aldea et al., 2006) [55].	29
Figure 3.7. Different FRP reinforcement configurations investigated by (Aldea et al., 2006) [55].	30
Figure 3.8. Example of a typical Horizontal Force – Displacement curve for CMG strengthened wall compared with URM wall [55].	30
Figure 3.9. Geometry of the masonry walls (a) and Finite Element micro-model (b) [56].	32
Figure 3.10. Assumed non-linear material models for units and mortar [56].	33
Figure 3.11. Comparison between numerical and experimental crack patterns for as-built panel (a) and strengthened panel (b) [56].	33
Figure 3.12. Different configuration of the strengthening system for masonry panels [58].	34
Figure 4.1. Outline of the wooden frame constructed for the casting of reinforced mortar specimens (dimensions in mm).	38
Figure 4.2. Geo-net employed for reinforced mortar specimens.	39
Figure 4.3. Preparation of the reinforcing mesh and orientation in the mortar specimens.	39
Figure 4.4. Phases of preparation of the mortar samples and positioning of the net.	40

Figure 4.5. Specimens casted in the wooden moulds: clay mortar (a) and lime mortar (b).	40
Figure 4.6. Climate chamber (a) and thermo-hygrometric conditions (b).	41
Figure 4.7. Reinforced mortar specimens in the climate chamber: clay mortar (a) and lime mortar (b).	41
Figure 4.8. Reinforced mortar specimens for tensile tests: clay mortar (a) and lime mortar (b).	42
Figure 4.9. Reinforced mortar specimens for three-points bending tests: clay mortar (a) and lime mortar (b).	42
Figure 4.10. Reinforced mortar specimens for compression tests: clay mortar (a) and lime mortar (b).	43
Figure 4.11. Force – displacement curves for unreinforced and reinforced mortar specimens under tensile load: clay mortar (a) and lime mortar (b).	44
Figure 4.12. Tested reinforced mortar specimens under tensile load: clay mortar specimen (a) and detail of crack in lime mortar specimen (b).	44
Figure 4.13. Force – displacement curves for unreinforced and reinforced mortar specimens under compression load: clay mortar (a) and lime mortar (b).	45
Figure 4.14. Tested reinforced mortar specimens under compression load: clay mortar (a) and lime mortar (b) specimens.	45
Figure 4.15. Force – deflection curves for unreinforced and reinforced mortar specimens under Shear load: clay mortar (a) and lime mortar (b).	47
Figure 4.16. Tested reinforced mortar specimens under shear load: clay mortar specimen (a) and detail of crack in lime mortar specimen (b).	47
Figure 5.1. Dimensions of the fundamental element used in the masonry specimens.	50
Figure 5.2. Overall dimensions of the masonry specimens and bricks arrangement (a) and position of the reinforcement grid (b).	51
Figure 5.3. Unreinforced masonry walls: (a) adobe, (b) burned clay bricks, (c) unburned clay bricks.	51
Figure 5.4. Geo-net employed for strengthening of masonry walls.	52
Figure 5.5. Testing walls strengthened with polymer nets: (a) a new undamaged wall; (b) wall after previous damage.	52
Figure 5.6. Adobe brick wall reinforced by means of X-shaped wire ropes (a) and detail of the anchoring system for wire ropes (b).	53
Figure 5.7. Testing rig and reaction wall for testing.	54
Figure 5.8. Scheme of the testing system.	54
Figure 5.9. Hydraulic jacks system for generating vertical compression pre-stress.	55
Figure 5.10. Servo-hydraulic actuator for horizontal loads.	55
Figure 5.11. Diagonal deformation measurements.	56
Figure 5.12. Loading pattern for each step of application of the horizontal force.	56

Figure 5.13. Crack pattern at failure of the plain masonry control wall under a combination of vertical compression and cyclic shear.	57
Figure 5.14. Crack pattern at failure of the adobe wall strengthened with reinforced mortar layers under a combination of vertical compression and cyclic shear.	58
Figure 5.15. Evidence of the detachment of the plaster from the wall surface.	59
Figure 5.16. Crack pattern at failure of the adobe wall strengthened with wire ropes under a combination of vertical compression and cyclic shear.	60
Figure 5.17. Details of the large damage at the wall base.	60
Figure 5.18. Detail of the damage due to the out-of-plane of the wire ropes reinforcement.	61
Figure 5.19. Cyclic curves for different steps of loading – Unreinforced adobe wall.	62
Figure 5.20. Cyclic curves for different steps of loading – Wall strengthened with reinforced mortar plaster.	63
Figure 5.21. Cyclic curves for different steps of loading – Wall strengthened with wire ropes.	64
Figure 5.22. Cyclic curve for unreinforced adobe wall.	65
Figure 5.23. Cyclic curve for wall strengthened with reinforced mortar plaster.	65
Figure 5.24. Cyclic curve for wall strengthened with wire ropes.	66
Figure 5.25. Envelop curves for unreinforced adobe wall.	66
Figure 5.26. Envelop curves for wall strengthened with reinforced mortar plaster.	67
Figure 5.27. Envelop curves for wall strengthened with wire ropes.	67
Figure 5.28. Behaviour of the wall strengthened with reinforced mortar plaster compared to the unreinforced wall.	68
Figure 5.29. Behaviour of the wall strengthened with wire ropes compared to the unreinforced wall.	68
Figure 5.30. Crack pattern at failure of the retrofitted adobe wall under a combination of vertical compression and cyclic shear.	69
Figure 5.31. Damage at the base of the wall: detachment of the mortar layer (a) and large vertical crack in the wall thickness.	70
Figure 5.32. Cyclic curves for different steps of loading – Retrofitted adobe wall.	71
Figure 5.33. Cyclic curve for retrofitted adobe wall.	72
Figure 5.34. Envelop curves for retrofitted adobe wall.	72
Figure 5.35. Behaviour of the retrofitted adobe wall to the unreinforced wall.	73
Figure 5.36. Comparison between undamaged wall strengthened with reinforced mortar layers and retrofitted wall.	73
Figure 6.1. Different iterative methods: Regular Newton-Raphson iteration (b); Modified Newton-Raphson iteration (b); Quasi-Newton iteration (c); Linear Stiffness iteration (d).	80
Figure 6.2. Possible incremental procedures: force controlled increment (a) and displacement controlled increment (b).	82

Figure 6.3. Arc-length method.	82
Figure 6.4. Material model adopted for mortar and bricks.	83
Figure 6.5. Mohr-Coulomb and Drucker-Prager yield conditions.	83
Figure 6.6. Tensile cut-off criterion.	84
Figure 6.7. Non-linear tension softening according to Hordijk.	85
Figure 6.8. Constant shear retention.	85
Figure 6.9. Finite Element (CHX60) used for 3-D model of mortar specimens.	86
Figure 6.10. 3-D Finite Elements model of the specimen for tensile test.	87
Figure 6.11. 3-D Finite Elements mesh (540 Elements x 2594 Nodes).	87
Figure 6.12. Deformed shape for Step 50.	88
Figure 6.13. Cracking pattern at final stage of the non-linear analysis.	89
Figure 6.14. Evolution of cracking pattern for some significant steps of the analysis.	89
Figure 6.15. Constraint condition 1: deformed shape (a) and cracking pattern (b).	90
Figure 6.16. Constraint condition 2: deformed shape (a) and cracking pattern (b).	91
Figure 6.17. Constraint condition 3: deformed shape (a) and cracking pattern (b).	91
Figure 6.18. Finite Element (HX24L) used for 3-D model of masonry wall.	92
Figure 6.19. Masonry wall: definition of the geometry (a) and meshing (b).	93
Figure 6.20. Constraint conditions (a) and assignment of materials (b).	93
Figure 6.21. Example of non-linear curve obtained through a non-linear analysis for model testing.	94

LIST OF TABLES

Table 4.1. Results of tensile tests on mortar specimens.	44
Table 4.2. Results of compression tests on mortar specimens.	46
Table 4.3. Results of shear tests on mortar specimens.	47
Table 4.4. Results of mechanical tests on unreinforced and reinforced mortar specimens.	48

1. INTRODUCTION

A large portion of the worldwide built heritage and most of the constructions currently present in European countries consist of existing buildings which recurring constructive typology is represented by structural masonry walls or non-structural infill masonry panels enclosed in reinforced concrete frames. The experience has shown that these classes of buildings are characterized by a high vulnerability when subjected to earthquakes. The seismic events occurred during the last years have revealed, in fact, that unreinforced masonry buildings (URM) exhibit poor capacities to withstand horizontal actions and are prone to suffer high damage.

The failure of URM walls produces loss of resistance capacity against actions induced by earthquake and, when occurring unevenly throughout the building, it is also cause of reduction in the energy dissipation capacity of the whole structure. The most widespread collapsing mechanisms commonly encountered in URM buildings subjected to seismic forces involve both the out-of-plane and in-plane failure modes. Since unreinforced masonry walls are the resistant system, or contribute to the lateral seismic resistance of the building, the first possible failure mode is due to in-plane shear failure. The other type of failure is represented by the out-of-plane flexural failure due to the orthogonal inertial forces induced by the earthquake. In addition, the excessive out-of-plane bending is also a major reason for the reduction in the vertical load carrying capacity of unreinforced masonry walls.

Composites offer an attractive strengthening possibility for existing and historical unreinforced masonry structures. In the past few decades, composites have successfully been used in different construction applications including strengthening of reinforced concrete, steel and timber structures. Lately, several studies have been conducted for evaluating the use of polymeric composites for repair and strengthening both unreinforced and reinforced masonry walls subjected to seismic, wind and lateral earth pressure. In most cases, both in-plane shear and out-of-plane flexural upgrades are required to upgrade the seismic performance of old and historical unreinforced masonry structures. In order to fulfil these demands, multidirectional composite systems are required (e.g. cross-ply, angle-ply or quasi-isotropic lamination) to achieve optimum retrofit design.

1.1 MOTIVATION

The high vulnerability and the extensive damaging suffered by particular classes of structures, including unreinforced masonry buildings, in case of seismic event, mining their serviceability and safety, have brought to light the necessity to strengthen them appropriately in order to achieve an

upgrading to the required seismic capacity in terms of resistance and ductility. The choice of the strengthening system should be calibrated in order to prevent the failure mechanisms of unreinforced masonry walls and in function of the way the structure is required to behave. If the seismic behaviour is taken into account, the structure should be retrofitted through the implementation of measures to prevent the previously described failure mechanisms and able to improve the overall ductility and energy dissipation capacity.

Masonry elements have been reinforced throughout the years by traditional methods involving, for example, filling of cracks or voids by grouting, stitching of large cracks or other weak areas with metallic elements or concrete, application of reinforced grouted perforations to improve the cohesion and tensile strength of masonry, post-tensioning with steel ties, single- or double-sided jacketing by steel mesh reinforced concrete. All the previously reported traditional technique are affected by some disadvantages that have more and more restricted their application and prompted researchers to seek better solutions. In order to overcome the drawbacks commonly encountered when facing with traditional techniques, the use of composite Fibre-Reinforced Polymers (FRP) has been thus successfully proposed.

Different strengthening methods based on the employment of FRP have been proposed and experimentally/numerically studied during the last decades have been conducted. All the developed techniques take advantage of the well known benefits proper of these materials including, above all, excellent mechanical properties, high strength-to-weight ratio, high resistance to corrosion in comparison to similar metallic strengthening systems, ease of application, preservation of the geometrical and architectural detail of the walls. The more common systems make use of FRP reinforcement in form of laminates or sheets externally bonded to the surface of the element to be strengthened (FRP-EBR) with different configurations and type of reinforcing or bonding materials. Other techniques recently studied involve the use of FRP rods mounted near the surface (NSM) of the wall in epoxy-filled grooves, that can also follow the bed and head joints of masonry. It is noted that the NSM technique can be more attractive since it does not require the installation of anchoring devices as in some cases is necessary for the externally applied FRP laminates and for aesthetic requirements. Also, it has been showed that NSM retrofitted elements exhibit no worse performances than the case of strengthening with externally bonded FRP.

Alternative possibilities to strengthen URM walls subjected to out-of-plane and in-plane loadings continue to be proposed. One of them is represented by the use of textile-reinforced mortar (TRM) in substitution to the classical FRP overlays. In more recent applications the textile reinforcement is replaced by commercial FRP bi-directional grids, and the polymeric bonding resins substituted by cement- or lime-based mortars.

The present study is focused on the investigation of the mechanical behaviour of a particular strengthening system for unreinforced masonry walls retrofitting. The reinforcing system for this purpose is realized by mortar layers embedding a FRP reinforcement in form of grid. It is intended to externally strengthen the masonry walls applying the FRP reinforced mortar layers on its surfaces. The

main interest in the study of this strengthening technique is related to the promising possibility it offers in the upgrading of the out-of-plane flexural behaviour and in-plane shear behaviour of the system to which it can be applied. Moreover, the performances of the whole assemblage need to be investigated for monotonic loading state as well as for cycling loading conditions. Another important issue to address is also the assessment of the effectiveness of the considered strengthening system in the improvement of the overall ductility of reinforced elements.

It is finally noted that in the last decades different aspect related to the field of retrofitting of URM have been explored by experimental campaigns and numerical studies. The previous researches have been focused on the investigation of the behaviour of retrofitted URM walls regarding the in-plane actions, the out-of-plane bending and, in some cases, the cyclic behaviour has been considered. In particular, the various possible strengthening technique have been studied with respect to the type of materials and reinforcing configuration. Nevertheless, many issues regarding the evaluation of the actual behaviour of these techniques, and the effectiveness of some of them in the improvement of the overall behaviour of structural members to which they are applied, remain still open.

1.2 AIMS, SCOPE AND LIMITATIONS

The main issues investigated in the present research program are related to the structural behaviour of masonry walls and non-structural infill masonry panels in reinforced concrete frames strengthened by means of FRP grid reinforced mortar layers.

The strengthening technique taken into account in the research is represented by externally applied mortar panels embedding a FRP reinforcement in form of bi-directional grid. The mortar encloses the reinforcement passing through the grid's openings allowing an effective mechanical interlocking that assure a composite behaviour of the system. In addition, the use of lime- or cement-based mortar allows the development of a better bonding between the strengthening system and the surface of the masonry panel. The effectiveness of the collaboration between reinforcement and substrate will be also investigated in the course of the research program.

The described FRP reinforced mortar panels will be applied on the surfaces of the unreinforced masonry wall in a symmetric configuration, and can be also connected to the substrate by means of an adequate anchoring system. The effectiveness of the reinforcing system will be explored in case of cyclic loading conditions.

The study will be firstly focused on the characterization of the mechanical behaviour of the considered strengthening system, namely the reinforced mortar layer reinforced with FRP grid, by means of tensile, compression and shear tests. For this purpose, the influence of different types of mortar with different strength for the reinforcing system will be investigated. The results collected throughout this experimental program will be employed in order to produce constitutive laws to

characterize the mechanical behaviour of the reinforced mortar layer and describe the cracking state of the system. Furthermore, the numerical modelling of the strengthening system will be performed in order to validate the experimental evidences.

Beside the comprehensive study of the described reinforcing system, the research aims to assess the effectiveness in the upgrading of the overall behaviour of the strengthened URM walls. The retrofitting of masonry elements through FRP grid reinforced mortar layer is expected to increase the in-plane shear resistance, provide the system an enhanced ductility, assure a higher integrity and reduce the damage of the panels in order to contain serviceability problems. Thus, the performances of the URM walls strengthened by means of this reinforcing system will be investigated under cyclic loading conditions. An experimental program on prototypes as well as the FEM modelling of the system will be carried out in order to replicate the structural behaviour of the assemblage.

1.3 OBJECTIVES OF THE THESIS

The main objectives of the present study can be, finally, summarized as follow:

- Characterization of the mechanical behaviour of the reinforced mortar layer reinforced with FRP grid by means of tensile, compression and shear tests;
- Study of the influence of different types of mortars with different strength for the reinforcing system;
- Investigation the effectiveness of the connection between the external reinforcing system and the masonry substrate;
- Assessment of the effectiveness of the FRP grid reinforced mortar layer in the upgrading and retrofitting of the overall behaviour of masonry walls with respect to the in-plane shear resistance and overall ductility;
- Numerical modelling of the strengthening system in order to validate the experimental evidences;
- Numerical modelling of the masonry wall in order to produce an instrument to replicate the structural behaviour of the whole system.

1.4 THESIS OUTLINE

The present thesis has been organized in seven chapters, including an introductory part (*Chapter 1*) in which an overall outline of the main issues investigated and the motivation at the base of the study is explained. Moreover, the aims and scope of the study and the principal objectives are illustrated. In *Chapter 2* a brief overview in relation to the traditional strengthening techniques for masonry walls used in the past decades is illustrated. In the same chapter, a research and summarize of all the possible modeling strategies for masonry structures is presented, with reference to their level of complexity and capability in the description of the actual behaviour of this material. *Chapter 3*

provides a comprehensive study of the relevant literature in the same field of interest of the issues investigated in the present thesis based on the bibliographical research. In particular, a review of the main aspects related to the strengthening of masonry walls is presented on the basis of some of the most relevant previous studies. Experimental and theoretical studies are reviewed, with reference to the available existing strengthening techniques for masonry walls, the use of Fibre Reinforced Polymers (FRP) with different arrangements, the evaluation of the contribution of these techniques to the improvement of the mechanical capacity of strengthened elements. Particular attention is paid to the studies concerning the employed of mortar layers reinforced with FRP. In *Chapter 4* the mechanical tests campaign carried out at ITAM Structural Laboratory on unreinforced and reinforced mortar specimens is described. In particular, the employed material, namely mortars and reinforcement, and the preparation of specimens is reported and the results of the characterization tests are collected. In *Chapter 5* the experimental tests on masonry walls carried out in the ITAM Structural Laboratory are described, reporting information about the specimens, in terms of geometry and employed materials, the strengthening systems and the test set-up. The experiments consist of in-plane shear tests on masonry walls strengthened with different techniques and subjected to a combination of compression and cyclic shear loading. The effectiveness of the strengthening system realized with reinforced mortar layers is tested also on brick walls severely damaged during a former experimental campaign cyclic tests. The numerical model through finite elements techniques is carried out in *Chapter 6*, with reference to the reinforced mortar specimens described in Chapter 4 and subjected to tensile and shear load conditions in order to reproduce the experimental results. Finally, the numerical modelling of the masonry wall is carried out in order to produce an instrument to replicate the structural behaviour of the whole system. In the final *Chapter 7* the major conclusion of the study are provided, together with a discussion and suggestion for future researches.

2. BACKGROUND

Existing unreinforced masonry (URM) buildings, many of which have historical and cultural importance, constitute a significant portion of existing buildings around the world. Recent earthquakes have repeatedly shown the vulnerability of URM buildings. This brought to light the urgent need to improve and develop better methods of retrofitting for existing seismically inadequate URM buildings. Several conventional techniques are available to improve the seismic performance of existing URM walls and are briefly reviewed in the following sections. Surface treatments (ferrocement, shotcrete, etc.), grout injections, external reinforcement, and center core are examples of such conventional techniques. Several researchers (ElGawady et al., 2004) [1] have discussed the disadvantages of these techniques: available space reduction, architecture impact, heavy mass, corrosion potential, etc. Modern fiber reinforced polymers FRP offer promising retrofitting possibilities for masonry buildings and present several well-known advantages over existing conventional techniques. Studies on shear retrofitting of URM using FRP are limited and a review of the most recent of them will be carried out in the following chapter.

Moreover, modelling the behaviour of URM walls in shear is a complex challenge that has not been completely resolved, due to the lack of suitable harmonized test method and input parameters for a suitable design model. In addition, several parameters influence shear behaviour of URM, primarily aspect ratio of the wall, the applied normal force, cohesion, coefficient of friction, unit tensile strength. In case of URM-FRP, other failure modes (e.g., debonding) are observed and new particularities related to the FRP are introduced which increase the complexity of shear problem. These include wide spectrum of commercial products with variations in types and orientations of fiber; FRP behaves linearly in tension up to failure, whereas conventional reinforced steel does not. Regarding masonry modelling, researchers have modelled it in the following two approaches:

(1) By considering masonry as a one phase homogenous material with mechanical properties differs from its constituents (i.e., brick and mortar). In this case, the mechanical properties of the homogenous material are the average mechanical properties of the components.

(2) By considering masonry as a two phase material where its constituents are considered separately.

The first modelling approach is relatively simple to use and requires less input data and the failure criterion has normally a simple form. Neglecting the influence of mortar joints which are acting as a plane of weakness makes this modelling approach suitable for the study of the global behaviour of masonry. The second modelling approach is more demanding because it requires more input data,

extensive computational facility, and complicated failure criterion. This approach well suited to the study of local behaviour of masonry.

2.1 TRADITIONAL STRENGTHENING TECHNIQUES FOR UNREINFORCED MASONRY PANELS

In many seismically active regions of the world there are large numbers of masonry buildings. Most of these buildings have not been designed for seismic loads. Recent earthquakes have shown that many of such buildings are seismically vulnerable and should be considered for retrofitting. Different conventional retrofitting techniques are available to increase the strength and/or ductility of unreinforced masonry walls. In the following sections a review on some seismic retrofitting techniques for masonry walls is presented.

Although a variety of technical solutions have been implemented for seismic retrofitting, there exists little information or technical guidelines with which an engineer can judge the relative merits of these methods. Furthermore, no reliable analytical techniques are available to evaluate the seismic resistance of retrofitted masonry structures.

2.1.1 Surface treatments

Surface treatment is a common method, which has largely developed through experience. Surface treatment incorporates different techniques such as ferrocement, reinforced plaster, and shotcrete. By nature this treatment covers the masonry exterior and affects the architectural or historical appearance of the structure.

Ferrocement consists of a thin cement mortar laid over wire mesh (Figure 2.1(a)), which acts as a reinforcement. It is relatively cheap, strong and durable, and the basic technique is easily acquired. Although ferrocement is not strictly a 'sustainable' technology as it uses cement and steel, it nevertheless employs them in a highly efficient and cost-effective manner. The mechanical properties of ferrocement depend on mesh properties. Ferrocement is ideal for low cost housing since it is cheap and can be done with unskilled workers. It improves both in-plane and out-of-plane behaviour. The mesh helps to confine the masonry units after cracking and thus improves in-plane inelastic deformation capacity. This retrofitting technique increases the in-plane lateral resistance and improves wall out-of-plane stability and arching action since it increases the wall height-to-thickness ratio.

Another technique is represented by the application of a reinforced plaster to the wall. A thin layer of cement plaster applied over high strength steel reinforcement can be used for retrofitting. The steel can be arranged as diagonal bars or as a vertical and horizontal mesh. A reinforced plaster can be applied as shown in Figure 2.1(b). In diagonal tension test and static cyclic tests, the technique was

able to improve the in-plane resistance by a factor of 1.25-3. The improvement in strength depends on the strengthening layer thickness, the cement mortar strength, the reinforcement quantity and the means of its bonding with the retrofitted wall, and the degree of masonry damage.

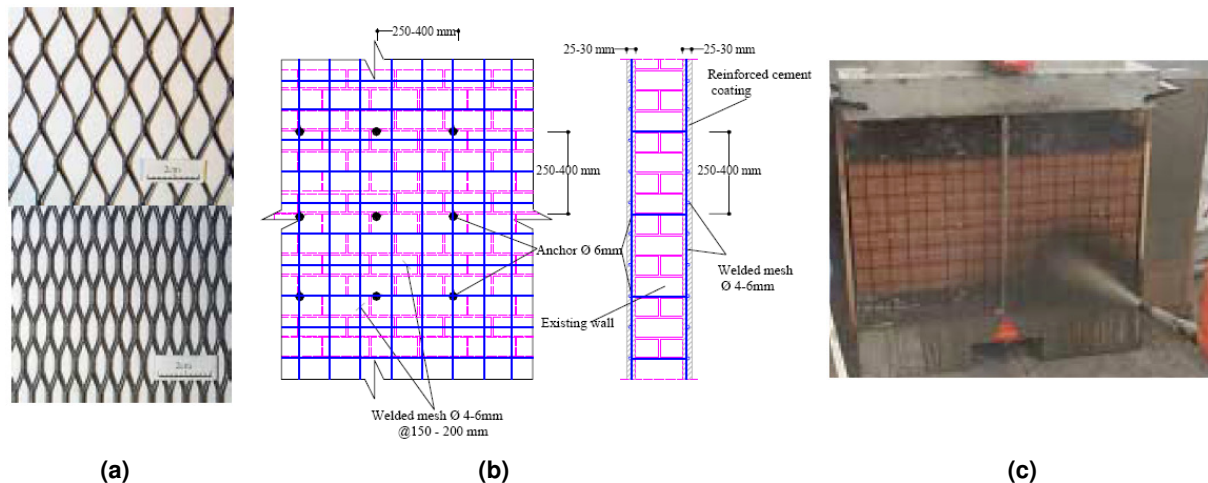


Figure 2.1. Surface treatments: samples of reinforcement used in ferrocement (a); typical layout of reinforced plaster (b); application of shotcrete (c) [1].

Shotcrete represents an alternative solution. Shotcrete overlays can be sprayed onto the surface of a masonry wall over a mesh of reinforcing bars (Figure 2.1(c)). Shotcrete is more convenient and less costly than casting-situ jackets. The thickness of the shotcrete can be adapted to the seismic demand. In general, the overlay thickness is at least 60 mm. In order to transfer the shear stress across shotcrete-masonry interface, shear dowels are fixed using epoxy or cement grout into holes drilled into the masonry wall.

Many of the physical properties of sound shotcrete are comparable or superior to those of conventional concrete or mortar having the same composition. Improperly applied shotcrete may create conditions much worse than the untreated condition. Shotcrete is used in lieu of conventional concrete, in most instances, for reasons of cost or convenience. Shotcrete is advantageous in situations when formwork is cost prohibitive or impractical and where forms can be reduced or eliminated, access to the work area is difficult, thin layers or variable thicknesses are required, or normal casting techniques cannot be employed. Additional savings are possible because shotcrete requires only a small, portable plant for manufacture and placement. Shotcreting operations can often be accomplished in areas of limited access to make repairs to structures. The selection of shotcrete for a particular application should be based on knowledge, experience, and a careful study of required and achievable material performance. Retrofitting using shotcrete significantly increases the ultimate load of the retrofitted walls. This retrofitting technique dissipates high-energy due to successive elongation and yield of reinforcement in tension.

2.1.2 Grout and epoxy injection

Grout injection is a popular strengthening technique, as it does not alter the aesthetic and architectural features of the existing buildings. The main purpose of injections is to restore the original integrity of the retrofitted wall and to fill the voids and cracks, which are present in the masonry due to physical and chemical deterioration and/or mechanical actions. For multi-leaves masonry walls, injecting grout into empty collar joint enhances composite action between adjacent leaves. The success of a retrofit by injection depends on the injectability of the mix used, and on the injection technique adopted. The injectability of the mix influences by mix's mechanical properties and its physical chemical compatibility with the masonry to be retrofitted.

The retrofit of walls by cement grouting can be carried out as follows:

- Placement of injection ports and sealing of the cracked areas in the basic wall as well as around injection ports.
- Washing of cracks and holes with water. Inject of water (soak of the bricks), from the bottom to the top of the wall, to check which tubes are active.
- Injection of grout (Figure 2.2), with injection pressure of less than 0.1 MPa, through each port in succession. Begin injection at the lower-most port. After filling all large voids, a second grout mix (cement-based or epoxy) is used for fine cracks.

This retrofitting technique improves the overall behaviour of the retrofitted URM and is effective at restoring the initial stiffness and strength of masonry.

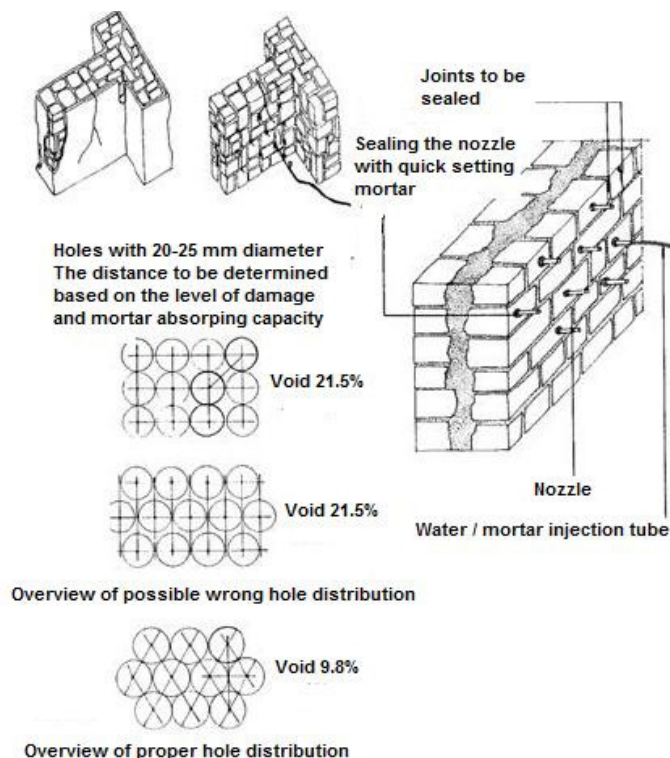


Figure 2.2. Overview of injection holes distribution.

2.1.3 External reinforcement

Steel plates or tubes can be used as external reinforcement for existing URM buildings. Steel system is attached directly to the existing diaphragm and wall (Figure 2.3(a)). The relative rigidities of the unretrofitted structure and the new steel bracing are an important factor that should be taken into consideration. In an earthquake, cracking in the original masonry structure is expected and after sufficient cracking has occurred, the new steel system will have comparable stiffness and be effective. The vertical and diagonal bracing improves the lateral in-plane resistance of the retrofitted wall. The increment in the lateral resistance is limited by crushing of the masonry at ends (toes) followed by vertical strips global buckling. In the case of creating infill panel, the rocking motion of the pier is associated with a vertical movement of its corner butting against the support masonries and the steel verticals resist the motion by restringing this vertical movement. This mechanism put both vertical members under tension forces (Figure 2.3(b)). The system increased the in-plane lateral resistance of the retrofitted wall and, in addition, the external steel system provides an effective energy dissipation mechanism.

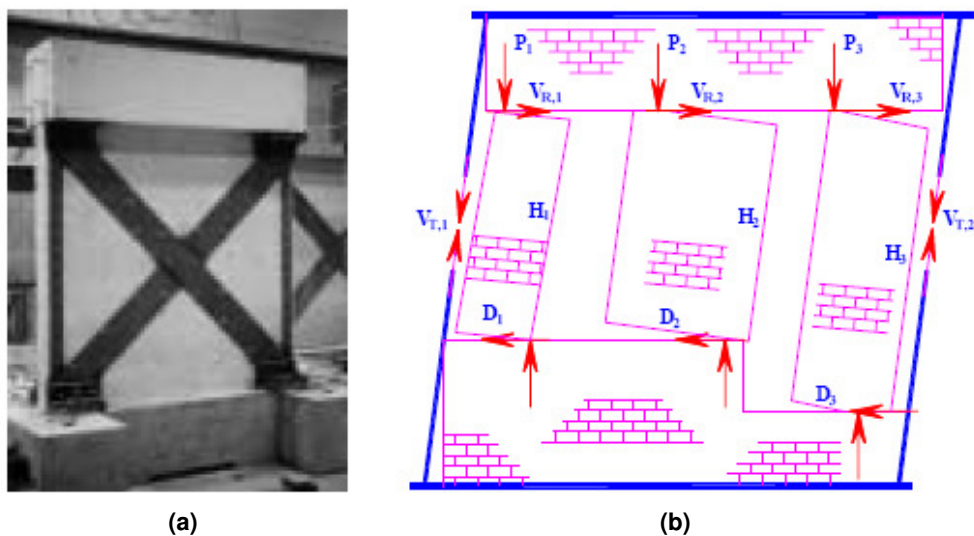


Figure 2.3. External reinforcement using vertical and diagonal bracing (a) or creating infill panel (b) [1].

2.1.4 Confinement of URM with R.C. tie columns

Confined masonry with R.C. weak frame represents one of the most widely used masonry construction system in Asia and Latin America. In China, they used such confinement in new masonry buildings as well as it is used as retrofitting for existing URM buildings. However, it is not easy to construct such confinement in existing masonry buildings. The basic feature of confined masonry structures is the vertical R.C. or reinforced masonry tie columns, which confine the walls at all corners

and wall intersections as well as the vertical borders of doors and windows openings. In order to be effective, tie columns should connect with a tie beam along the walls at floors levels.

The confinement prevents disintegration and improves ductility and energy dissipation of URM buildings, but has limited effect on the ultimate load resistance. The amount of reinforcement and concrete dimensions for this system is determined on the basis of experience, and depends on the height and size of the building.

2.1.5 Post-tensioning

Post-tensioning involves a compressive force applied to masonry wall; this force counteracts the tensile stresses resulting from lateral loads. There has been little application of this technique; post-tensioning is mainly used to retrofit structures characterized as monuments. This is due in part to lack of knowledge about the behaviour of post-tensioning masonry. In addition, the codification of post-tensioning masonry has only begun recently. Post-tensioning tendons are usually in the form of alloy steel thread bars, although mono-strand tendons are not uncommon. Bars typically show higher relaxation losses (2-3 times strand losses) and much lower strength/weight ratio; in addition, a major drawback for using of steel bars is corrosion. However, fiber reinforced plastic presents a promising solution for this problem.

Tendons are placed inside steel tube (duct) either within holes drilled along the midplane of the wall or along grooves symmetrically cut on both surfaces of the wall. Holes are cement grouted and external grooves are filled with shotcrete. In this case, the tendons are fully restrained (i.e. it is not free to move in the holes). This is true even if the tendon is unbonded, i.e. no grout is injected between the duct and the tendons. However, the holes can be left un-grouted (unguided unrestrained). This simplifies the strengthening procedure and allows future surveillance, re-tensioning, or even removal of the post-tensioning bars. It is also important for un-bonded bars to continue the protection of the bar inside the foundation to avoid differential oxidation.

Anchorage of post-tensioning in masonry is more complicated than in R.C. as masonry has a relatively low compressive strength. The self-activating dead end can be encasing to continuous and heavy R.C. foundation beams, constructed on either side of the wall bottom and connected well with it. At the top, post-tensioning is anchored in the existing R.C. elements or in a new precast R.C. special beam or specially stiffened steel plates. Anchorage devices and plates are usually placed in a recess of the surface, and covered later on with shotcrete or cement mortar. The requirement for bottom anchorage penalizes considerably this retrofitting technique. Vertical post-tensioning resulting in substantial improvement in wall ultimate behaviour for both in-plane and out-of-plane; in addition, it improves both cracking load and distribution.

For bonded grouted post-tensioning the ultimate tendon force may be determined assuming rigid bond and plane sections similar to design of R.C. post-tensioning. Thus, the tendon will reach

their yield force. For un-bonded post-tensioning the tendon force will increase from service up to ultimate load depending on the deformations. This increment in the tendon force may be estimated by applying rigid mechanisms. For short time behaviour and under the same post-tensioning force, strand configuration and amount has insignificant effect on wall behaviour.

2.1.6 Center core technique

The center core system consists of a reinforced, grouted core placed in the center of an existing URM wall. A continuous vertical hole is drilled from the top of the wall into its basement wall. The core achieved by this oil-well drilling technique may be 50-125 mm in diameter, depending on the thickness of the URM wall and the retrofitting required. After placing the reinforcement in the center of the hole, a filler material is pumped from the top of the wall to the bottom such that the core is filled from the bottom under pressure controlled by the height of the grout.

The placement of the grout under pressure provided by the height of the core provides a beneficial migration of the grout into all voids adjacent to the core shaft. The strong bonding of the grout to the inner and outer wythes of brick provides a homogeneous structural element much larger than the core itself. This reinforced homogeneous vertical beam provides strength to the wall with a capacity to resist both in-plane and out-of-plane loading. Wall anchors for lateral ties to the roof and floors are placed at the core location to make a positive connection to the wall. The filler material itself consists of a binder material (e.g. epoxy, cement, and polyester) and a filler material (e.g. sand). For cement-based grout, the volume proportions of the components play an essential role in the shear resistance.

This technique is successfully used to enhance the resistance of URM wall under cyclic actions, and lateral maximum lateral displacement, even if the energy dissipated is not so high. However, the system has several advantages: it will not alter the appearance of wall surface as well as the function of the building will not be impaired since the drilling and reinforcing operation can be done externally from the roof. The main disadvantage is this technique tends to create zones with widely varying stiffness and strength properties.

2.2 NUMERICAL MODELLING OF MASONRY

It is known that masonry is a material whose behaviour differs depending on the considered direction, due to the fact that the mortar joints surrounding masonry units, acting as planes of weakness, modify the mechanical properties and introduce a level of anisotropy. The characteristics of masonry should be reflected in the modelling technique adopted to study a particular mechanical aspect of such material, which also determines the level of accuracy of the model. This aspect clarifies

that all modelling strategies are useful for understanding of masonry structures behaviour with different scale of observation.

Figure 2.4 illustrates two different techniques for material description each of which has his own characteristics and field of application; in particular one can refer either to a micro-modelling or to a macro-modelling strategy. Micro-modelling is generally applied to small elements or portion of structures which require a more detailed representation, allowing the investigation of localized phenomena, while macro-modelling is employed for global modelling of entire structures in which the dimensions of the elements are large enough to neglect any unevenness in the stress distribution along the element. The characteristics of the macro-models and the small computational effort involved allow using them in cases that require fast analysis with a not very high level of detail.

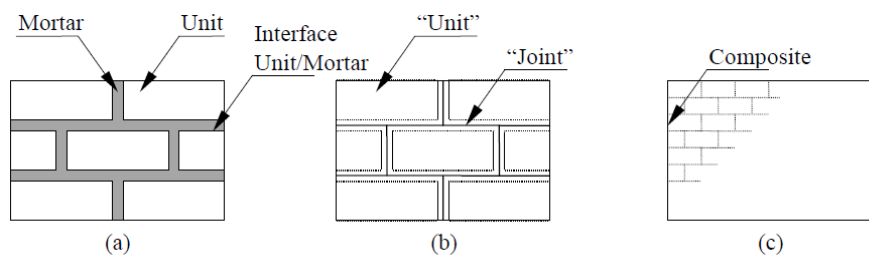


Figure 2.4. Modelling techniques for masonry: masonry element (a); micro-modelling (b); macro-modelling (c) [2].

In literature works it is possible to find analyses carried out on structural masonry models implemented with different levels of accuracy and precision. In the following, a brief revision of such models is made with particular concern to a macro-elements approach, when the model is realized through entire structural components, to a macro-modelling approach, when finite element continuous structural models are used, and to a micro-modelling approach, when discontinuous structural models are employed.

2.2.1 Macro-elements modelling technique

When a simple model of a masonry structure is needed one can refer to a modelling approach based on the use of structural elements as components of the entire structure. This kind of approach is the simplest method to describe the whole structure and its overall behaviour; it is based on the use of different mono- and bi-dimensional elements, such as beams, plates or shells, to model piers, walls, slabs, constituting the building. In particular, the use of structural components through which define an equivalent analytical model of a masonry walls structure gives different modelling options (Figure 2.5) such as a lumped mass model, a beam model, a macro-panel model (Seible and Kingsley, 1991) [3].

The simplest analytical model of a masonry structure is based on the use of lumped masses and structural parameters at each floor level (Figure 2.5(b)); this type of modelling permits to study the global behaviour of the structure taking into account the dynamic features and the material non-

linearity with a reasonable approximation. Due to the simplicity of this model, it is not serviceable to predict global failure mechanism or local damage of masonry elements.

To describe the actual geometry of the structural components in a more accurate manner one can be used beam elements connected through joints (Figure 2.5(c)). Using an equivalent frame it is possible to obtain more static and dynamical information on the behaviour of the structure, namely the pattern of local failure mechanisms development and the global collapse type, and also tri-dimensional analyses can be carried out.

The higher level of detail that a macro-elements modelling approach permits to achieve is represented by the approximation of the structure by panel components (Figure 2.5(d)). Examples are (Brencich et al., 1998) [4], (Cattari et al., 2005) [5]. The wall-system building is approximated by bi-dimensional elements, which can be either rigid or deformable, principally subjected to in-plane actions. Also, such bi-dimensional elements can be employed to study the evolution of damage phenomena while subjected to increasing loads or for kinematic limit analysis.

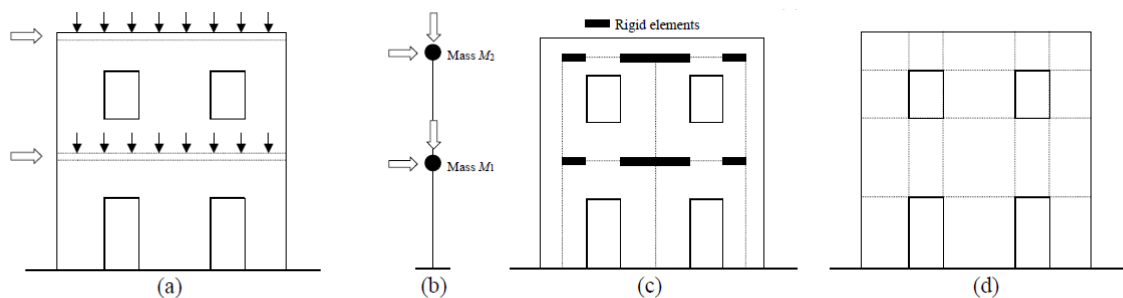


Figure 2.5. Structural components modelling techniques for masonry wall system (a): lumped masses (b); equivalent frame (c); panel system (d) [2].

2.2.2 Continuous modelling and homogenization techniques

Continuous modelling is a feasible approach to evaluate the behaviour of complete masonry structures, in which the approximation to consider a homogeneous material, described through a relation between average values of stresses and strains, is reasonable. The study of masonry structures through continuous numerical models is complex principally because the available experimental data are often lacking and it is not always possible to describe comprehensively the mechanical behaviour of the material. Furthermore, in non-linear analysis the knowledge of the post-peak phase of material plays a fundamental role in the reliability of the analysis results. These difficulties are further stressed by the complex anisotropic behaviour of masonry. For a proper description of anisotropic quasi-brittle materials behaviour different criteria for tension and compression should be formulated, with the implementation of plasticity concepts including different hardening and softening laws along each material axis.

Many theoretical anisotropic plasticity models are available (Hill, 1948) [6], (Hoffman, 1967) [7], (Tsai and Wu, 1971) [8], some of which successively have been numerically implemented in the works of (De Borst and Feenstra, 1990) [9], (Shellekens and De Borst, 1990) [10], considering an elastic-perfectly-plastic Hill yield criterion and an elastic-perfectly-plastic Hoffman yield criterion, respectively. Recently, attempts are given to simulate the hardening behaviour, but there are very poor numerical implementation and numerical testing data.

A step forward in the formulation of anisotropic models was done by establishing a composite yield criterion to describe anisotropic materials subjected to plane stress (Lourenço, 2000) [11]. In particular, tension and compression were treated as two independent yield criteria, with reference to different mechanisms of crisis. In particular, traditional formulations for isotropic quasi-brittle materials have been considered and extended to describe the orthotropic behavior. The formulations of isotropic quasi-brittle materials generally consider different inelastic criteria for tension and compression, namely the Drucker-Prager and Rankine criteria, also used for concrete. To model the behaviour of orthotropic materials as masonry, a Hill type yield criterion for compression and a Rankine type yield criterion for tension can be considered.

Other simplified modelling techniques (Sacco, 2009) [12], (Avossa et al., 2009) [13] are based on the description of the plastic and cracked material behaviour using a Drucker-Prager plasticity model, which is able to simulate the typical friction behaviour of masonry, or a concrete-type model. In the concrete-type model the elastic behaviour of material can be bounded by a surface, as that proposed by William and Warnke for ceramic materials, associated to a smeared cracking model for tension behaviour and a crushing behaviour for compression. A softening law and a tension cut-off for tensile behaviour are also defined.

A certain importance in the modelling of anisotropic and non-homogeneous materials is played by the homogenization techniques (Anthoine, 1997) [14], (Lourenço et al., 2006) [15]. In (Lourenço et al., 2006) [15] a review of different homogenization techniques of masonry components is presented. In particular, in the case of masonry brick walls modelling, such methodology can help to describe the material with a medium-high level of accuracy, keeping a certain degree of simplicity in the characteristics of the finite element model. The regularity of the assemblage and the recurring of a basic cell are the basic requirements the masonry element should have for the application of a homogenization procedure.

2.2.3 Discontinuous modelling

Discontinuous modelling produces micro-models which can be used to study the behaviour of masonry at a more detailed level and useful to calibrate some physical or mechanical material parameters. The weakness introduced by the presence of the horizontal and vertical mortar joints plays an important role in the anisotropic behaviour of the masonry element, making necessary a

more detailed material description which can be able to directly take into account the presence of units, joints and interface behaviour. It is outlined that all the possible failure mechanisms (Figure 2.6) of a masonry element could be taken into account to consider cracking of joints, vertical or diagonal cracking of units, sliding of blocks over head/bed joints, crushing of masonry (Lourenço and Rots, 1997) [16].

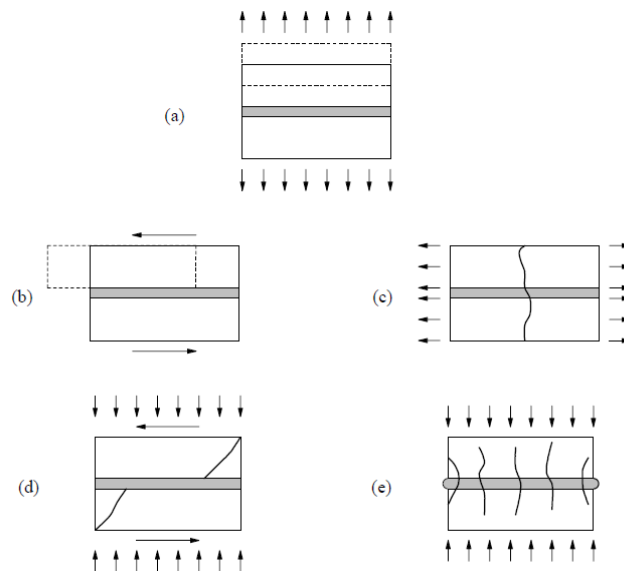


Figure 2.6. Masonry failure mechanism: joint cracking (a); joint sliding (b); unit vertical cracking (c); unit diagonal cracking (d); masonry crushing (e).

Analyses based on a discontinuous model of masonry are indicated for small elements or portion of structures, because of the high number of material parameters to be known, with particular focus on the non-linear properties of the unit-joint interface. Attempts over the years to model masonry non-linearity via interface elements are very few and neither all failure mechanisms nor the softening behaviour after cracking are comprehensively taken into account, limiting the applicability of such model to the pre-peak field.

Different modelling strategies can be pursued taking into account a different level of detail and ways to represent the non linear behaviour, which can be concentrated in the mortar joints and in potential vertical cracks in the centre of the block. Also, discontinuous modelling analysis can be carried out using finite elements (Lofti and Shing, 1994) [17], (Lourenço and Rots, 1997) [16], discrete elements (Lemos, 1998) [18] or limit analysis (Baggio and Trovalusci, 1998) [19], (Orduña, 2003) [20].

A finite element-based modelling technique allows to describe potential unit cracks, mortar joint cracks, slip and crushing surfaces through interface elements, able to represent the material non-linearity. In particular, a numerical implementation of this simplified modelling strategy is presented in (Lourenço, 1994) [21], which has been assumed that all the inelastic phenomena occur in the interface elements; also, such type of models are able to follow the entire load path of a structure until total degradation of stiffness. This is a case of a composite interface model defined by a tension cut-off

failure, a Coulomb friction envelope for shear failure and a cap mode for compressive failure, described on the basis of the modern plasticity concepts and, unlike from previous cases, taking into account the softening behaviour after crack slip.

While referring to discrete elements, they can be rigid or deformable elements connected between their vertexes, sides or faces and allow considering potential interpenetration and a real or adjusted damping coefficient. The contacts between elements are not fixed and during the deformation process there can be the formation of new points of connection. Discrete elements permit to grasp the behaviour of large displacement systems and each block has the advantage to be mesh independent, but a correct modelling of the structure require a high number of contact points at the interfaces.

For limit analysis rigid blocks not allowing elements interpenetration description are generally used, giving the possibility to obtain only the collapse load and mechanism of the structure.

3. STATE-OF-THE-ART

In the following sections a review of the main aspects related to the strengthening of masonry walls is presented. Some of the most relevant previous studies carried out by different authors in the recent years are examined. In particular, the state of previous knowledge and the information so far obtained through experimental and theoretical studies are investigated with reference to the available existing strengthening techniques for masonry walls, the use of Fibre Reinforced Polymers (FRP) with different arrangements, the evaluation of the contribution of these techniques to the improvement of the overall mechanical capacity of the strengthened element, in terms of shear capacity and energy dissipation. Furthermore, the last development regarding the upgrading of structural masonry walls in terms of seismic behaviour will be outlined and the last innovative reinforcing methodologies proposed during the last years will be reviewed. In addition, the new issues requiring further investigations in terms of experimental studies and numerical modelling are outlined and described in the framework of the present work.

3.1 GENERAL ASPECTS

The high vulnerability of buildings based on systems of structural masonry walls to the actions induced by earthquakes, and the increased serviceability and safety requirements imposed by the new codes, make clear the necessity of such existing buildings to be upgraded. In fact, it is necessary to strengthen this particular class of structures with appropriate reinforcing systems, in order to achieve the required upgrading of their seismic and energy dissipation performances. Furthermore, the damage patterns experienced by two-dimensional elements in masonry structures observed after the stroke during seismic events require development of new types of strengthening techniques and systems, effectiveness of which has to be quantitatively evaluated through experimental and numerical analyses.

The reinforcement of two-dimensional masonry elements has been carried out during the last years by means of different strengthening methods. Some of the most used traditional methods in order to upgrade structural elements in masonry buildings are represented by: (a) filling of cracks and voids by grouting; (b) stitching of large cracks and other weak areas with metallic or brick elements or concrete zones; (c) application of reinforced grouted perforations to improve the cohesion and tensile strength of masonry; (d) external or internal post-tensioning with steel ties, joining structural elements together into an integrated three dimensional system; and (e) single or double sided jacketing by

shotcrete or by cast-in-situ concrete, in combination with steel reinforcement (e.g. in the form of two-directional welded mesh). It has been seen that these traditional strengthening techniques are affected by many problems and drawbacks; thus sundry new methods based on the use of innovative materials, such as the Fibre Reinforced Polymers (FRP), have been developed in the last decades (Triantafillou, 1998) [22]. All the last developed techniques take advantage of the well known benefits proper to the FRP materials including, above all, a light weight, resistance to corrosive environment, excellent mechanical properties such as stiffness and strength, and simplicity to put in place.

One of the early studies on the use of non-metallic reinforcement for strengthening of masonry walls was that by (Croci et al., 1987) [23], in which it is presented a campaign of tests carried out on shear walls with vertical or inclined reinforcement realized by low modulus polypropylene braids. Furthermore, detailed concepts and analytical results on the applicability and effectiveness of FRP tendons used to apply circumferential pre-stressing to historic masonry structures are given by (Triantafillou and Fardis, 1997, 1993) [24, 25]. In the work of (Schwegler, 1994) [26] the use of carbon laminates (CFRP) as non-seismic strengthening elements of masonry structures was investigated. The laminates used as tensile reinforcement were bonded to the masonry surface by means of epoxy resin. The tests carried out in order to clarify the effectiveness of this technique were conducted on full-scale, both in-plane and out-of-plane, cyclic testing of one-story masonry walls, and was developed an analytical model for the in-plane behaviour of CFRP-strengthened walls within the framework of stress fields theory. Also, the studies by (Saadatmanesh, 1994) [27] and (Ehsani, 1995) [28] focused on experimental investigations, involving monotonic static tests of unreinforced masonry specimens strengthened with epoxy-bonded glass fabrics. The results obtained from these studies led to the conclusion that for the sake of both economy and mechanical response, unidirectional FRP reinforcement in the form of laminates or fabric strips is preferable to two-dimensional fabrics which cover the whole surface of masonry walls.

3.2 STRENGTHENING TECHNIQUES FOR IN-PLANE BEHAVIOUR

As previously outlined, during the years the researchers developed different strengthening techniques based on the use of Fibre Reinforced Polymers (FRP) externally bonded to the surfaces of the element to be reinforced. These techniques can be described in terms of the FRP typology, reinforcement arrangement, connection system to the substrate. In general, the strengthening techniques can be devoted to the improvement of the out-of-plane flexural capacity, the in-plane shear resistance and the ductility of the system to which the reinforcement is applied.

Several experimental or analytical research works have been carried out on the in-plane response of walls strengthened with FRP sheets or laminates. In (Roca and Araiza, 2010) [29] a review of some in-plane tests configurations used to study the shear response of reinforced elements is reported (Figure 3.1). In these cases the strengthening strategy is represented by an externally

chemically bonded Fibre Reinforced Polymers in form of sheets or laminates. It is noted that such externally chemical bonded reinforcement involves complex mechanical phenomena such as the peeling off of the substrate bricks surface or the influence of friction and dilatancy in the brick-mortar interface on the response of the strengthening itself.

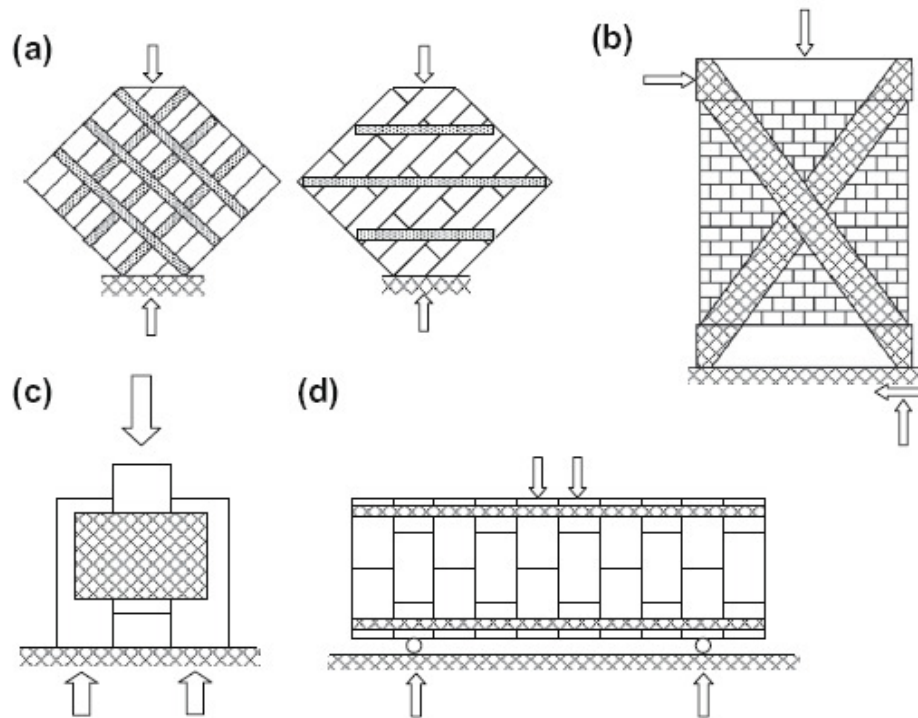


Figure 3.1. Different in-plane test configurations to investigate the shear response of FRP reinforced brick masonry elements: (a) (Valluzzi et al., 2002) [30], (b) (ElGawady et al., 2005) [31], (c) (Eshani and Saadatmanesh, 1997) [43], (d) (Triantafillou, 1998) [40]. [29].

In particular, (Valluzzi et al., 2002) [30] used the classical diagonal compressive tests (Figure 3.1(a)) to explore the in-plane shear response of brick masonry panels strengthened with FRP laminates and compared the experimental results with the predictions yielded by different analytical models. In the cited study the difference in the effectiveness of the reinforcement has been investigated for both side (symmetric) or for one side (non-symmetric) strengthening configurations. In (ElGawady et al., 2005) [31] and (Avramidou et al., 1999) [32] the effectiveness of FRP strengthening is evaluated through tests on masonry walls reinforced with externally bonded laminates applied diagonally to the joints, as shown in Figure 3.1(b). Moreover, in (ElGawady et al., 2007) [33] the cyclic behaviour of masonry shear walls, employing specimens similar to those in Figure 3.1(b), is investigated by the authors. Also, similar experimental campaigns have been carried out, for example, by (Santa Maria et al., 2006) [34] using CFRP, and by (Fam et al., 2008) [35], (Al-Salloum and Almusallam, 2005) [36], (Wang et al., 2006) [37], (Stratford et al., 2004) [38] using GFRP. In particular, in (Fam et al., 2008) [35] has been studied the effect of the combination of two repair techniques for

damaged walls, namely grout injection of mortar and application of GFRP sheets, showing that it is possible to fully recover and even upgrade the capacity of the walls.

As previously outlined, (Valluzzi et al., 2002) [30] performed a study in order to investigate the efficiency of the strengthening system considering different configurations, namely strips with grid arrangement or diagonal strips, and the influence of the eccentricity of the reinforcement, strengthening the panels on both sides or only at one side. It is noted that, first of all, the asymmetrical application of the reinforcement is associated to a limited effectiveness in the improvement of the shear resistance of masonry panels. Moreover, it is shown that the diagonal configuration can be more efficient concerning the enhancement of the shear capacity, while the configuration of strips as a grid allows a better stress redistribution producing a less brittle failure due to crack spreading (Valluzzi et al., 2002) [30], (Santa Maria et al., 2006) [34], (Luccioni and Rougier, 2010) [41]. In general, for masonry panels externally reinforced with FRP and subjected to diagonal compression it is observed an increase of strength between 15 and 70%.

(ElGawady et al., 2005, 2007) [31, 33] and (Santa Maria et al., 2006) [34] studied the response of half scale masonry panels strengthened with FRP laminates applied diagonally to the joints subjected to both static and cyclic loading. The tests showed that the increase of lateral strength was proportional to the FRP axial rigidity and, also, using high amount of FRP brittle failure occurred.

A number of researches have been performed in order to study the seismic strengthening of unreinforced masonry walls with FRP. Some results have shown that the reinforcement improves significantly the lateral stability of the walls, increases the shear strength, the maximum displacement before the failure, and the displacement and load at first crack (ElGawady et al., 2005) [31], (Santa Maria et al., 2006) [34], (Chuang et al., 2003) [42].

Finally, some studies have been carried out on elementary shear masonry assemblages, such as that represented in Figure 3.1(c), rather than entire masonry walls or panels, in order to identify and study the elementary mechanisms involved in the strength response of reinforced masonry instead of the evaluation of the overall efficiency of the strengthening (Roca and Araiza, 2010) [29]. Moreover, in such studies the difference with respect to some previous research works lays on the consideration of strengthening strips applied perpendicular to the mortar joints, considered important not only regarding the brick cracking but also for the sliding mode failure of elements. A similar approach, also using simple shear assemblages strengthened by means of overlay reinforcement placed through the mortar joints, has been previously considered by (Eshani and Saadatmanesh, 1997) [43] (Figure 3.1(c)). In (Haroun et al., 2003) [44] shear tests on small wall strengthened transversely to the mortar joints have been also carried out.

A number of experimental procedures and numerical models have been proposed for the study of the bond performances between FRP sheets and bricks. An example is the test procedure described in (Aiello and Sciolti, 2006) [45], allowing the evaluation of bond stress-slip relationship. Another example of investigation of the bond behaviour of the FRP reinforcement on clay bricks is in

(Liu et al., 2005) [46], (Willis et al., 2009) [47]. Also some numerical models for the masonry-FRP interface have been recently proposed (Grande et al., 2010) [48].

It is further noted that this technique may lead to some problems that can limit more or less considerably its application for all cases, requiring additional studies. Since the reinforcement is made by continuous strips or sheets externally applied on the surface of masonry wall, this may create a water-proof barrier and produce difficulties for the natural transpiration of stone or ceramic material. In addition, some problems may arise regarding the fire resistance of the strengthening systems that, especially when used in combination with epoxy-based matrix or bonding material, can be particularly vulnerable.

3.3 EXTERNALLY APPLIED FRP GRID REINFORCED MORTAR LAYERS

An alternative strengthening method to previously described ones has been recently proposed by (Papanicolau et al., 2007, 2008, 2011) [49, 50, 51] for strengthening of unreinforced masonry walls subjected to in-plane and out-of-plane cyclic loadings. As already described, numerous techniques have been developed in order to rehabilitate and strengthen URM structures; these may be roughly categorized as ‘conventional’ and as ‘modern’. The former include surface treatments (such as shotcrete or ferrocement overlays), grout injections and internal or external prestressing with steel ties. The latter include the use of metallic or polymer-based grid-reinforced surface coatings, externally bonded fiber-reinforced polymers (FRP, such as epoxy-bonded strips or in situ impregnated fabrics) and near-surface mounted (NSM) FRP reinforcement.

In the cited case, a technique that combines the benefits of both types of interventions, conventional and modern, is the one in which the reinforcement consists of a textile reinforced mortar (TRM) in substitution of the FRP used as overlays or near surface mounted reinforcement. The researchers introduced the TRM in the strengthening of unreinforced masonry walls in order to address the numerous drawbacks related to the use of FRP externally bonded to element surface and mainly associated to the employment of organic binders.

These drawbacks are attributed mainly to the use of organic binders (resins) and can be summarized as follows:

- (a) poor behaviour of resins at temperatures above the glass transition temperature;
- (b) relatively high cost of epoxies;
- (c) potential hazards for the manual worker;
- (d) difficulty to apply FRPs on wet surfaces or at low temperatures;
- (e) lack of vapour permeability;
- (f) incompatibility of epoxy resins and some substrate materials (e.g. clay);
- (g) difficulty to conduct post-earthquake assessment of the damage suffered by the masonry behind the FRP.

In addition, certain properties of clay masonry, such as the porosity and surface unevenness and/or roughness, which affect the epoxy-brick bond behaviour, as well as restrictions related to intervention strategies for historic masonry buildings (e.g. requirements for reversibility), may possibly inhibit the success of FRP application (Papanicolau et al., 2007) [49].

In Figure 3.2 a snapshot of the TRM strengthening is shown, considering the different phases of the application of the reinforcement system. The benefits of this technique have been compared to the classical application of FRP in forms of strips, considering both the in-plane shear and out-of-plane flexural increase of strength for the cases of monotonic and cyclic loading conditions.



Figure 3.2. Textile-reinforced mortar (TRM) strengthening of a masonry panel. Phases of application [51].

The specimens used by the authors in this study are represented by medium-scale clay brick shear walls, beam-column type walls and beam type walls subjected to cyclic out-of-plane or in-plane loading. On the basis of the experimental results, it has been noted that the textile-reinforced mortar system lead to an increase of the load carrying capacity and deformability of unreinforced masonry walls. Furthermore, for the case of out-of-plane loading the TRM overlays perform even better than the ordinary FRP reinforcement in terms of maximum load and displacement at failure, in the cases in which tensile fracture of textile reinforcement does not occur. For the case of in-plane loading, TRM results in reduced effectiveness for strength (but not more than 30%), if compared with FRP-EBR strengthening. In terms of deformation capacity, representing a fundamental characteristic in seismic retrofitting of masonry structural elements, TRM reinforcement is found to be more effective than FRP, up to about 15–30% in shear walls. In addition, the strength generally increases with the number of layers and the axial load, at the expense of deformation capacity (Papanicolau et al., 2011) [51].

The experimental study highlighted the effectiveness of the TRM jacketing technique as a solution for strengthening of unreinforced masonry walls subjected to either out-of-plane or in-plane loading. The authors also suggest further investigation in order to expand the amount of experimental data and to optimize this technique for the seismic retrofitting.

In (Faella et al., 2010) [52] a similar technique has been employed in order to strengthen yellow-tuff-masonry walls, which are rather common in the South of Italy as well as in the Mediterranean basin. The composite material utilized for strengthening is made out of a carbon fiber mesh, arranged according the configuration shown in Figure 3.3(a), placed within two layers of mortar, according to the usual procedure currently carried out for spreading a plaster layer upon the wall faces: in particular, two mortar layers have to be placed for embedding carbon fibers and developing composite interaction between fibers and matrix (Figure 3.3(b)).

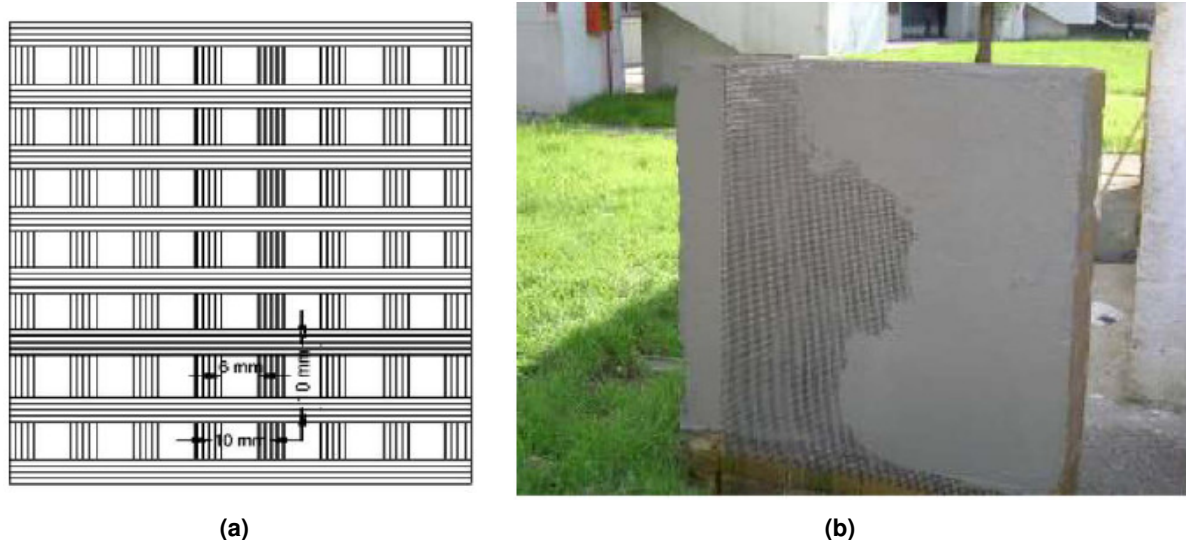


Figure 3.3. Carbon fiber reinforcement mesh texture (a) and application of the TRM layer [52].

The experimental campaign carried out on these reinforced elements showed that strengthened walls did not fail for the characteristic diagonal sliding fracture at the mortar-to-brick interface, that generally develops in unreinforced masonry walls. In fact, the strengthening layer restrain the possible formation of such diagonal crack, as indicated by the change in stiffness which can be observed on the load–displacement curves. Consequently, the ultimate load in diagonal compression, and the corresponding shear strength, for strengthened walls was found to be between four and six times greater than the one observed for bare walls.

Furthermore, no fiber tearing failure has been observed, but failure usually occurs prematurely after loss of adhesion between the strengthening layer and the masonry substrate. Due to this evidence, the same increase in shear strength would have been observed even if a less resistant layer would be employed; in particular, based on characteristics compatible with mechanical properties of masonry substrate, namely strength and stiffness.

In any case, the system examined represents a reliable solution for enhancing shear strength on tuff-masonry, confirmed in its effectiveness by the significant increment in shear resistance observed in strengthened walls compared to the non-strengthened ones.

Another innovative strengthening method developed in the last years features, on the basis of the previous described technique, that the textile reinforcement is replaced by commercial grids made of long fibre rovings, usually made of carbon, glass or aramid, arranged in two orthogonal directions. In addition, the polymer resins are substituted by cement- or lime-based mortars. The composite action is achieved in this case through mechanical interlock of the grid structure and the mortar passing through the grid's openings. An important aspect to be remarked is represented by the fact that the use of an inorganic material as a binder rather than an organic resin can be more advantageous and can solve some problems, such as poor behaviour at high temperatures, vapour impermeability, incompatibility with masonry substrate (Prota et al., 2006) [53].

The specimen employed by (Prota et al., 2006) [53] are represented by tuff masonry walls reinforced by a cementitious matrix–grid (CMG) system externally applied to the masonry wall surface. Yellow tuff stone represents the main volcanic product widely spread particularly in Southern Italy where seismic hazard is relevant and represents a crucial aspect in the preservation process of historical constructions. Due to high porosity and low abrasion resistance, tuff surfaces need to be pretreated by using proper coating primers in order to consolidate the support and improve the adhesion of strengthening FRP materials. High compatibility and reversibility are concepts of particular relevance for application on historical buildings, and are also required when selecting the strengthening methods using FRP.

The grid used for the strengthening system, as shown in Figure 3.4, was a bi-directional alkali resistant AR glass coated open grid, SRG 45, consisting of machine and cross direction strands connected perpendicularly at about 25.4 mm spacing, while the matrix was a polymer modified AR-glass fiber reinforced mortar. The choice of such cementitious composite material was due to some advantages, mainly due to its highly compatibility in terms of physical and mechanical properties with the tuff substrate. Among the advantages of the CMG strengthening system, the following can be mentioned:

- (a) ease of installation;
- (b) no need for any surface preparation or high levels of workmanship;
- (c) fire resistance;
- (d) excellent bond with the substrate;
- (e) breathability of the system which allows transport of air and moisture through the matrix, and reversibility.

Moreover, as already stated, for strengthened walls exposed to high temperature or environmental effects, the application of a thick layer of cementitious mortar substantially ensures a protection for the reinforcing grid and improves the long-term behaviour of the strengthening system. Due to these key

advantages and unique properties, this system is a potential alternative to the traditional strengthening techniques used for masonry structures.

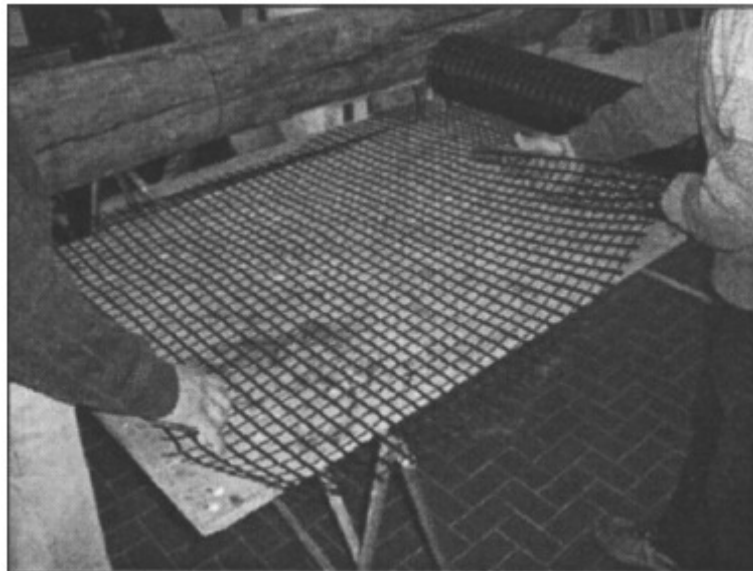


Figure 3.4. Bi-directional alkali resistant AR glass coated open grid, SRG 45 [53].

The installation of the strengthening system on the masonry substrate has been done considering controlled procedure. First of all the wall was properly prewetted and the mortar, previously mixed with water and an acrylic hardener, was then trowelled onto the wall in a 5 mm thick layer. The first 900 mm² fabric sheet was firmly hand pressed into the wet binder to ensure its adequate embedding to the support wall. The first ply was laid up with the primary fibers aligned horizontally to the bottom of the wall (Figure 3.5(a)). Then, a second layer of mortar was applied by trowelling an additional 5 mm thick layer. Finally, the second ply was applied with the primary fibers aligned vertically. A 15 mm offset of the second ply with respect to the first was ensured in order to avoid that any fracture plane could originate from the overlap. The second ply was covered by a relatively smooth surface, and the resulting CMG system nominal thickness was of about 10 mm (Figure 3.5(b)). In the cited tests, the installation of the CMG system involved one or both sides of tuff masonry walls.

The experimental campaign carried out by the authors allows to recognize that the CMG system reduces the high anisotropy of the as-built panels; the engineered composite masonry–CMG wall is made of two components: the CMG system that ensures the required shear strength to the mortar–stone interface, and the stone blocks providing the compressive strength. The obtained results indicate that relevant increases of shear strength can be obtained using the CMG reinforcement, especially when a double layer of CMG is applied on both sides of the panel. This configuration also provides a better post-peak response and a significant increase in ductility (Prota et al., 2006) [53].

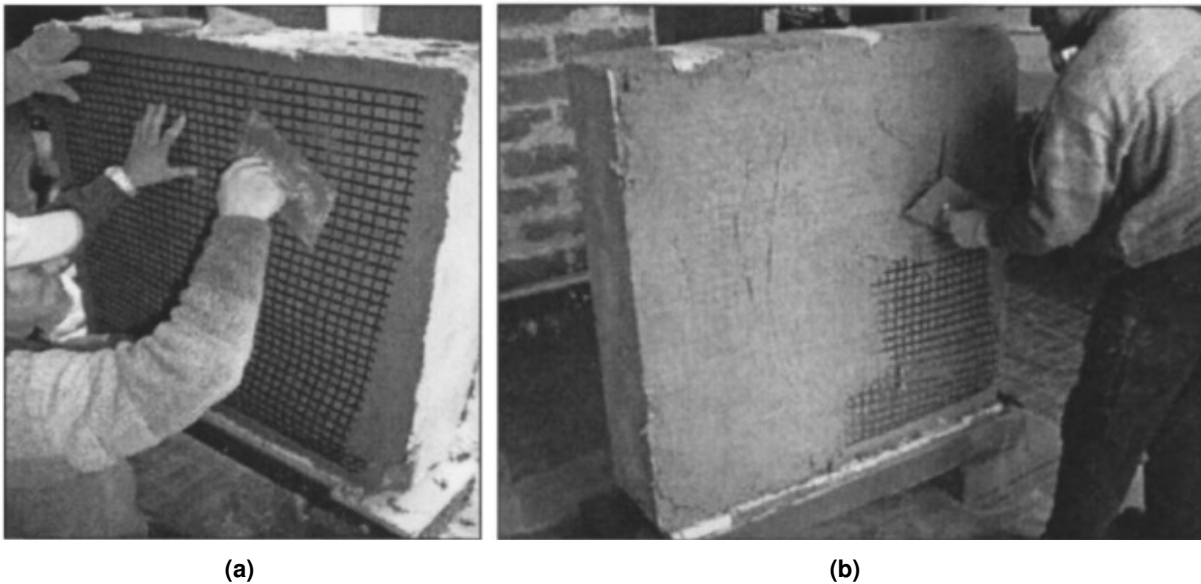


Figure 3.5. CMG system: reinforcing grid installation (a) and troweling of final mortar layer (b) [53].

It can be finally observed that the CMG system satisfies basic design requirements such as compatibility with the support, high bond properties, and reversibility of the intervention. Significant improvements of strength and ductility of panels were achieved installing different layouts of the CMG grid, while there is a negligible influence on the initial stiffness of the strengthened walls. Moreover, the impact of the intervention on the existing structure is very low and compatible with conservation requirements. The comparison of results provided by different reinforcement layouts gives important, even though not comprehensive, information for the design of in-plane strengthening of masonry walls. Further research is needed to assess the effectiveness of the proposed strengthening solution when applied to different brickworks and structural layouts and further experimental investigations are necessary as well in order to assess the performance under cyclic actions of masonry elements strengthened with the CMG system.

In (Drdácký and Lesák, 2009) [54] a test campaign on masonry walls strengthened by different techniques has been carried out, including also the use of geo-net reinforced plaster layers applied to the specimen surface. For the masonry walls strengthened with geo-nets, three different cases were considered by varying geometrical and mechanical characteristics. The rendering used to embed the geo-net reinforced consisted in lime mortar containing a small percentage of Portland cement. Some of the specimen tested by the authors were represented by damaged specimen used in previous test under the application of a horizontal load, repaired with the same system. The test were carried out applying a cyclic load with a stepwise increase in the maximum cyclic limits.

The tested specimens presented a particular crack pattern, that is different from the one that can be found in specimens reinforced with X-shaped FRP strips. In fact, the cracks visible on the surface represent a combination of two sets of damages: masonry cracks, and cracks which occur in the plaster only and originate from the differential movement of a plastic mesh. In general geo-nets

have a better ratio of strength to the strength of brick, if compared with FRP laminate reinforcement, and it is advisable to apply them on masonry substrates.

Systems similar to the previous ones have started to be studied using again cement-based matrix grid systems to strengthen unreinforced masonry walls. In (Aldea et al., 2006) [55] a composite system consisting of a sequence of layers of cement-based matrix and alkali resistant glass coated reinforcing grid has been used (Figure 3.6). The characterization of the considered strengthened systems has been carried out and the assessment of its effectiveness for improving unreinforced masonry walls seismic performance has been investigated by the authors. The experimental campaign resulted in the evidence of the ability of the cement-based system to strengthen the walls and showed a better performance compared to other FRP reinforcement alternatives.

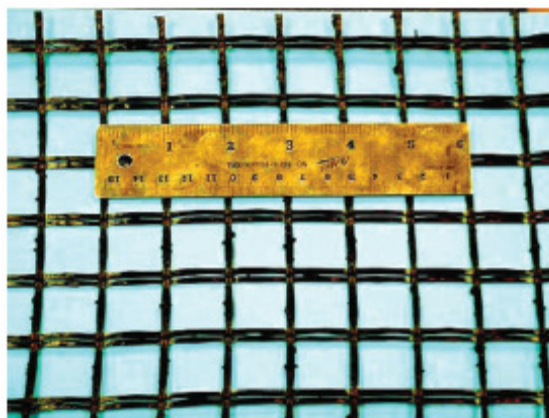


Figure 3.6. Coated AR-glass grid employed by (Aldea et al., 2006) [55].

The tests have been carried out on lightly reinforced single-wythe masonry walls to simulate typical piers between windows of a building. The concrete masonry full scale walls were tested under in-plane shear loading in order to simulate seismic action. In the experimental campaign carried out by the authors, as illustrated in Figure 3.7, different commercially available FRP systems using E-glass fabrics applied in various reinforcement configurations and the CMG system were considered. In particular, CMG system application was full coverage, on one side of the wall only.

X-cracking was the failure mode observed for all the walls strengthened with CMG system. The bond between the strengthening system and the substrate plays a critical role in providing adequate load carrying capacity to the structural element strengthened. Multiple cracking of CMG system surface was observed during the tests, which suggests stress distribution and energy absorption provided by the reinforcing grid.

Since in this study, the reinforcement was placed on only one side of the walls, it can be observed the difference between the reinforced face and the unreinforced back at failure: in particular, the reinforced face of the wall held the masonry wall together at failure, whereas the material was spall away from the back. In all tests the structural integrity of the walls at failure was ensured by

CMG system. This suggests that its use may be able to prevent the collapse of unstrengthened walls, which is a major source of hazard during earthquakes.

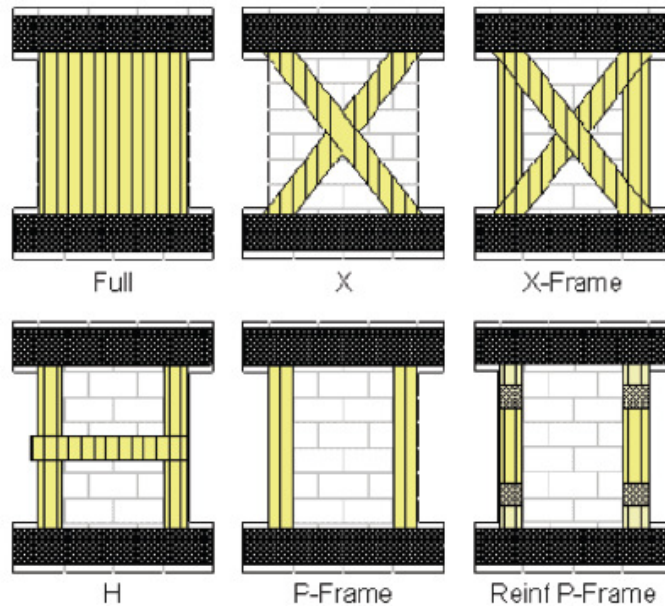


Figure 3.7. Different FRP reinforcement configurations investigated by (Aldea et al., 2006) [55].

Finally, in Figure 3.8, typical horizontal force - displacement curves for a reference and a strengthened wall using CGM system are presented. It can be observed that the addition of the strengthening system significantly improves the performance of the wall, both in terms of strength and ductility. In all cases the engineered load improved for the strengthened walls tested compared to reference.

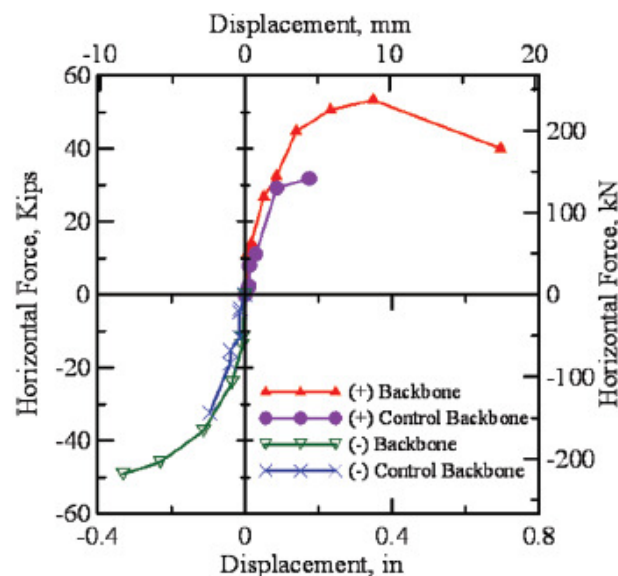


Figure 3.8. Example of a typical Horizontal Force – Displacement curve for CMG strengthened wall compared with URM wall [55].

In conclusion, as already described, the strengthening of masonry walls by means of fibre reinforced polymer grid embedded in a cement- or lime-based mortars, constituting also the bonding material on the substrate to which it is applied, is an effective strengthening technique for both in-plane and out-of-plane actions. Also, this reinforcing methodology allows to overcome some of the main disadvantages characterizing the employment of the externally bonded FRP in forms of strips or sheets and the FRP elements applied via the near-surface mounted (NSM) technique.

In the present thesis the strengthening technique that will be considered is represented by mortar layers embedding a FRP reinforcement in form of a grid. The FRP-Reinforced Mortar Layers are symmetrically externally applied to the walls surfaces. This technique is characterized by a number of advantages if compared to other possible FRP-based strengthening methods; particularly, a superior resistance to fire action has to be remarked, a good compatibility and bond with the substrate material, particularly in the case of masonry, vapour permeability. The main interest in the study of this strengthening technique is related to the promising possibility it offers in the upgrading in-plane shear behaviour of the system to which it is applied. The performances of the whole assemblage need to be investigated for monotonic loading state as well as for cycling loading conditions. Another important issue to address is also the assessment of the effectiveness of the considered strengthening system in the improvement of the overall ductility of reinforced elements.

3.4 MODELLING OF THE BEHAVIOUR OF THE REINFORCED SYSTEM

Some numerical analysis have been also carried out on masonry panels strengthened with cementitious matrix grid composites with the aim of investigate the scattered results due to workmanship defects through FEM parametric analyses (Lignola et al., 2009) [56]. In addition, it has been shown that the presence of the external reinforcement reduces the anisotropy of the as-built panels leading to a better redistribution of the stresses and a more uniform and diffused crack pattern, allowing for higher shear strength and deformability. For that reason, strengthened panels are less sensitive to the workmanship defects. Moreover, it has been observed that the strengthening also provides a good post-peak response and a better ductility for the panels.

In order to conduct the analyses, finite-element method (FEM) models of the elements have been compared by the authors. Experimental data obtained through a past test campaign carried out by (Prota et al., 2006) [53] can represent the database of results about how fiber density and layout could influence the strength and ductility performance of strengthened panels. Moreover, in a previous work conducted by (Lignola et al., 2007) [57], a parametric analysis was carried out on a geometrical ideal panel focusing mainly on the variability of mortar and tuff properties. The experimental data were compared to numerical model. Regarding the numerical modelling strategy of the elements, a micro-modelling approach was adopted to fully understand the contribution of basic constitutive materials, namely mortar and tuff blocks, and to quantify the effect of the eventual workmanship defects on the

masonry behaviour by means of many parametric analyses on the numerical model. At the micro level, the interaction between mortar joints and brick units is analyzed by means of a detailed analysis involving discrete nonlinear models of single elements layered according to predefined patterns.

The details of the specimen geometry are given in Figure 3.9(a). The overall dimensions of the panels tested by the authors were: 1030 mm height, 1030 mm length, and 250 mm width, with an aspect height-to-length ratio of 1, commonly found in multi-storey buildings.

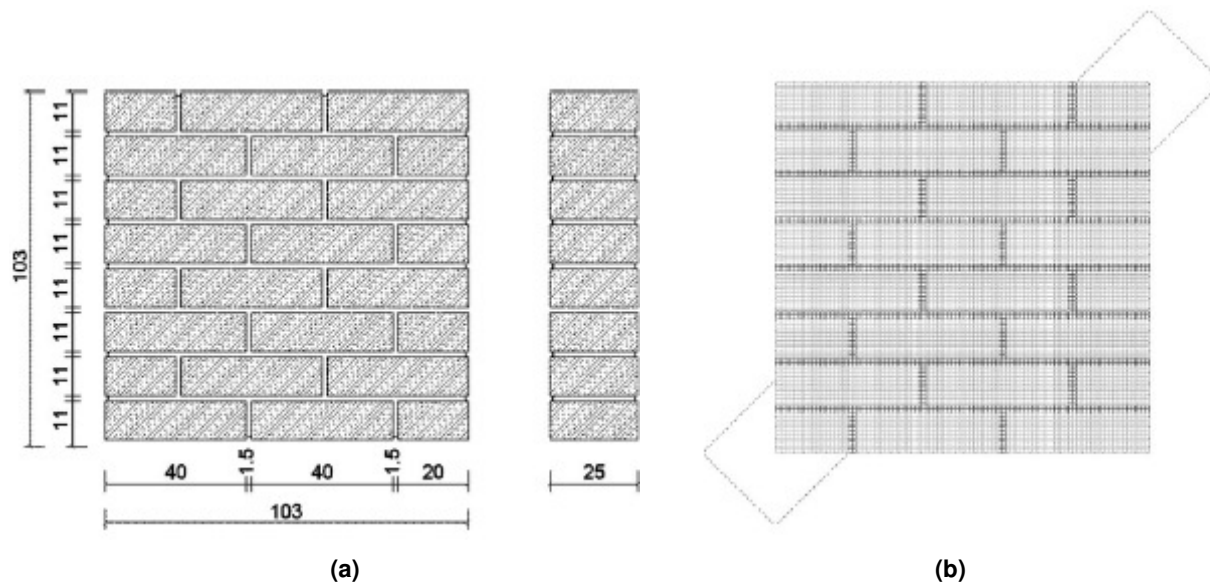


Figure 3.9. Geometry of the masonry walls (a) and Finite Element micro-model (b) [56].

The panels were modelled by eight-node quadrilateral isoparametric plane stress elements; the resulting finite element model is shown in Figure 3.9(b). These elements are based on quadratic interpolation and Gauss integration. At the micro level the tuff and the mortar are modelled independently, without frictional interfaces between them, according to a smeared-crack approach with exponential strain softening in tension and plasticity in compression by means of a parabolic curve formulation both based on tensile and compressive fracture energy Figure 3.10. The biaxial stress state in the two materials has been modelled by a combination of the yield conditions of Rankine and Von Mises. The former is adopted to describe the tensile regime, the latter to describe the compressive regime. This combined yield surface is especially applicable in plane stress situations. CMG is modelled as an additional material bonded to the masonry panel. The cement based mortar, representing the matrix, is modelled like the mortar of the masonry substrate, while the composite grid material is linear elastic up to failure (brittle) in tension and no strength is considered in compression. In all the experimental tests, the wall structural integrity at failure was ensured by the CMG strengthening system, revealing the high bond performance between CMG and the support even without any mechanical anchorage (Prota et al., 2006) [53]. This suggests that the strengthening system can be perfectly bonded to the masonry panel in the FEM simulations. Thus, in the model it

was simulated with eight-node quadrilateral elements over the first masonry substrate mesh, connecting the same nodes, but with their own properties.

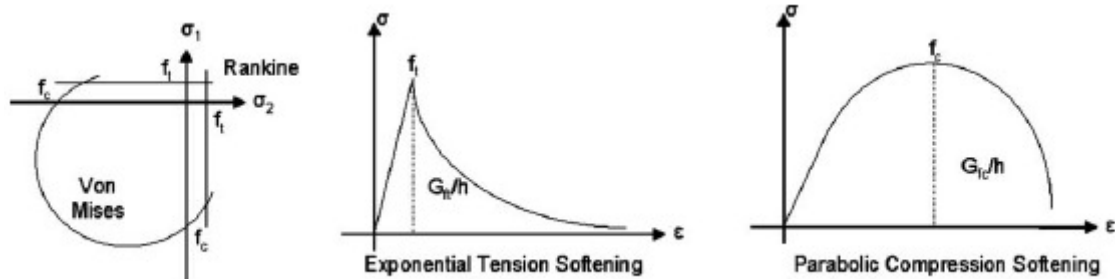


Figure 3.10. Assumed non-linear material models for units and mortar [56].

The response of the reference, as-built, panels was characterized by the development of early cracks through the diagonal mortar joints starting at the middle of the diagonal of the wall (example is shown in Figure 11(a)). The composite fibers led to a better redistribution of the stresses in the panel, and a more uniform and diffused crack pattern was achieved, instead of few localized cracks allowing for higher shear strength and deformations. The CMG system reduces the anisotropy of the as-built panels; the strengthened wall is then made of two components: the CMG system that ensures the required tensile strength and the masonry substrate providing the compressive strength. The load applied to the panel passed through the matrix and induced tension forces in the composite grid. Figure 11(b) shows multiple and spread cracking of the panel after the CMG system application, which confirms the better stress distribution and, consequently energy absorption, provided by the reinforcing grid. This means also that once the composite action is ensured between masonry and strengthening system, doubling the number of plies does not produce a proportional performance improvement, but smaller strength increases are expected to be achieved.

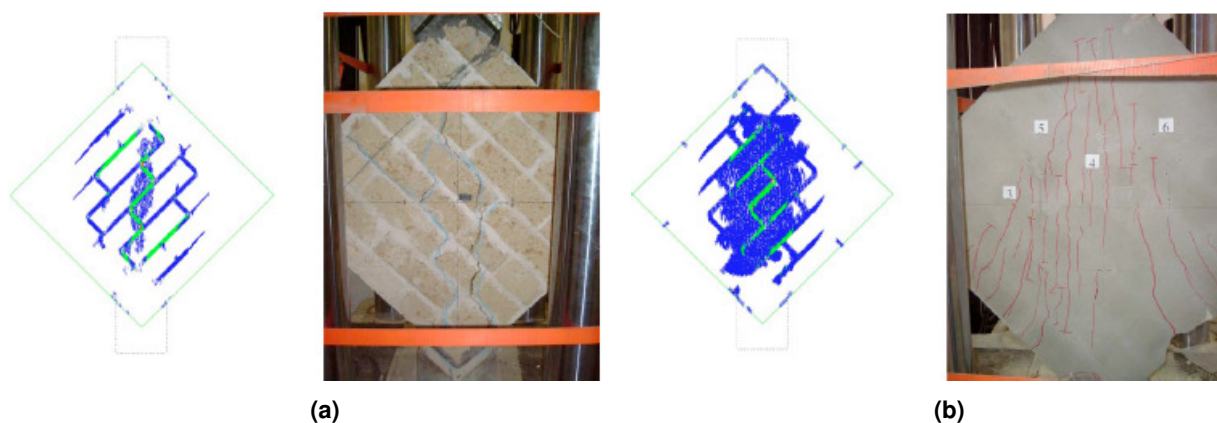


Figure 3.11. Comparison between numerical and experimental crack patterns for as-built panel (a) and strengthened panel (b) [56].

In (Gabor et al., 2007) [58] are presented different finite element modelling approaches for the analysis of the behaviour of unreinforced and FRP strengthened masonry walls when they are subjected to a predominant shear load. Three models have been analyzed, having different complexity levels, and used for the simulation of diagonal compression tests on masonry panels.

The models have different complexity levels:

- (a) Detailed modelling, which considers the real configuration of the masonry panels (constituted from bricks and mortar) and the composite reinforcement.
- (b) Simplified modelling, considering the experimentally measured global mechanical parameters of the masonry panels.
- (c) Simplified modelling, based on homogenization theory, where bricks and mortar are replaced by an equivalent continuum.

As illustrated in Figure 3.12, three types of FRP composites are employed: a unidirectional glass fiber, a unidirectional carbon fiber and a bidirectional glass fiber. The mechanical properties of the composites have been determined in tension on coupons. The composite coupons are manufactured in the same conditions as they are overlayed on the walls: embedding the composite fibers in the epoxy resin.

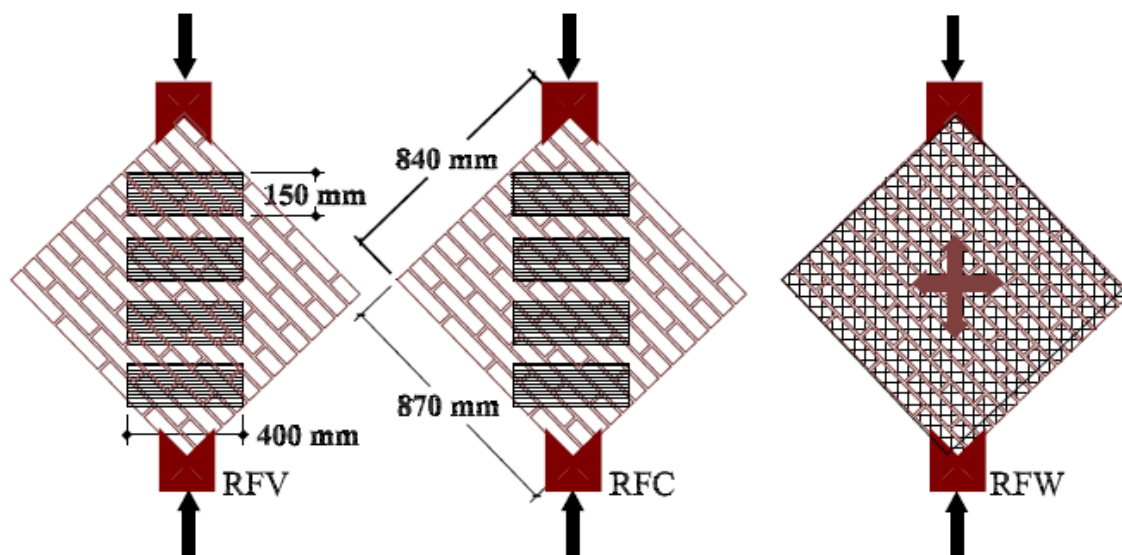


Figure 3.12. Different configuration of the strengthening system for masonry panels [58].

Firstly, the authors considered a detailed micro-modelling of the unreinforced masonry. This approach considers the detailed structure of the masonry: it is built as a regular inclusion of bricks into a matrix of mortar. The mortar is considered as a net which perfectly bonds to bricks. The geometrical configuration and the boundary conditions are identical to the real ones. The bricks are fully elastic and the mortar joint is characterized by an appropriate elasto-plastic model; thus, the non-linearity of the brick/mortar interface is transposed onto the behaviour of the mortar joint. A plane stress modelling is carried out using four node standard elements having two degrees of freedom per nodes, four

Gauss integration points and Lagrangian polynomials as shape functions. This model is found to give a relatively good prediction of the behaviour of the unreinforced masonry panel.

It is noted that the detailed modelling of the geometrical structure of the masonry requires important computational resources and renders the modelling quite laborious. Thus, if the goal of the modelling is to obtain an approximation of the average behaviour of the masonry in terms of loads and strains, it is conceivable to build an equivalent material model without considering the internal geometry of the masonry. In addition, in this case the model parameters are considered independent: the elastic modulus does not act on the global resistance as well as the shear strength does not modify the global stiffness of the masonry. In these conditions, an equivalent material having the global elastic properties of the masonry panel and the plastic parameters of the joint/brick interface can be considered.

Another approach followed by the authors is the modelling of panels using homogenized medium. Through the homogenization is possible to obtain the mechanical parameters of an equivalent material, based on the establishment of average stresses and strains on a representative volume element.

For the simulation of the behaviour of the reinforced masonry panels the detailed modelling, considering separately the bricks, the mortar and the composite reinforcement, have been only used. Even if the homogenized model for the unreinforced masonry gives a quite accurate response of the structure, it needs some improvements for taking into account the composite reinforcement. The elements used in the model allow membrane stiffness and tension-only option for the composite layers. The elements are standard tri-dimensional element having three degrees of freedom at each node. The behaviour law of the composite sheets is considered as elastic, and the real thicknesses of the composite reinforcements were considered. The model of the reinforced masonry panel is obtained by coupling the nodes of the elements of the masonry with those of composite strips. This corresponds to a perfect bonding between the masonry constituents and the composite strips.

Finally, the parametrical study carried out by the authors based on the finite element modelling underlined again the effectiveness of bi-directional composites applied on the entire surface, since the increase of the thickness of composite strips that are applied in strips does not induce a proportional increase of the strength or of the deformation capability.

4. MECHANICAL TESTS ON UNREINFORCED AND REINFORCED MORTAR SPECIMENS

In order to study the mechanical behaviour of the strengthening system employed to reinforce the masonry walls a test campaign on reinforced mortar specimen has been carried out at the ITAM Structural Laboratory. Four series of specimens have been prepared considering two different types of mortar: in particular, the for first group of specimens clay mortar with a low percentage of sand has been employed, while the second group has been realized with lime mortar with addition of Portland cement. For each type of mortar two series of specimens have been casted without net, while other two series of specimens have been prepared enclosing a polyethylene mesh as a reinforcement, also employed in the strengthening of masonry walls. Two identical wooden formworks have been prepared for casting of specimens, whose dimensions and arrangement have been studied in order to allow to obtain elements of different shape to be used for testing under tension, compression and shear forces.

In the present chapter, the details of the specimens preparation, of the type of mechanical tests carried out and the results obtained will be outlined. The tests carried can be used in order to verify the numerical model in order to asses the accuracy of the theoretical approach.

4.1 EXPERIMENTAL SPECIMENS PREPARATION

The mechanical tests on unreinforced mortar elements and on mortar elements reinforced with the polyethylene net have been carried out on specimens of different dimensions according to the type of test. In particular, the casting of the different elements has been done employing some wooden frames adequately designed in order to obtain the required specimens. The outline and the indication of dimensions of the frame are reported in Figure 4.1. Two wooden moulds with identical geometry have been prepared, since the experimental campaign includes two identical sets of specimens in terms of dimensions, casted using two different types of mortar. For the first set of specimens the mortar consisted in clay with a low percentage of sand, while for the second set a lime mortar with Portland cement was used. In particular, clay-sand mortar consists of natural clay (5 mm) with mixed-grain sand (0-2 mm), prepared with addition of 25% in volume of water; while lime-Portland cement mortar is composed by grain mixture between 0.0-1.2 mm. The water content is 7.7 litres per 40 kg of material, the bulk density of fresh mortar is 1.7 kg/dm^3 with a time of workability of 3 hours.

For both set the internal reinforcement is represented by a polyethylene TENCATE geo-net, also employed for the strengthening of masonry walls and showed in Figure 4.2. The same moulds have been also used to cast the unreinforced specimens. The linear temperature expansion coefficient of polyethylene is about $200 \cdot 10^{-6}$ m/mK, while for lime mortar and clay mortar is around $8 \cdot 10^{-6}$ m/mK and $9 \cdot 10^{-6}$ m/mK, respectively. For brick masonry this coefficient is about $5.5 \cdot 10^{-6}$ m/mK.

Each of the wooden frames prepared for the realization of the reinforced mortar samples have been designed in a way to obtain two specimens for tensile tests, which dimensions are 82 x 300 x 20 mm, two specimens for shear tests, which dimensions are 85 x 85 x 20 mm, and two groups of four elements which dimensions are 85 x 80 x 20 mm. These eight elements have been employed in order to construct two specimens in shape of a box to be used for compression tests.

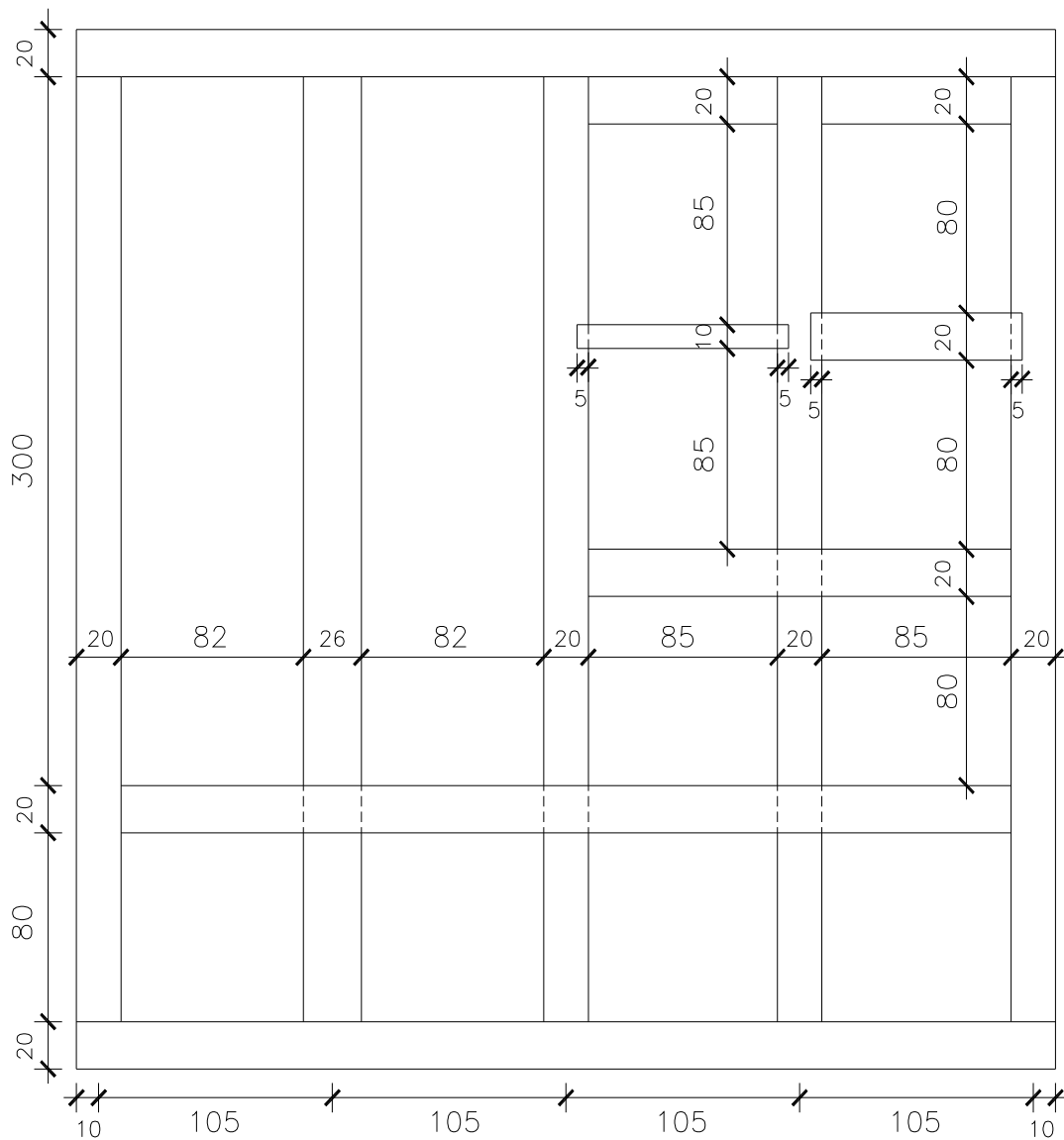


Figure 4.1. Outline of the wooden frame constructed for the casting of reinforced mortar specimens (dimensions in mm).

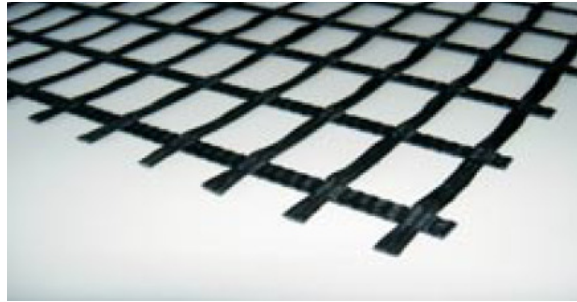


Figure 4.2. Geo-net employed for reinforced mortar specimens.

Prior to cast the specimens in the wooden moulds, all the reinforcement elements have been cut according to the dimensions of each elements. In particular, for the elements belonging to the two specimens to be constructed and tested under compression, both orientations of the grid have been considered. The outline of the grid elements and the orientation with which they have been placed in the moulds are illustrated in Figure 4.3.



Figure 4.3. Preparation of the reinforcing mesh and orientation in the mortar specimens.

After the preparation of the net, the two different types of mortar have been prepared and the specimens casted in the wooden moulds, placing the reinforcement in the middle plane of the samples' thickness, as showed in Figure 4.4. The final results for the two sets of specimens is reported in Figure 4.5, for both types of mortar, and with the representation of the position of the mesh on the surface.

After four days of curing the mortar elements have been removed from the moulds and placed in a climate chamber (Figure 4.6(a)) at constant values of temperature and humidity, set at 20°C and 65%, respectively (Figure 4.6(b)). The clay mortar specimens (Figure 4.7(a)) and the lime mortar specimens (Figure 4.7(b)) have been kept in the climate chamber for 28 days prior to be tested. The same procedure has been followed for the unreinforced mortar specimens.



Figure 4.4. Phases of preparation of the mortar samples and positioning of the net.

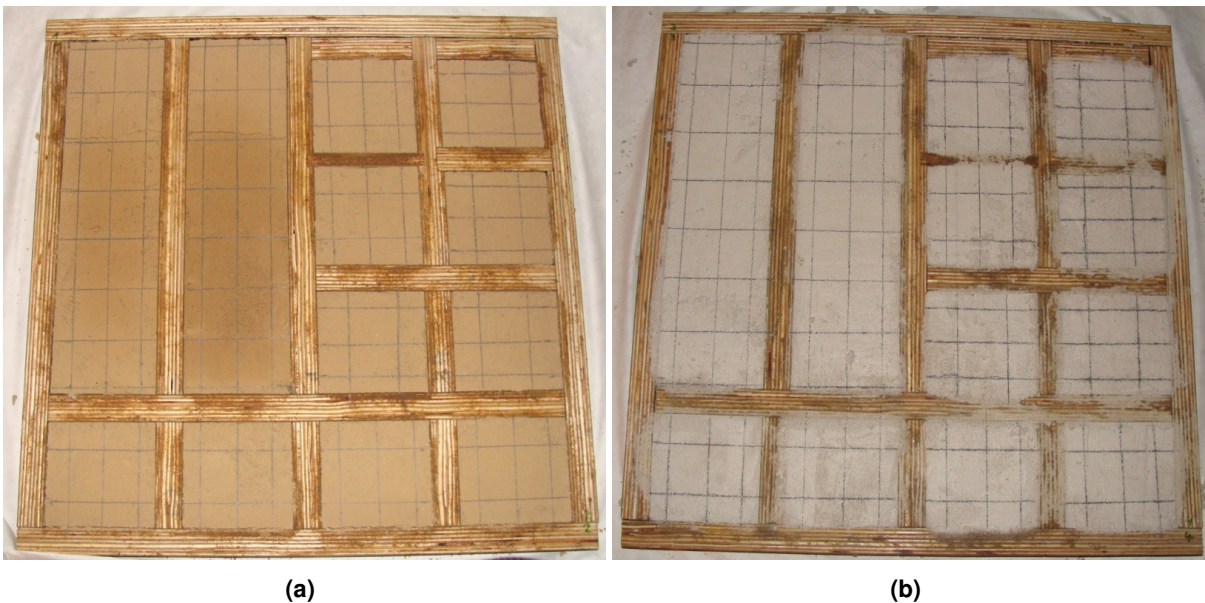


Figure 4.5. Specimens casted in the wooden moulds: clay mortar (a) and lime mortar (b).



(a)



(b)

Figure 4.6. Climate chamber (a) and thermo-hygrometric conditions (b).

(a)



(b)

Figure 4.7. Reinforced mortar specimens in the climate chamber: clay mortar (a) and lime mortar (b).

After waiting the 28 days for all the sets of mortar elements, the preparation of the specimens for testing has been done; in particular, the pieces for compression specimens, and for shear specimens have been glued in order to obtain the final specimens. In the following pictures, the obtained reinforced mortar specimens are shown: in particular in Figure 4.8 are illustrated the specimens for tensile tests for both clay-sand and lime-Portland cement mortars. It is noticed that, due to an imperfection occurred in the clay-sand mortar, namely a crack in the shorter direction, these two specimens have been cut resulting in a length of 200 mm. In Figure 4.9, the specimens for shear tests

have been reported; in particular, two mortar elements have been glued together in order to allow to test the specimen under three points bending test, inducing shear stresses in the two halves of the specimen. Finally, in Figure 4.10 the specimens for compression tests are also shown; four mortar elements have been glued together in order to form a sort of box to be tested under compression. As already said, both orientations of the grid have been considered. The same set of specimens has been realized for the unreinforced elements also, for both type of mortar.

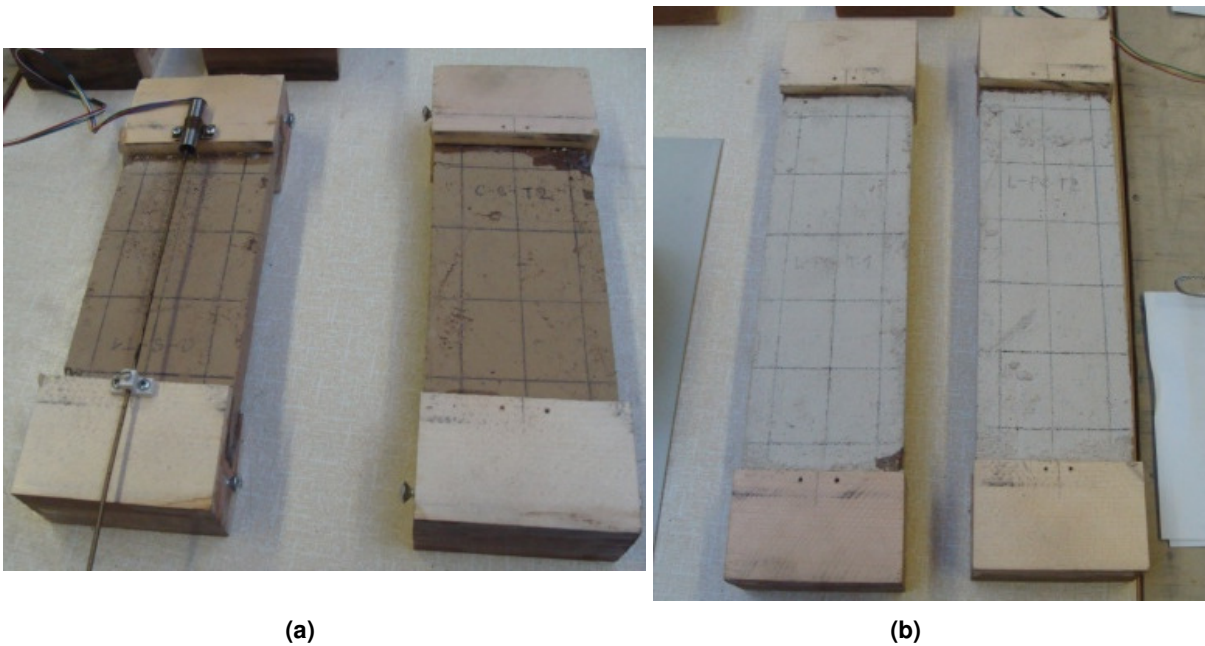


Figure 4.8. Reinforced mortar specimens for tensile tests: clay mortar (a) and lime mortar (b).

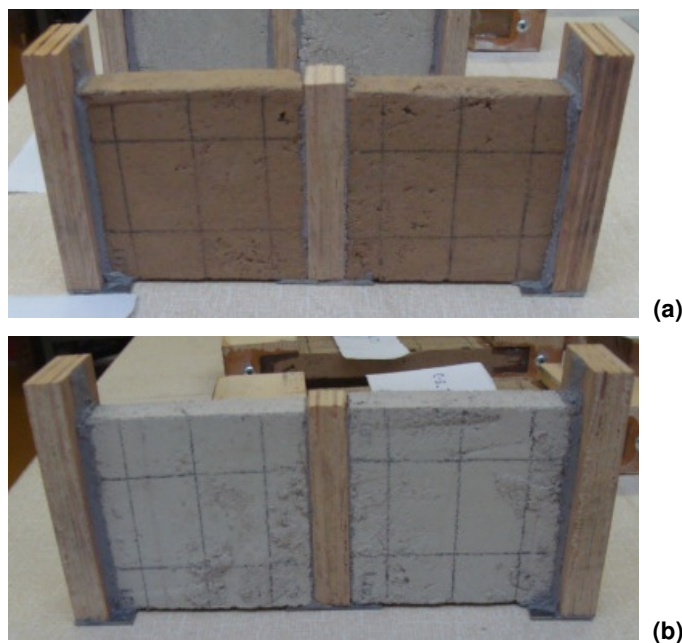


Figure 4.9. Reinforced mortar specimens for three-points bending tests: clay mortar (a) and lime mortar (b).

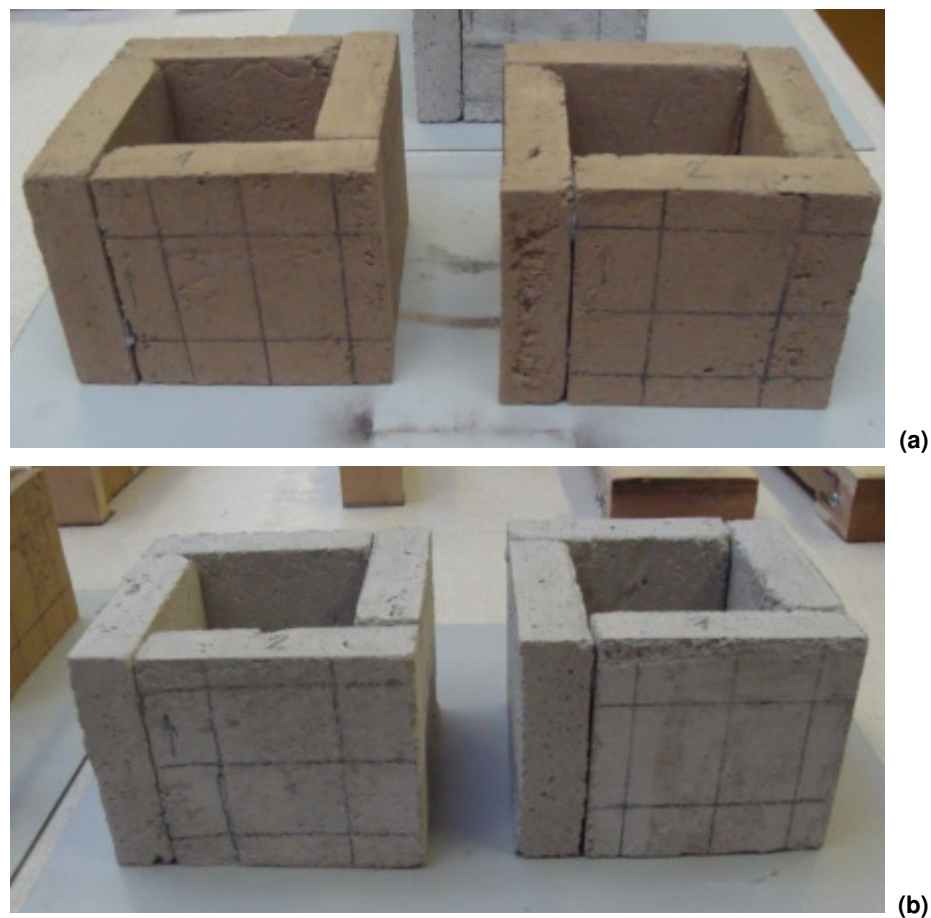


Figure 4.10. Reinforced mortar specimens for compression tests: clay mortar (a) and lime mortar (b).

4.2 TENSILE TESTS

In the following section the results obtained from the tensile tests on unreinforced and reinforced mortar specimens are reported.

In the graphs of Figure 4.11 the force – displacement curves for the unreinforced and reinforced mortar specimens have been collected; in particular, Figure 4.11(a) refers to the clay-sand mortar specimens, while Figure 4.11(b) to the lime-Portland cement mortar specimens. The Table 4.1 summarizes the results from the tensile tests on unreinforced and reinforced specimens. Moreover, in the pictures of Figure 4.12 two of the tested reinforced mortar specimens for both types of mortar are illustrated. As it can be seen from the pictures, the failure occurred upon the formation of a crack in the direction normal to the tensile load.

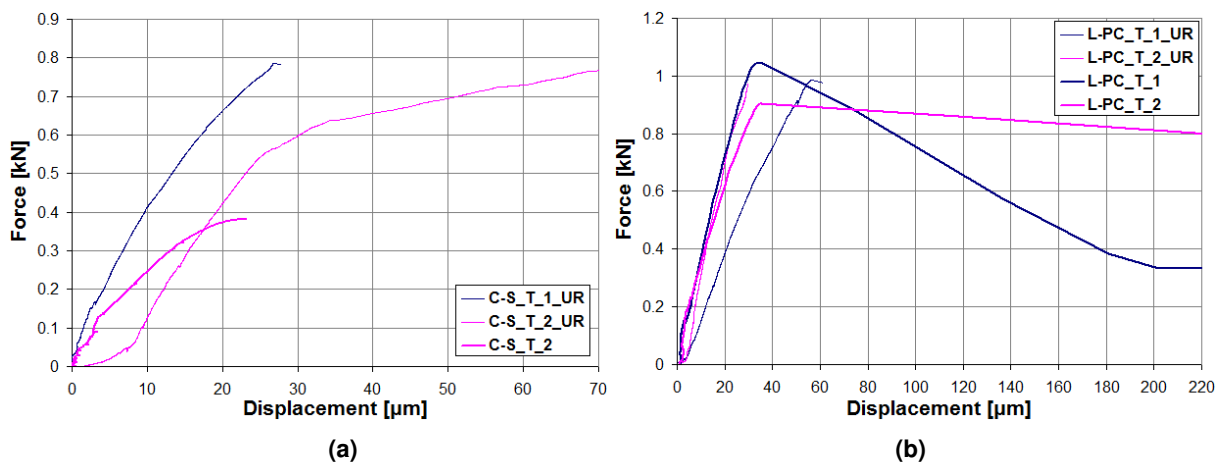


Figure 4.11. Force – displacement curves for unreinforced and reinforced mortar specimens under tensile load: clay mortar (a) and lime mortar (b).

Tensile Tests							
Specimen Name	Fmax [N]	Width [mm]	Thickness [mm]	Length [mm]	σ_t [MPa]	Mortar Type	Reinforcement
C-S T 1	–	80.4	19.78	144	–	clay-sand	YES
C-S T 2	382	81.2	19.94	150	0.24	clay-sand	YES
L-PC T 1	1045	81.63	20.12	241	0.64	lime-portland	YES
L-PC T 2	904	81.8	20.68	242	0.53	lime-portland	YES
C-S_T_1_UR	785	81.33	21.57	243	0.45	clay-sand	NO
C-S_T_2_UR	767	83.87	21.79	241	0.42	clay-sand	NO
L-PC_T_1_UR	987	81.3	21.6	244	0.56	lime-portland	NO
L-PC_T_2_UR	972	81.83	21.9	244	0.54	lime-portland	NO

Table 4.1. Results of tensile tests on mortar specimens.



Figure 4.12. Tested reinforced mortar specimens under tensile load: clay mortar specimen (a) and detail of crack in lime mortar specimen (b).

4.3 COMPRESSION TESTS

Compression tests have been also carried out on unreinforced and reinforced specimens, made by two different types of mortar.

In the graphs of Figure 4.13 the force – displacement curves for the unreinforced and reinforced mortar specimens have been collected; in particular, Figure 4.13(a) refers to the clay-sand mortar specimens, while Figure 4.13(b) to the lime-Portland cement mortar specimens. The Table 4.2 summarizes the results from the compression tests on unreinforced and reinforced specimens. Moreover, in the pictures of Figure 4.14 two of the tested reinforced mortar specimens for both types of mortar are illustrated. It is reminded that, for each type of mortar, both orientations of the reinforcing grid have been considered.

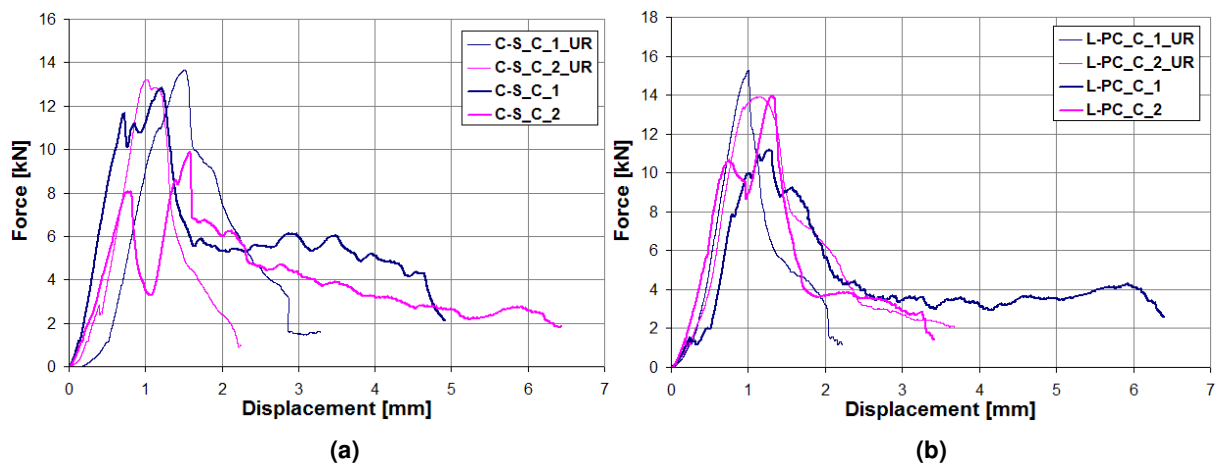


Figure 4.13. Force – displacement curves for unreinforced and reinforced mortar specimens under compression load: clay mortar (a) and lime mortar (b).



Figure 4.14. Tested reinforced mortar specimens under compression load: clay mortar (a) and lime mortar (b) specimens.

Compression Tests											
Specimen Name	F _{max} [N]	a ₁ [mm]	a ₂ [mm]	thickness ₁ [mm]	b ₁ [mm]	b ₂ [mm]	thickness ₂ [mm]	height [mm]	σ _c [MPa]	Mortar Type	Reinforcement
C-S_C_1	12830	104.3	63.06	41.24	104.4	64.7	39.7	79.55	1.88	clay-sand	YES
C-S_C_2	9895	104.2	64.4	39.8	103.8	64.6	39.2	78.6	1.49	clay-sand	YES
L-PC_C_1	11203	105.4	61.75	43.65	105.5	63.65	41.85	80.7	1.56	lime-portland	YES
L-PC_C_2	13950	106.6	64.8	41.8	105.7	64	41.7	79.5	1.96	lime-portland	YES
C-S_C_1_UR	13645	105.8	63.9	41.9	107.3	64.5	42.8	77.65	1.89	clay-sand	NO
C-S_C_2_UR	13213	106.2	64.55	41.65	104.9	61.1	43.8	77.9	1.84	clay-sand	NO
L-PC_C_1_UR	15256	106.8	62.1	44.7	107.8	63.25	44.55	77.2	2.01	lime-portland	NO
L-PC_C_2_UR	13925	106.6	62.5	44.1	106.7	61.25	45.45	77.6	1.85	lime-portland	NO

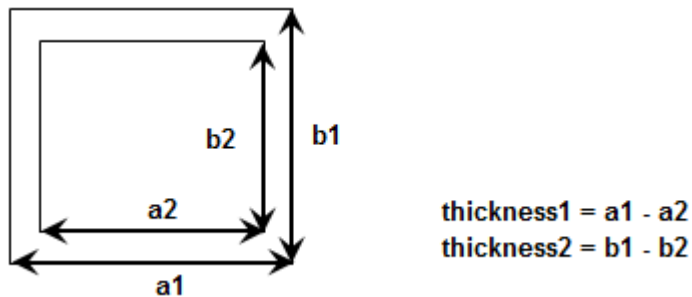


Table 4.2. Results of compression tests on mortar specimens.

4.4 SHEAR TESTS

Shear tests have been also carried out in order to induce shear stresses in specimens. In the following section the results obtained from tests on unreinforced and reinforced mortar specimens are reported. In the graphs of Figure 4.15 the force – deflection curves for the unreinforced and reinforced mortar specimens have been collected; in particular, Figure 4.15(a) refers to the clay-sand mortar specimens, while Figure 4.15(b) to the lime-Portland cement mortar specimens. The Table 4.3 summarizes the results from the tensile tests on unreinforced and reinforced specimens. Moreover, in the pictures of Figure 4.16 two of the tested reinforced mortar specimens for both types of mortar are illustrated. As it can be seen from the pictures, the failure occurred upon the formation of a crack in the direction normal to the tensile load.

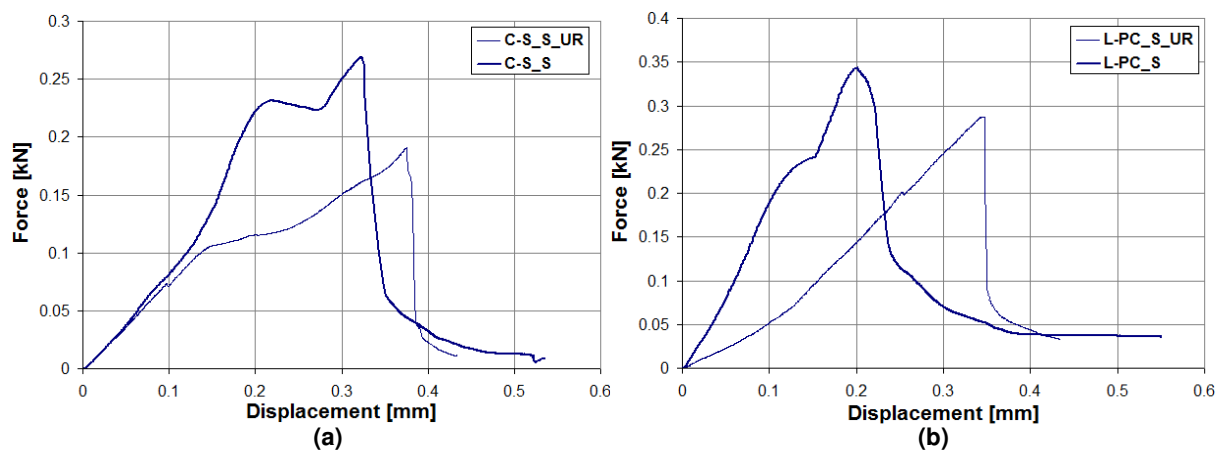


Figure 4.15. Force – deflection curves for unreinforced and reinforced mortar specimens under shear load: clay mortar (a) and lime mortar (b).

Shear Tests								
Specimen Name	Fmax [N]	Width [mm]	Thickness [mm]	Length [mm]	Supports [mm]	τ [MPa]	Mortar Type	Reinforcement
C-S_S	269	82	20.03	185	200	0.082	clay-sand	YES
L-PC_S	344	84.7	19.76	186	200	0.103	lime-portland	YES
C-S_S_UR	190.9	83.5	20.7	184	200	0.055	clay-sand	NO
L-PC_S_UR	287.4	82.8	20.82	187	200	0.083	lime-portland	NO

Table 4.3. Results of shear tests on mortar specimens.

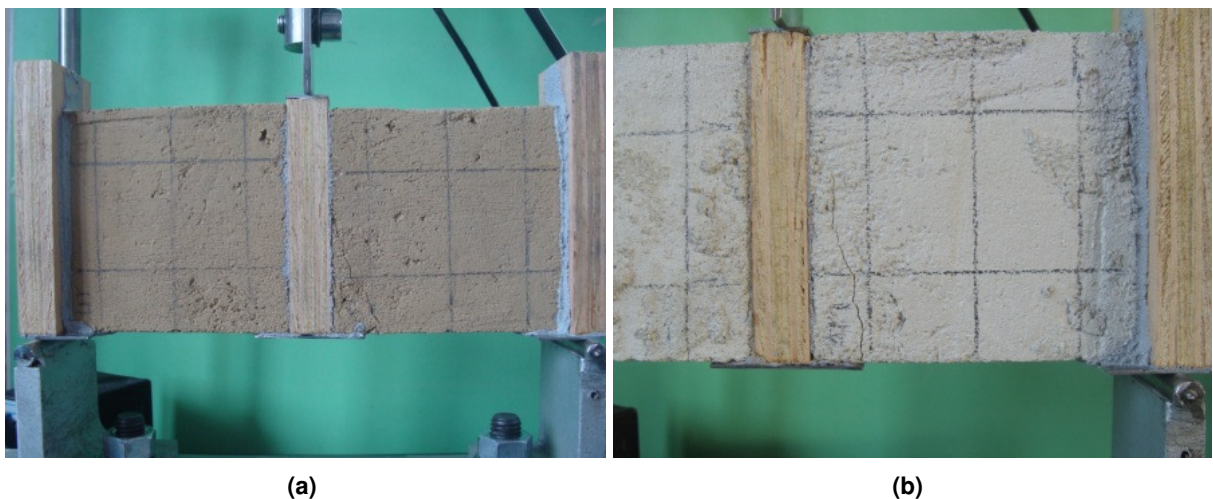


Figure 4.16. Tested reinforced mortar specimens under shear load: clay mortar specimen (a) and detail of crack in lime mortar specimen (b).

4.5 SUMMARY OF RESULTS

In the following table a summary of all the results obtained from the mechanical characterization tests is reported:

Tensile Tests			
Specimen Name	σ_t [MPa]	Mortar Type	Reinforcement
C-S_T_1	–	clay-sand	YES
C-S_T_2	0.24	clay-sand	YES
L-PC_T_1	0.64	lime-portland	YES
L-PC_T_2	0.53	lime-portland	YES
C-S_T_1_UR	0.45	clay-sand	NO
C-S_T_2_UR	0.42	clay-sand	NO
L-PC_T_1_UR	0.56	lime-portland	NO
L-PC_T_2_UR	0.54	lime-portland	NO
Compression Tests			
Specimen Name	σ_c [MPa]	Mortar Type	Reinforcement
C-S_C_1	1.88	clay-sand	YES
C-S_C_2	1.49	clay-sand	YES
L-PC_C_1	1.56	lime-portland	YES
L-PC_C_2	1.96	lime-portland	YES
C-S_C_1_UR	1.89	clay-sand	NO
C-S_C_2_UR	1.84	clay-sand	NO
L-PC_C_1_UR	2.01	lime-portland	NO
L-PC_C_2_UR	1.85	lime-portland	NO
Specimen Name	τ [MPa]	Mortar Type	Reinforcement
C-S_S	0.082	clay-sand	YES
L-PC_S	0.103	lime-portland	YES
C-S_S_UR	0.055	clay-sand	NO
L-PC_S_UR	0.083	lime-portland	NO

Table 4.4. Results of mechanical tests on unreinforced and reinforced mortar specimens.

5. EXPERIMENTAL TESTS ON REINFORCED MASONRY WALLS

In the present chapter the experimental tests on masonry walls carried out in the ITAM Structural Laboratory will be described. In particular, the description of the specimens, in terms of geometry and employed materials, the strengthening systems and the test set-up will be outlined. Finally the results obtained from the test campaign will be presented and some comparisons and evaluations will be performed between the different cases. The tests carried out can be successively used in order to verify the numerical model described in the following chapter in order to assess the accuracy of the theoretical approach.

The laboratory tests consist of in-plane shear tests on masonry walls strengthened with different techniques and subjected to a combination of compression and cyclic shear loading. A total of five specimens was tested, in which the masonry was made with bricks of different materials. In particular, adobe bricks, burned clay bricks and unburned clay bricks were used according to the same arrangement. For the reinforcing systems, in one case it is realized using steel rods mechanically fastened to the wall and disposed according to an X shape, and in all the other cases it is represented by a mortar layer externally applied to the wall surface and reinforced with a Fiber Reinforced Polymer (FRP) grid. For all the specimens the configuration of the reinforcement was done in a symmetric fashion, namely on both surfaces of the masonry wall.

The experimental campaign presented in this work represents a continuation of previous researches carried out by (Drdácký and Lesák, 2009) [54] on brick walls strengthened by fibre reinforced plastics strips with an epoxy resin matrix. The experimental evidences in that case led to the conclusion that even though the strips increased the load carrying capacity of brick walls and might be effectively used for repair of damaged walls after earthquake, the method is very costly, labour consuming and utilising material of a very high quality non-comparable to the co-operating bricks. Other important issues are also related to the possible fire protection of the reinforcement system, that is questionable and lowering practical applications in interior of buildings. The experimentation is thus continued in order to investigate brick walls strengthened with plastic nets of rectangular grids. The effectiveness of nets was tested also on brick walls severely damaged during the previous cyclic tests. New as well as damaged walls were strengthened with geo-nets.

5.1 EXPERIMENTAL SPECIMENS

In the ITAM Laboratory for Experimental Mechanics, 5 test specimens have been prepared for the experimental campaign presented in this thesis. The overall dimensions of the walls are 250 mm in thickness, 1140 mm in width and 1500 mm in height. The specimens have been walled up on steel-supported channels with fixtures that enabled the specimens to be lifted by a crane and positioned into the testing rig. Three types of bricks have been used to wall up the masonry panels: adobe bricks, burned clay bricks and unburned clay bricks were used according to the same arrangement. The dimensions of the fundamental element employed to construct the panels are reported in Figure 5.1.

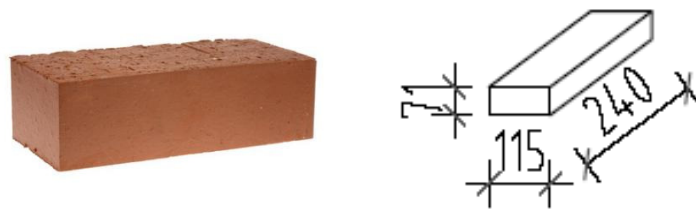


Figure 5.1. Dimensions of the fundamental element used in the masonry specimens.

A SAK-RET mortar was used, which belongs to HM group II of mortars, according DIN 1053. It has a minimum nominal compressive strength of 5 N/mm^2 and a minimum adhesion and shear strength of 0.2 N/mm^2 . The material characteristics of the mortar were checked on standard specimens made during production of the testing walls.

In Figure 5.2(a) the overall arrangement of the walls is presented, while in Figure 5.2(b) the position of the reinforcement net is illustrated.

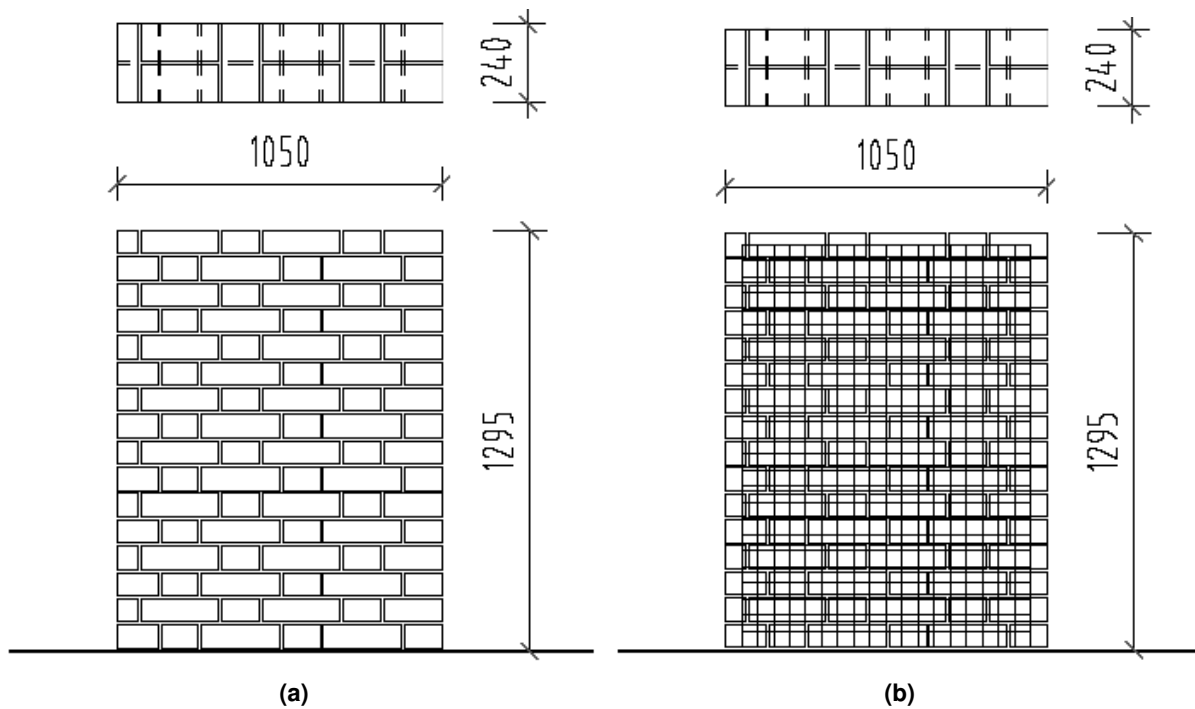


Figure 5.2. Overall dimensions of the masonry specimens and bricks arrangement (a) and position of the reinforcement grid (b).

In a previous experimental campaign, test specimens without reinforcement were prepared, and they were tested to failure, when pronounced cracks occurred. At the beginning, the deformation characteristics of the plain masonry were measured (compressive deformation modulus). In Figure 5.3 the control panels of plane masonry are illustrated for the three types of masonry considered in this study.

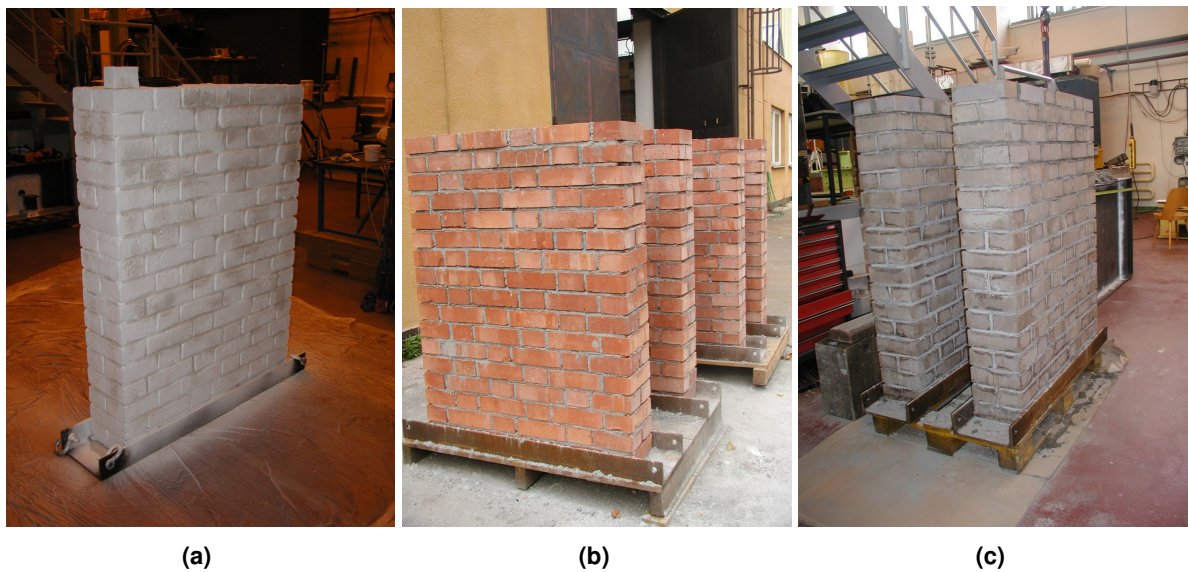


Figure 5.3. Unreinforced masonry walls: (a) adobe, (b) burned clay bricks, (c) unburned clay bricks.

For the reinforced specimens a polyethylene TENCATE geo-net externally applied onto the wall surfaces has been used (Figure 5.4).

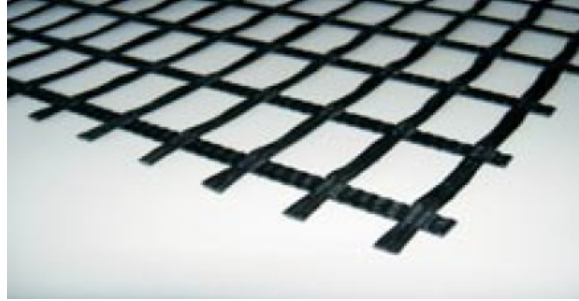
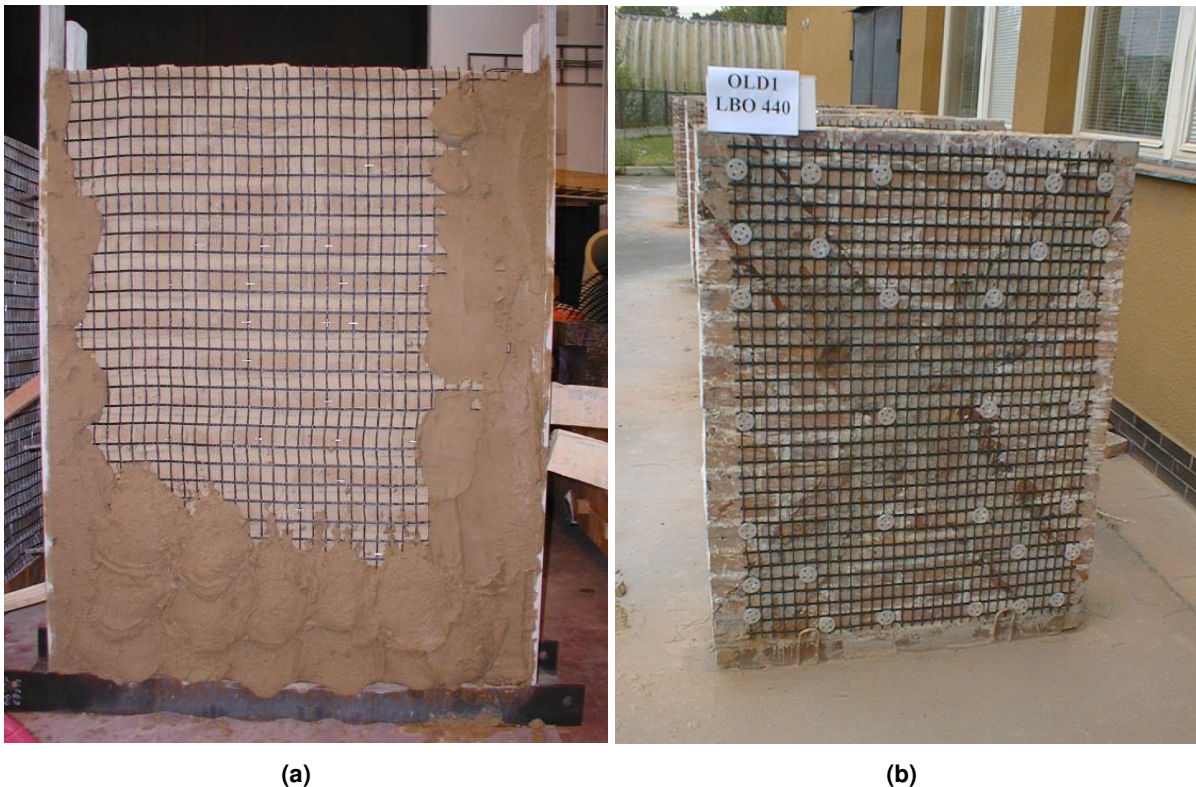


Figure 5.4. Geo-net employed for strengthening of masonry walls.

After they have been mechanically fastened, the walls were rendered with about 2 cm thick plaster made with lime mortar containing a small percentage of Portland cement. In Figure 5.5(a) is showed one of the masonry walls onto which the reinforcement net was applied. For the experimental program is also prepared a specimen severely damaged in a previous test, which has been repaired using the same system of geo-nets, after removing the remains of the composite strips previously applied, and tested again (Figure 5.5(b)). The cracks have been only plastered with a thin cement mortar in order to smooth the surface for fixation of geo-nets.



(a)

(b)

Figure 5.5. Testing walls strengthened with polymer nets: (a) a new undamaged wall; (b) wall after previous damage [54].

Finally, in the experimental campaign described in this thesis one of the specimens tested consisted of an adobe brick wall reinforced by means of a different system. The reinforcing elements used in this case are represented by steel wire ropes placed diagonally and in two direction on the wall surfaces. In Figure 5.6(a) the overall arrangement of the reinforced is shown. The wire ropes are installed in three grooves per direction previously produced on the surface of the wall and adequately anchored at their extremities by means of mechanics fasteners. A detail of the anchoring system is illustrated in Figure 5.6(b).

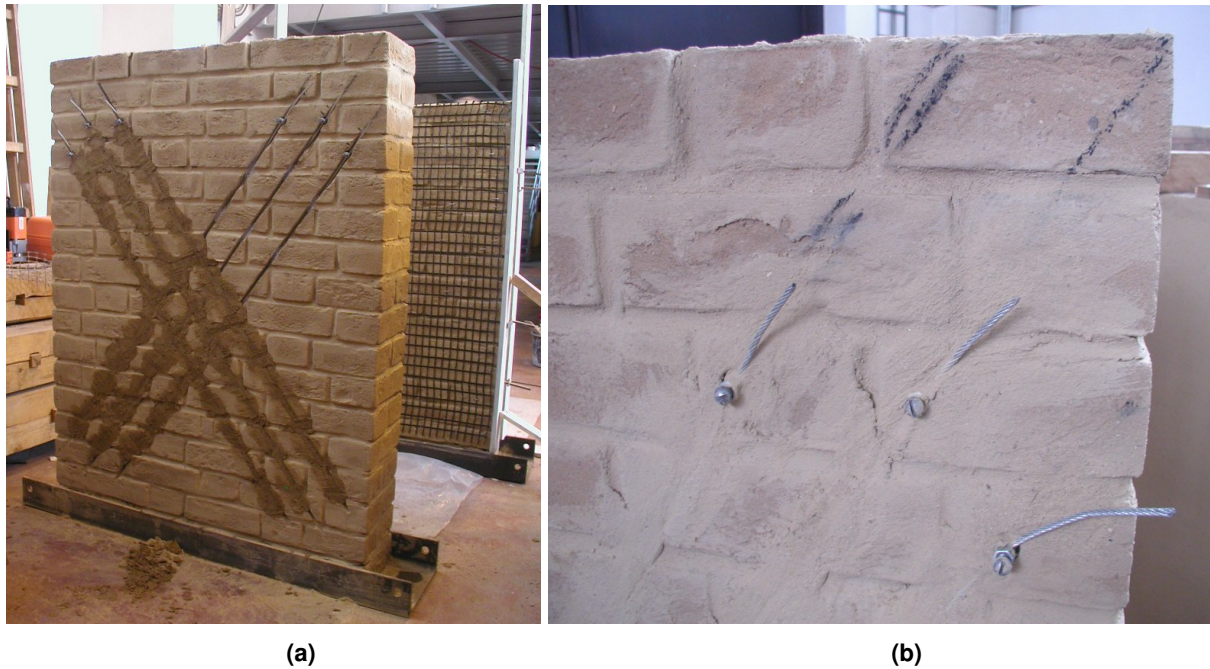


Figure 5.6. Adobe brick wall reinforced by means of X-shaped wire ropes (a) and detail of the anchoring system for wire ropes (b).

5.2 EXPERIMENTAL EQUIPMENT AND TEST SET-UP

The test specimens were mounted into a special testing rig that enabled simultaneous uniform compression and cyclic horizontal loading on the top of the tested specimen. The outline of the experimental equipment is illustrated in Figure 5.7, while in Figure 5.8 the scheme of the specimen placed in the testing system is shown.

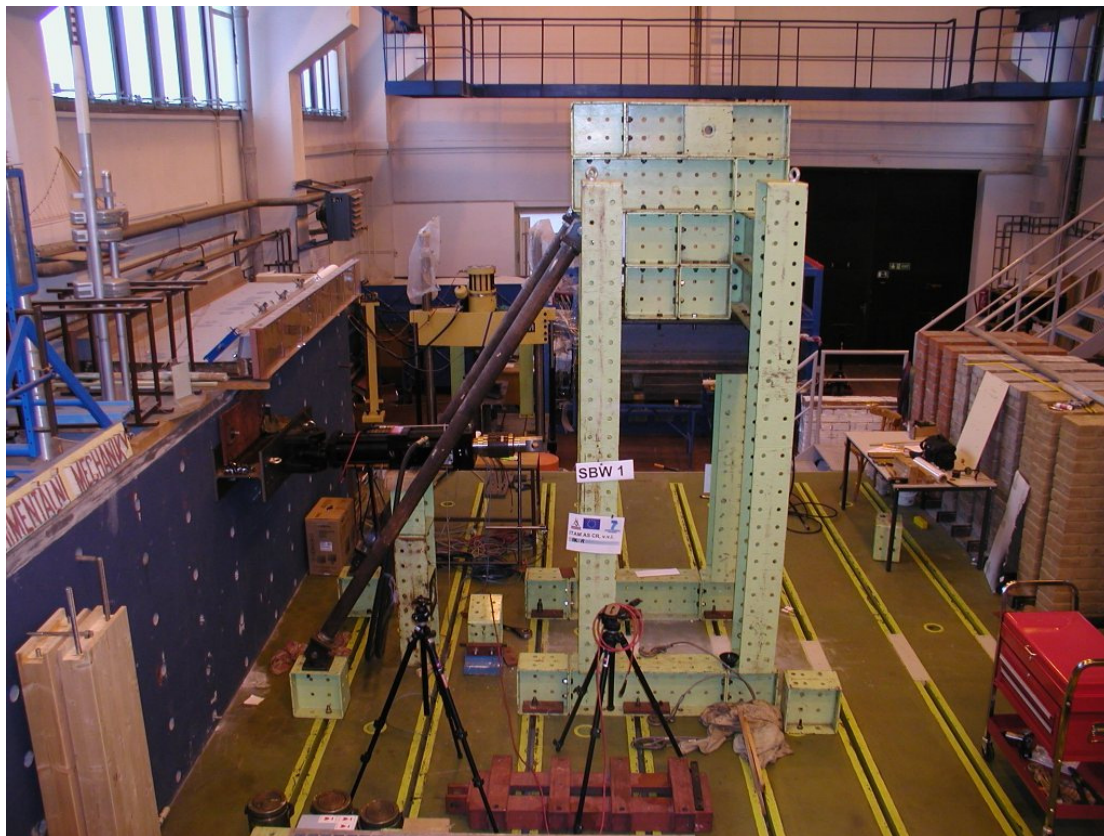


Figure 5.7. Testing rig and reaction wall for testing.

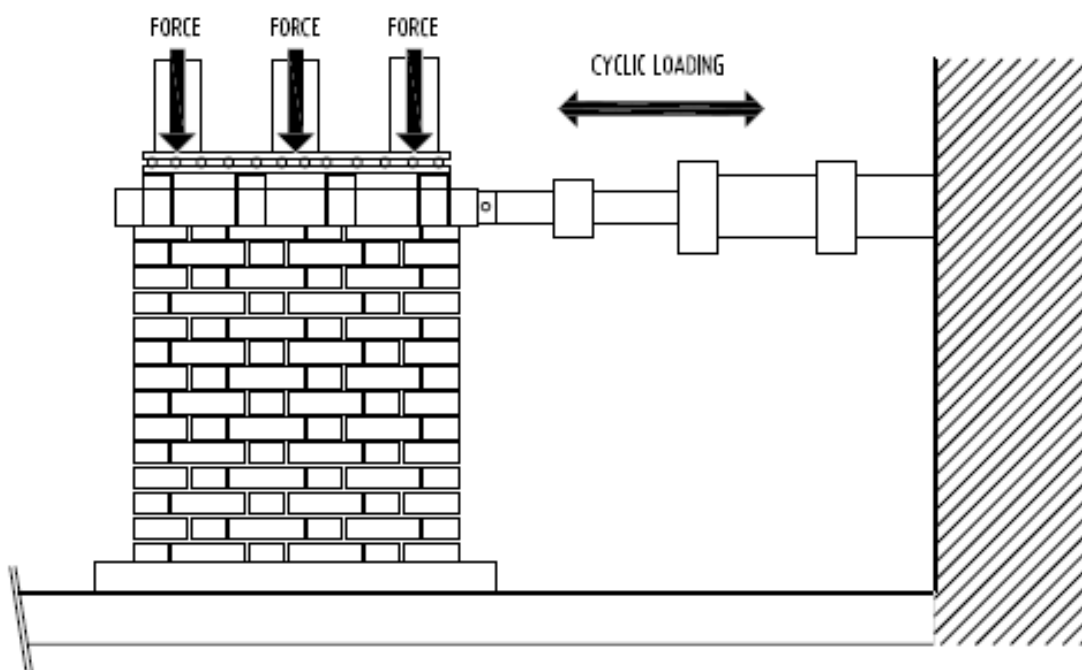


Figure 5.8. Scheme of the testing system.

Four hydraulic jacks (Figure 5.9) generated the vertical load, which was transmitted to the wall by eight ties and a steel 'hat' on the top of the wall. A horizontal displacement (force) on the top of the wall was introduced using a servo-hydraulic MTS actuator of 250 kN capacity, shown in Figure 5.10.



Figure 5.9. Hydraulic jacks system for generating vertical compression pre-stress.

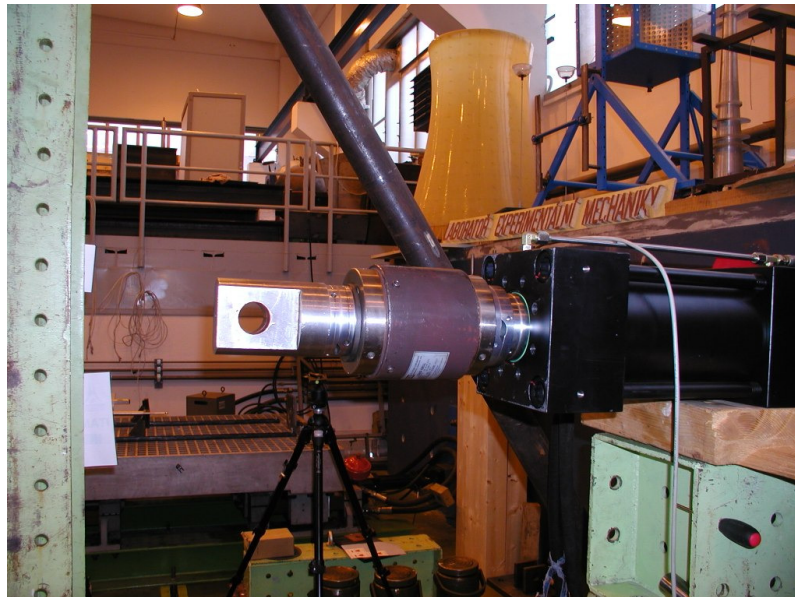


Figure 5.10. Servo-hydraulic actuator for horizontal loads.

During the first loading combination, with static vertical loading only, the deformation characteristics of the masonry wall were obtained. The horizontal displacement on the top of the wall and the deformations perpendicular to the shear diagonals of the panels were measured during combined loading. The position of one set of transducers is shown in Figure 5.11.

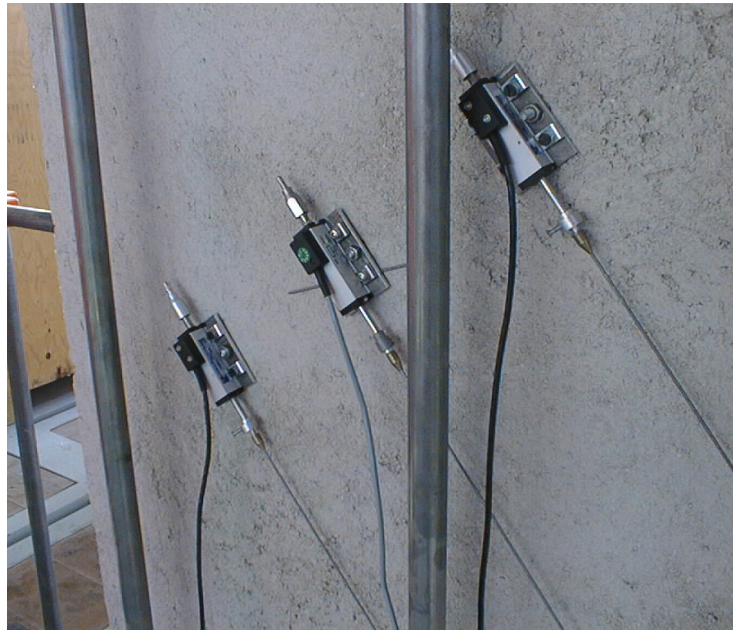


Figure 5.11. Diagonal deformation measurements.

In the experimental campaign carried out in this thesis the following loading condition has been considered. First, the above-mentioned compressive loading only was applied, and was increased continually up to a value of 80 kN, evenly distributed across the cross-section. Then, the vertical compressive pre-stress was combined with cyclic horizontal loading mode with a stepwise increase in the maximum cycling limits.

The application of the horizontal load follows the sinusoidal pattern illustrated in Figure 5.12. In particular, for each step of loading defined by a maximum value of the amplitude of the displacement imposed by the actuator, three cycles were performed. For each step of loading, the frequency of application of the horizontal force is kept constant and equal to 0.1 Hz.

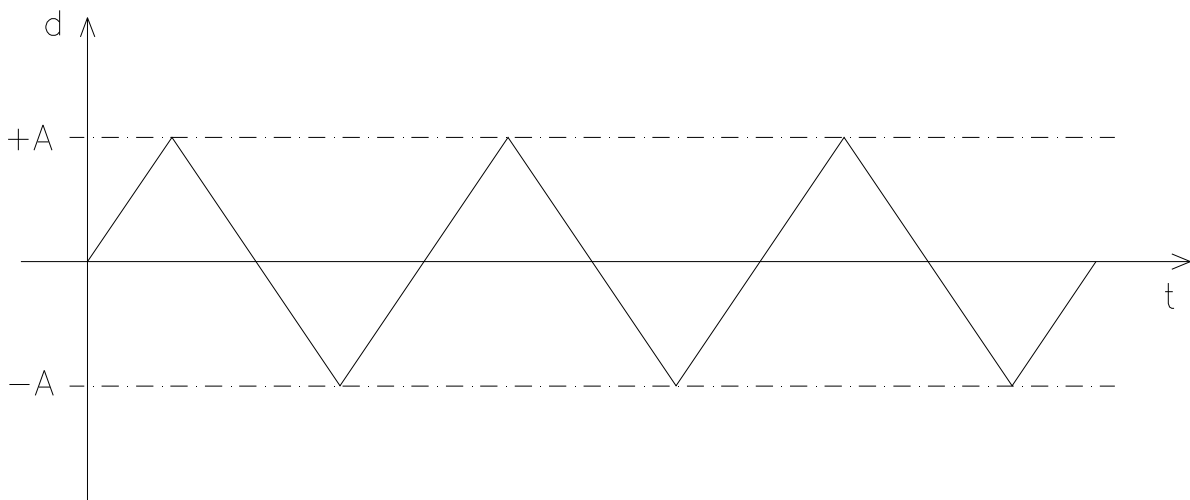


Figure 5.12. Loading pattern for each step of application of the horizontal force.

During the test the forces on the vertical hydraulic jacks as well as on the horizontal actuator were recorded. Further, horizontal displacements at the bottom and top of the wall and diagonal deformations of four lines on both surfaces were measured. The sequence of initiation and development of cracks on both surfaces were recorded in all loading steps using different colours and by photography. Loading was terminated in a moment when the force started to decrease at the controlled deformation.

5.3 EXPERIMENTAL RESULTS

5.3.1 Adobe brick walls

The results presented in the following section are related to the tests carried out on walls made by adobe bricks. Three types of tests are considered, namely the ones related to the unreinforced wall used as control specimen, to the specimen reinforced with geo-nets and mortar layers onto the wall surfaces and to the specimen reinforced with X-shaped wire ropes.

Typical failure cracking of a plain masonry wall loaded by combined uniformly distributed vertical static stress and a horizontal cyclic load is shown in Figure 5.13.

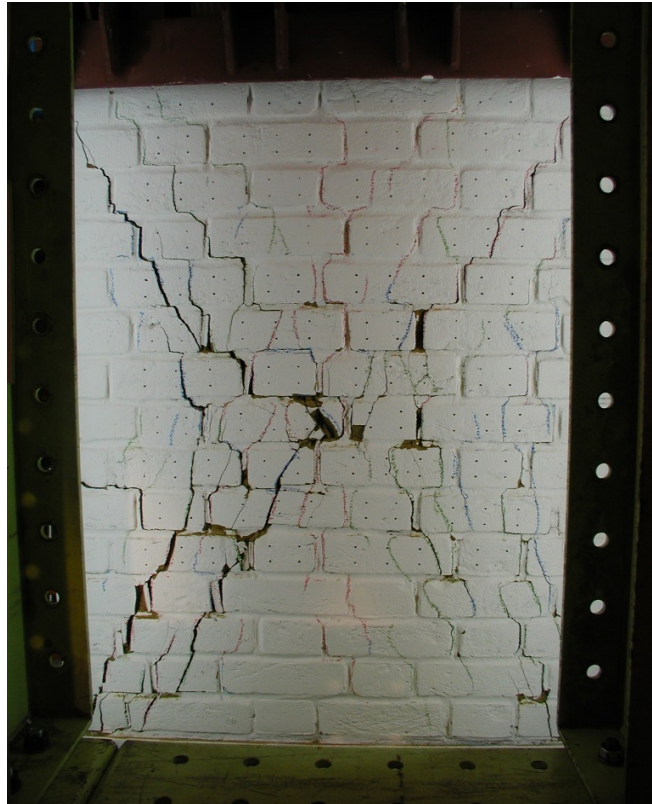


Figure 5.13. Crack pattern at failure of the plain masonry control wall under a combination of vertical compression and cyclic shear.

Figure 5.14 presents the crack pattern at failure registered for the wall strengthened with reinforced mortar layers. It is, thus, evidenced the typical behaviour of walls strengthened by means of this technique. It is noticed that the cracks visible on the surface represent a combination of two sets of damages: masonry cracks, and cracks which occur in the plaster only and originate from the differential movement of the FRP mesh.

It is observed that compared to the typical crack pattern usually found in plane masonry walls, the case of the wall strengthened with reinforced mortar layer present a more widespread and diffused crack pattern. In fact, when unreinforced masonry wall is subjected to a combination of vertical pre-stress and horizontal cyclic load cracks are localized in the two diagonal lines of the walls evidencing the typical X-shaped pattern. The application of the reinforced mortar layers reinforced with a FRP grid to the surfaces of the wall has also the effect to redistribute the stresses originated upon loading along the two diagonal lines of the wall and, thus, to spread the pattern over a wider area of the wall surface.

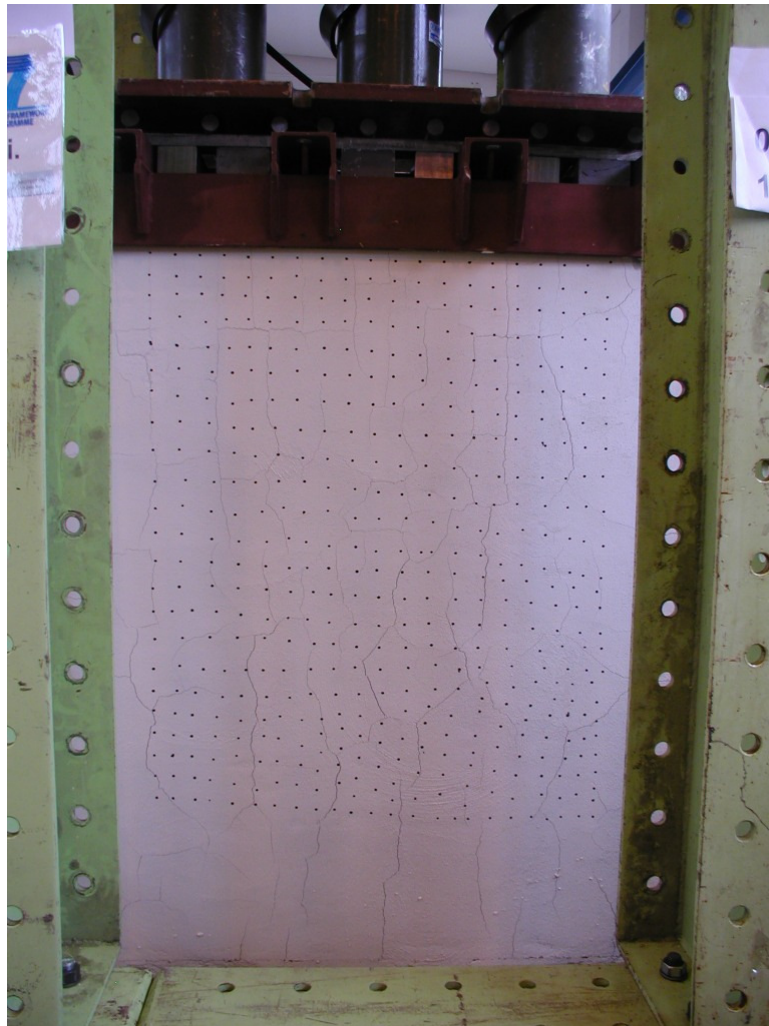


Figure 5.14. Crack pattern at failure of the adobe wall strengthened with reinforced mortar layers under a combination of vertical compression and cyclic shear.

An important aspect to be taken into account in the evaluation of the effectiveness of this kind of reinforcement is the interface behaviour between the external reinforcement and the masonry substrate to which it is applied represented by the wall. Since the reinforced mortar layer applied on the wall surfaces is slightly thin ($1.5 \div 2.0$ cm), and due to the different stiffness compared to the substrate, it can be subjected to out-of-plane forces that may cause its detachment. The experimental evidence of the detachment of this layer is much more evident when the difference in stiffness is larger. This happens particularly in the cases of application to this kind of reinforcement to clay bricks walls, while in case of adobe walls it is not so evident since the plaster has been made of the same material of the bricks. In Figure 5.15 it is shown a detail of the detachment of the plaster from the surface of the masonry wall; in this case, the polymeric grid is still anchored to the substrate and the detachment involved only the thin layer of plaster.



Figure 5.15. Evidence of the detachment of the plaster from the wall surface.

The adobe brick wall reinforced by means of steel wire ropes has been also tested. In Figure 5.16 the crack pattern upon failure of the specimen is shown. In case this kind of reinforcement is

adopted an important improvement in terms of resistance can be attained. The wall strengthened by means of this technique behaves in a quite compact manner since the wire ropes play a very effective role in sewing up the cracks and keeping the masonry blocks together. Some cracks can appear along the mortar joints in the surroundings of the reinforcement and, in general, there is a good redistribution of the stresses and a more widespread crack pattern compared to the unreinforced wall. The failure of the wall feature the formation of large damage in the wall at the level of the toe over the anchorage of the ropes, in the area where the reinforcement is not present. In Figure 5.17 it is shown the damage at the toe of the wall, with the formation of a plastic hinge at the base.



Figure 5.16. Crack pattern at failure of the adobe wall strengthened with wire ropes under a combination of vertical compression and cyclic shear.



Figure 5.17. Details of the large damage at the wall base.

Another important aspect brought to light by the experiments is related to the damage due to the possible out-of-plane of the reinforcement. In particular, the wire ropes are placed quite superficially in grooves made on the wall faces and just plastered with mortar. Since during the application of cyclic horizontal loading, or during the shake imposed by a seismic event, both direction of reinforcement can be subjected alternatively to compression, causing the tendency to the ropes to go out of the grooves, hitting the small filling of mortar. However, since the reinforcement is made by steel wire, during tension phase they can easily be able to continue to be effective, involving only superficial damage of the wall, as shown in Figure 5.18.



Figure 5.18. Detail of the damage due to the out-of-plane of the wire ropes reinforcement.

In the following the results of the three tests presented in this section are reported in terms of cyclic curves horizontal force versus displacement of the wall top. In particular in the graphs of Figure 5.19, 5.20 and 5.21, the cyclic curves for each step of loading are presented for the unreinforced wall, for the wall reinforced with grid and for the wall reinforced with wire ropes, respectively. The tests have been carried out considering fixed the frequency of the sinusoidal load and equal to 0.1 Hz, and incrementing the maximum displacement imposed in the actuator, starting from 2.5 mm and with increment of 2.5 mm.

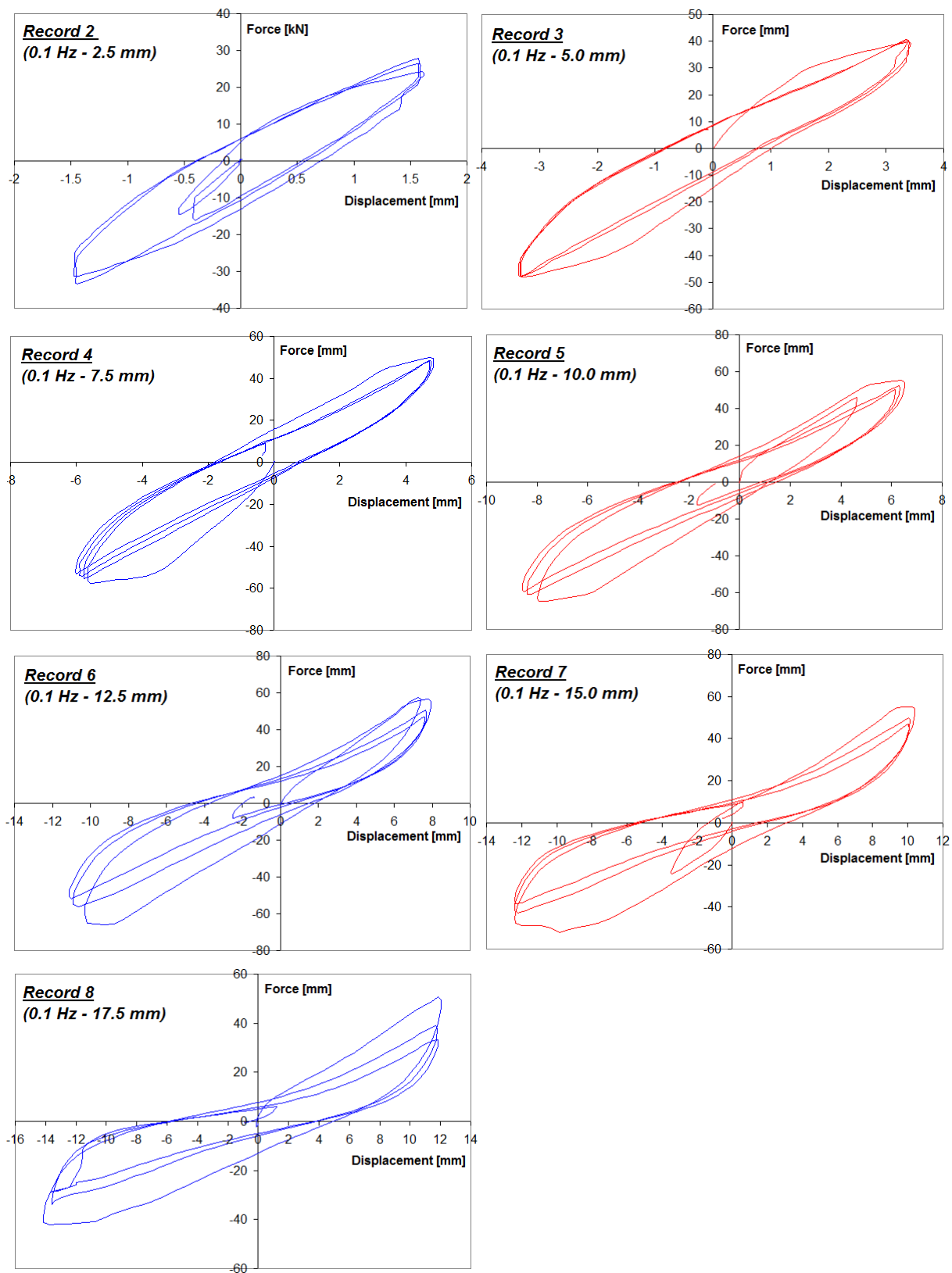


Figure 5.19. Cyclic curves for different steps of loading – Unreinforced adobe wall.

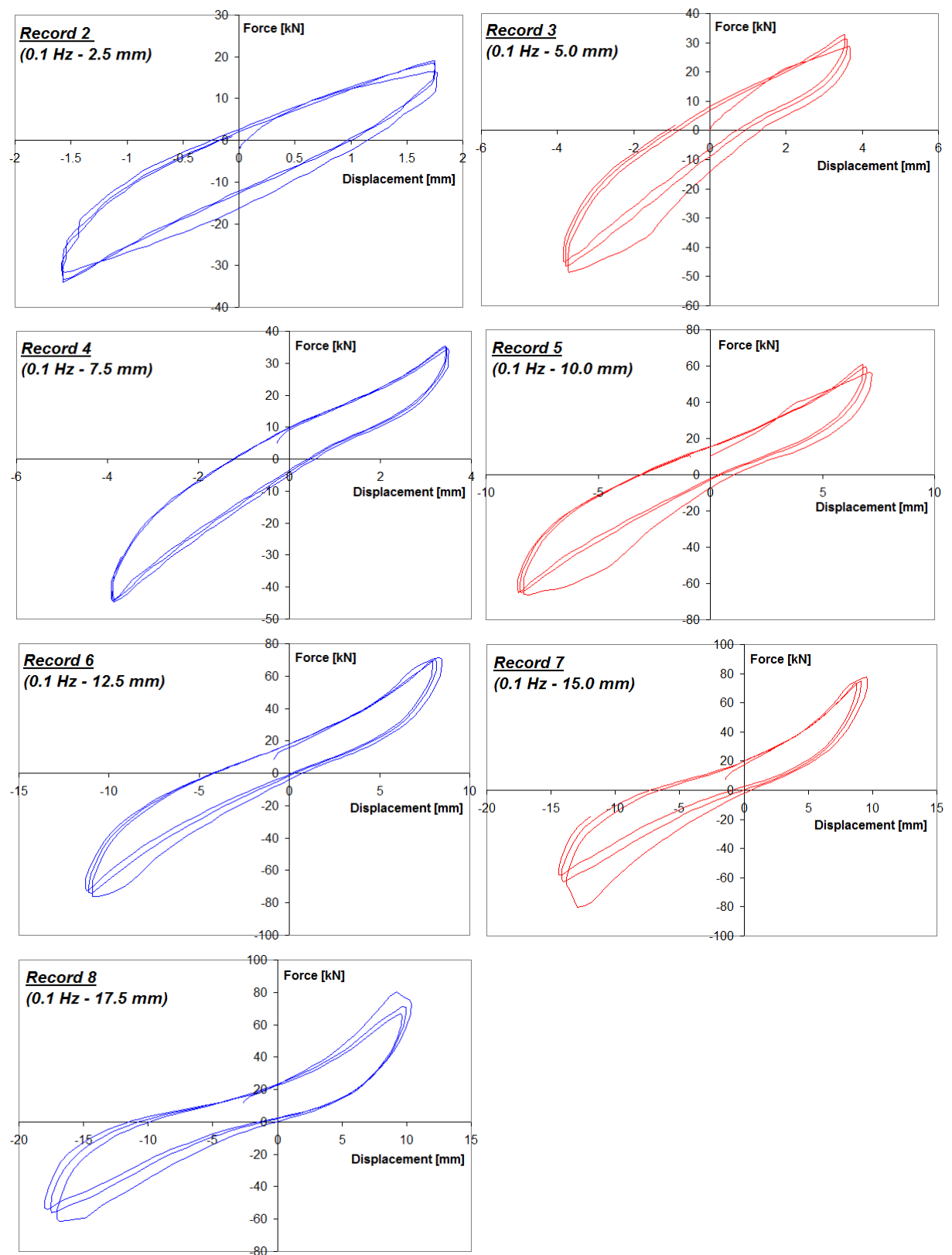


Figure 5.20. Cyclic curves for different steps of loading – Wall strengthened with reinforced mortar plaster.

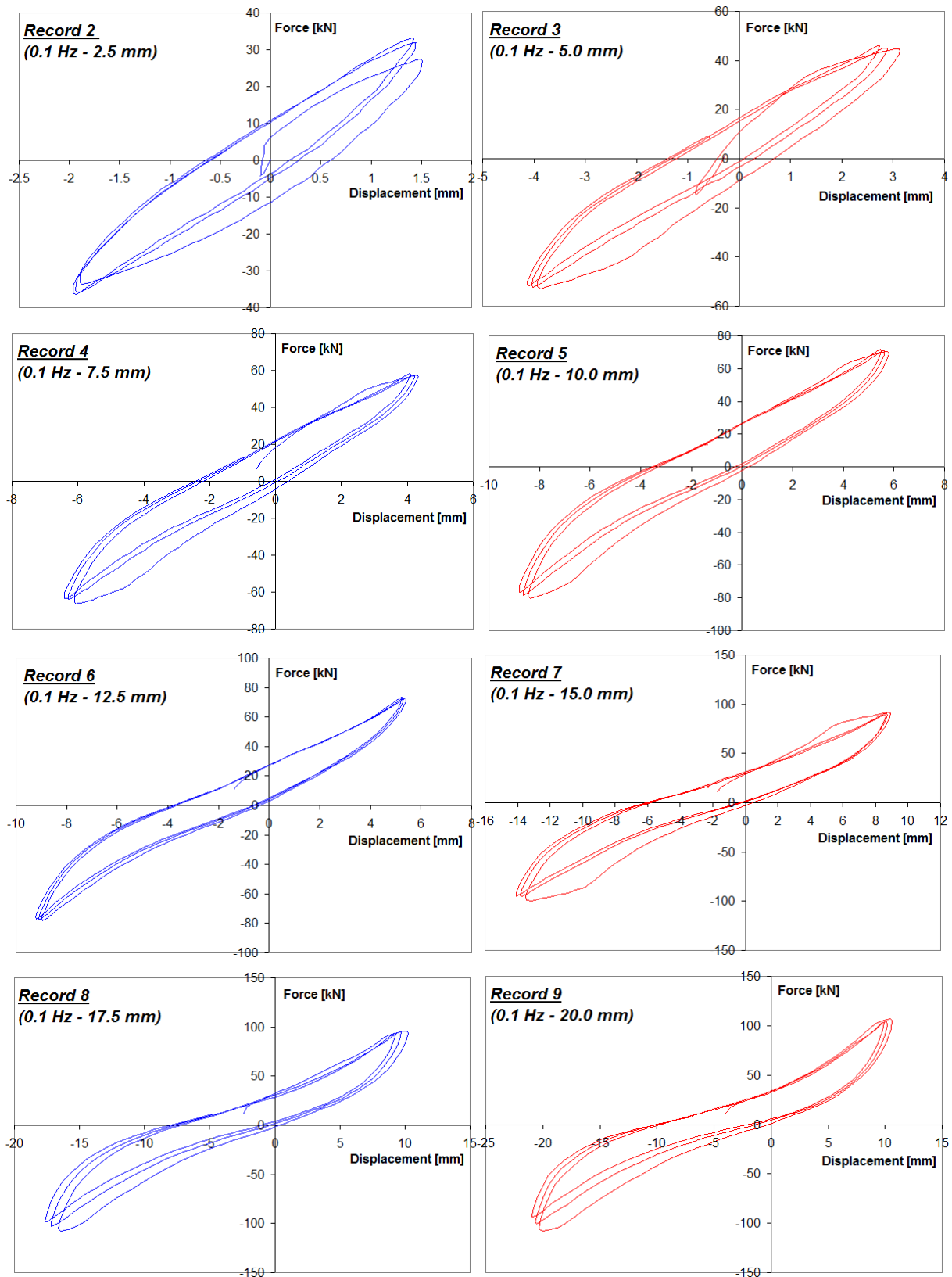


Figure 5.21. Cyclic curves for different steps of loading – Wall strengthened with wire ropes.

In the following graphs the overall cyclic curves for the three different walls are presented. In particular Figure 5.22 is referred to the unreinforced masonry wall, Figure 5.23 to the wall reinforced with FRP grid, Figure 5.24 to the wall reinforced with wire ropes.

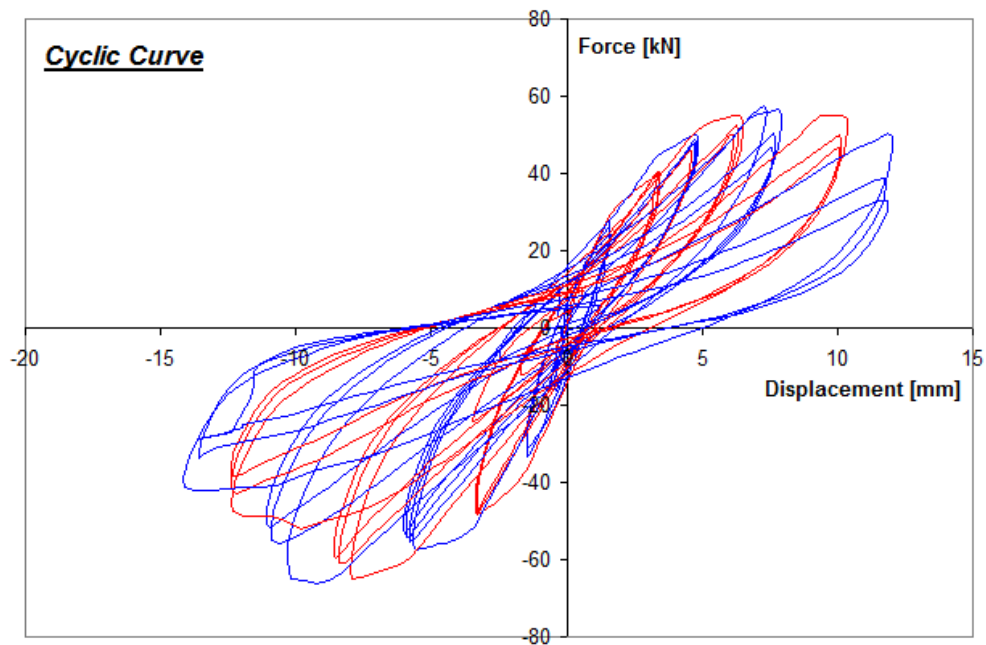


Figure 5.22. Cyclic curve for unreinforced adobe wall.

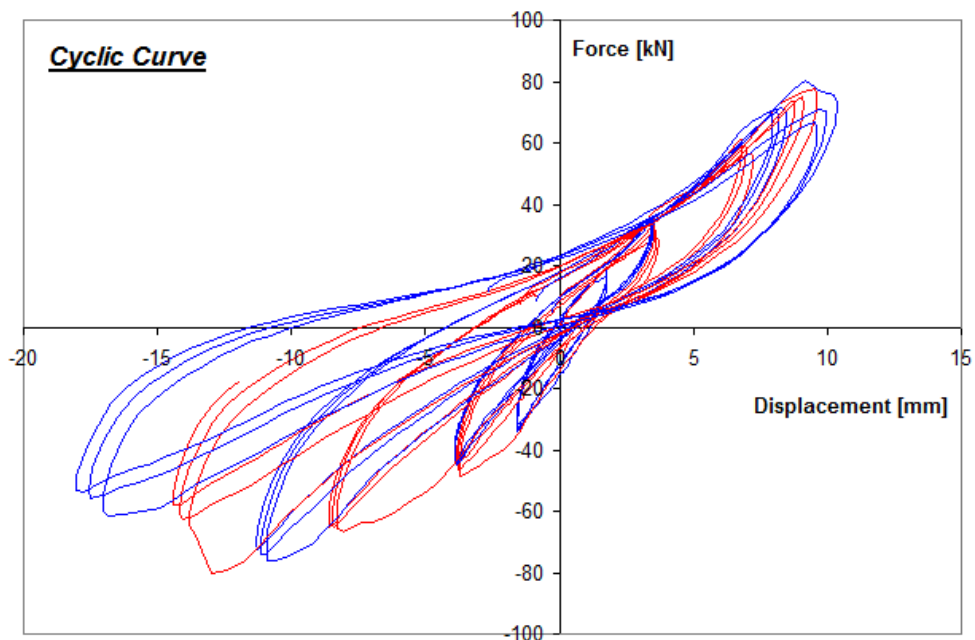


Figure 5.23. Cyclic curve for wall strengthened with reinforced mortar plaster.

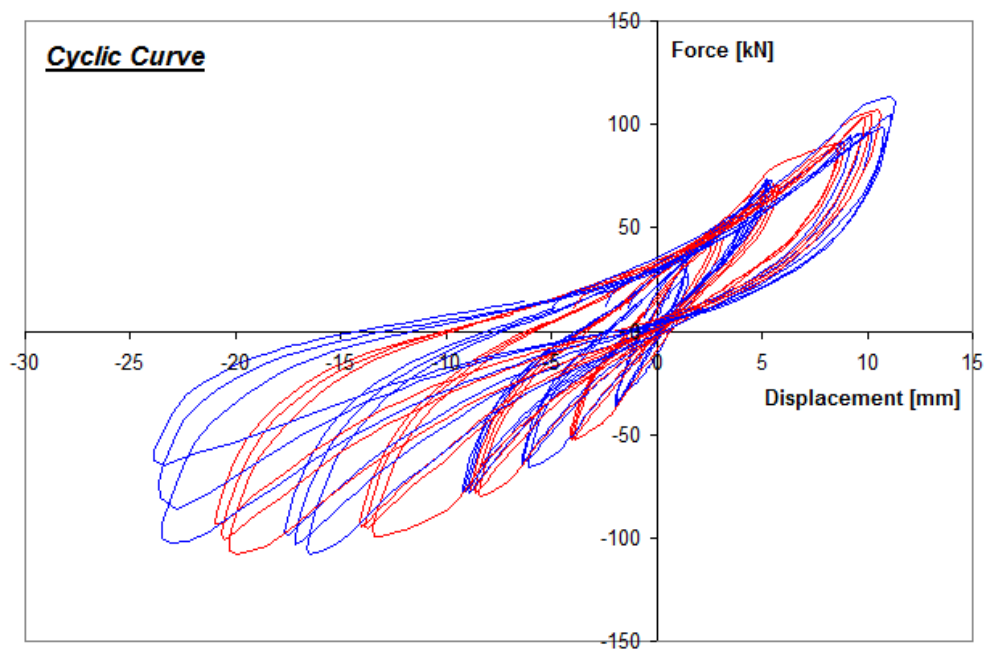


Figure 5.24. Cyclic curve for wall strengthened with wire ropes.

Finally, for each of the tested walls the envelop curves obtained from the cyclic curves are plotted. In particular both the extension side and the compression side of the cyclic curves are obtained, considering the maximum horizontal force and the correspondent displacement at each step of loading, and presented in Figure 5.25, 5.26 and 5.26 for the three cases.

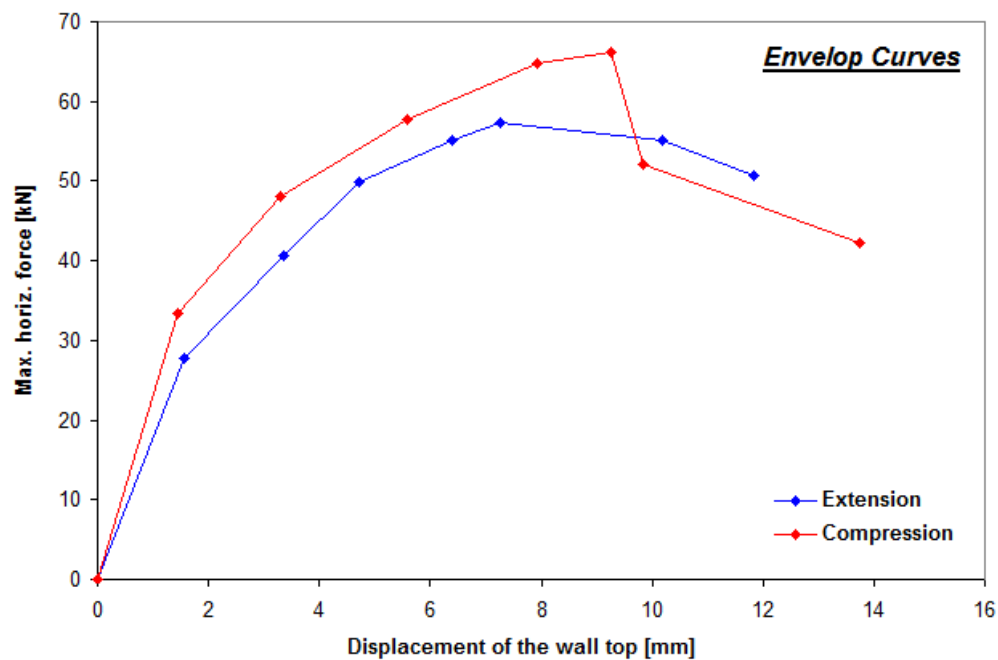


Figure 5.25. Envelop curves for unreinforced adobe wall.

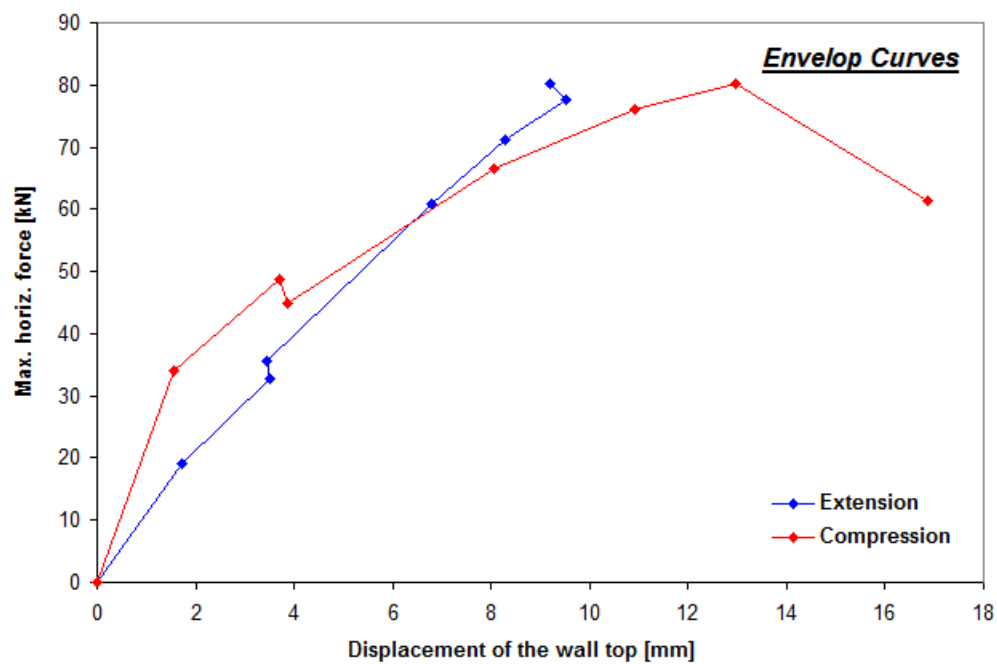


Figure 5.26. Envelop curves for wall strengthened with reinforced mortar plaster.

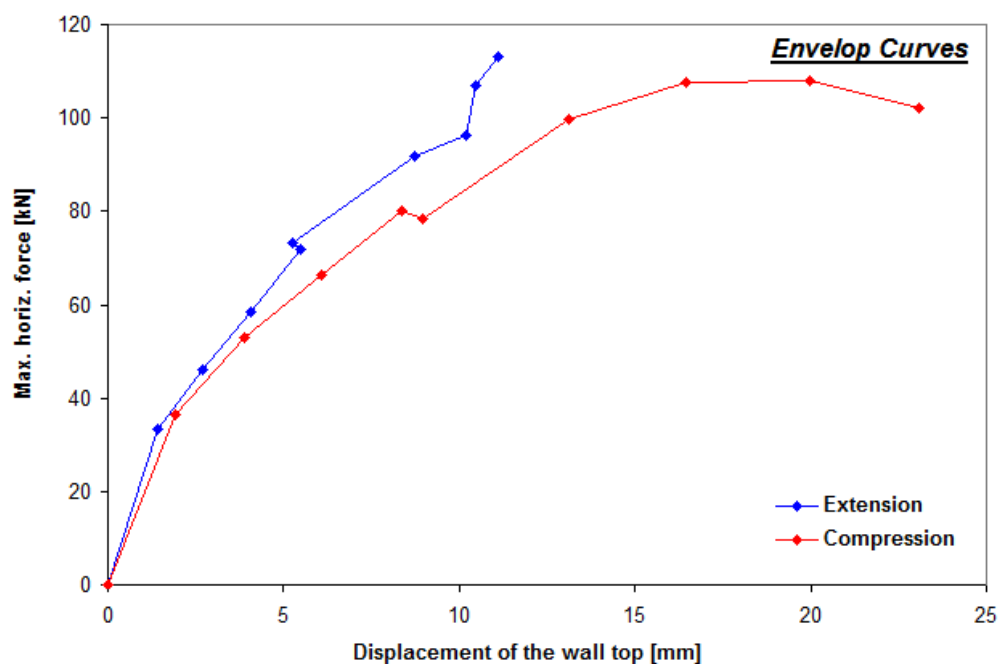


Figure 5.27. Envelop curves for wall strengthened with wire ropes.

In the following figures, some comparisons between the behaviour of the reinforced specimens with respect to the unreinforced control panel are reported. In Figure 5.28 the force-displacement curves for the unreinforced wall and for the wall reinforced with geo-net are plotted in the same graph. It is observed that the application of the reinforced mortar layers onto the wall's surfaces

allows the specimen to reach a higher value of strength, with an increment of about 20%. Moreover, an increment in terms of ductility is also registered.

When considering the comparison between the behaviour of the wall reinforced with wire ropes and the unreinforced wall, reported in Figure 5.29, it is observed that the strengthening system is more effective leading to an increment of strength of about 60%. The effectiveness of the system is evident also in terms of increment of the displacement capacity of the wall.

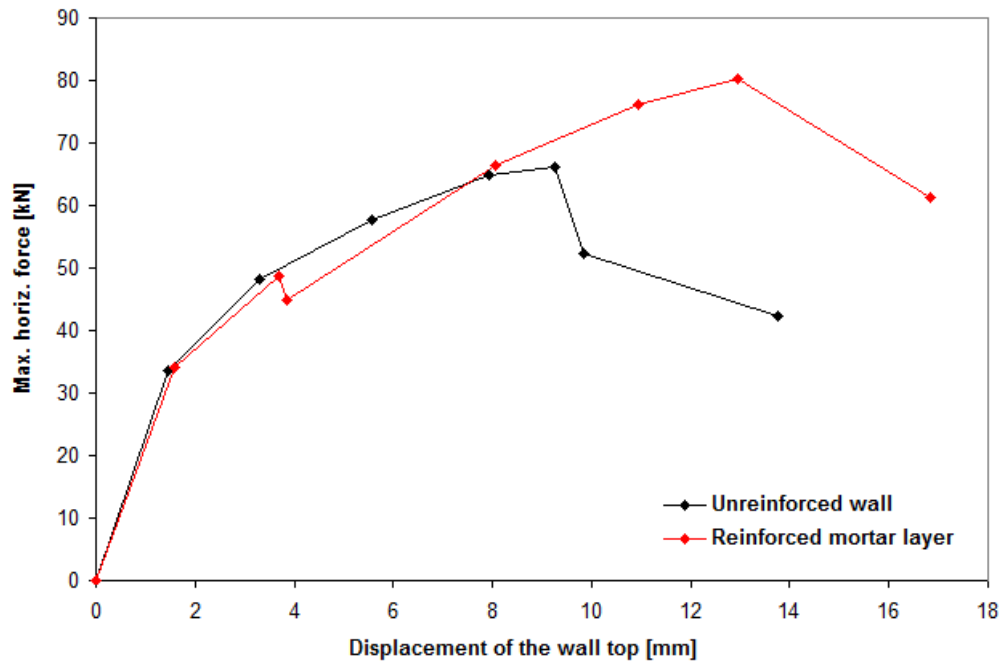


Figure 5.28. Behaviour of the wall strengthened with reinforced mortar plaster compared to the unreinforced wall.

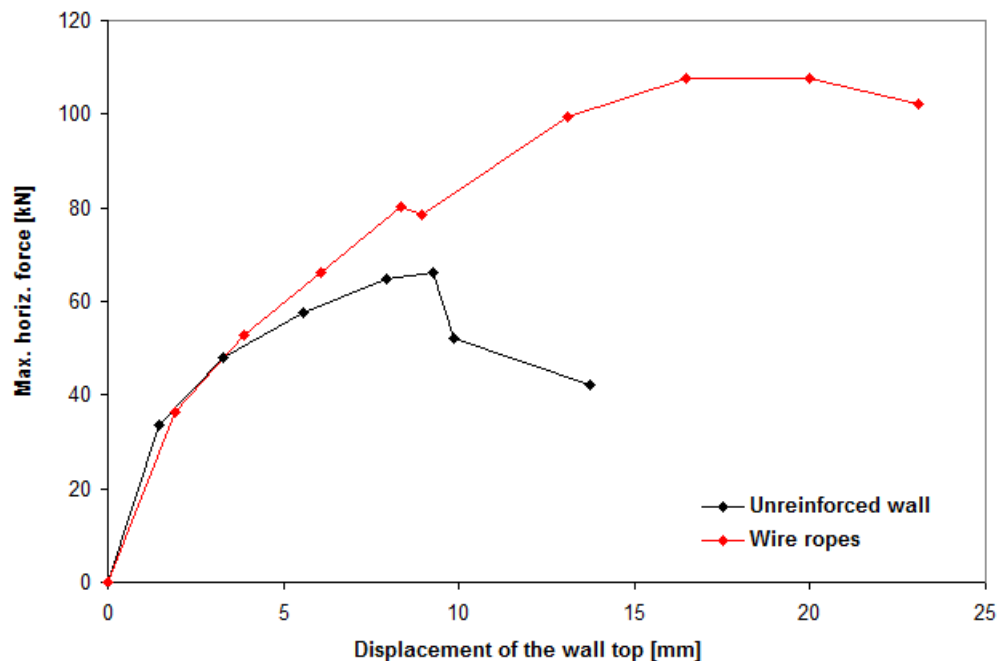


Figure 5.29. Behaviour of the wall strengthened with wire ropes compared to the unreinforced wall.

5.3.2 Damaged adobe brick wall retrofitted with reinforced mortar plaster

The experimental campaign carried out features also a test on a retrofitted wall. It is the case of an adobe brick wall severely damaged under cyclic loading conditions in a test carried out in a previous study at the ITAM. The damaged specimen has been repaired employing the same strengthening technique of the other walls, using geo-nets and plastering the surface with about 2 cm thick layer of mortar. In particular, the retrofitting intervention has been materialized after removing the remains of composite strips previously applied and properly cleaning the surface of the wall for the correct application of new materials.

The retrofitted wall has been, thus, tested again under combination of vertical prestressing load and cyclic horizontal load. In Figure 5.30 the crack pattern at failure registered on the wall surface; it can be observed a diffusion of cracking in the central area of the panel, with detachment of mortar plaster, and a concentration of damage at the base corners of the specimen.

Also in this case, as already observed in the case of the undamaged wall strengthened with reinforced mortar layers, the wall experienced the detachment of the mortar in the central area of the specimen and, for higher values of the top displacement, the out-of-plane of the plaster in the lower part of the wall close to the corners (Figure 5.31(a)). Moreover, due to a very high stress concentration in that area, a significant crack appeared and spread in the wall thickness, as reported in Figure 5.31(b).

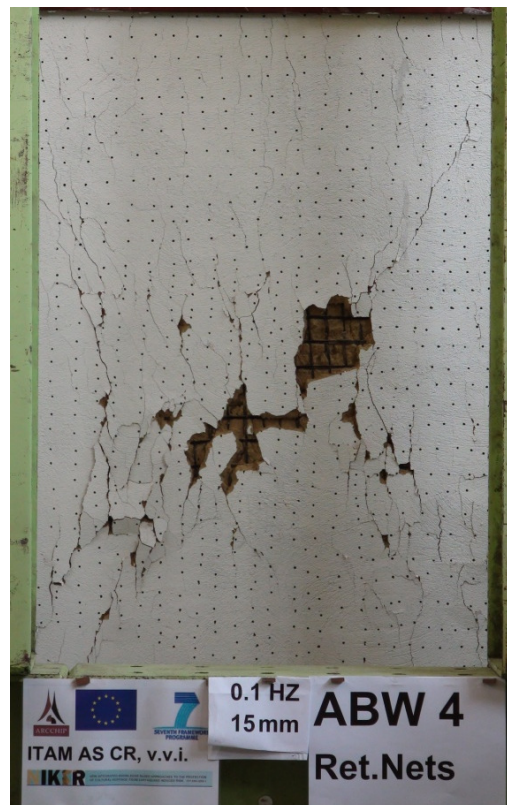


Figure 5.30. Crack pattern at failure of the retrofitted adobe wall under a combination of vertical compression and cyclic shear.

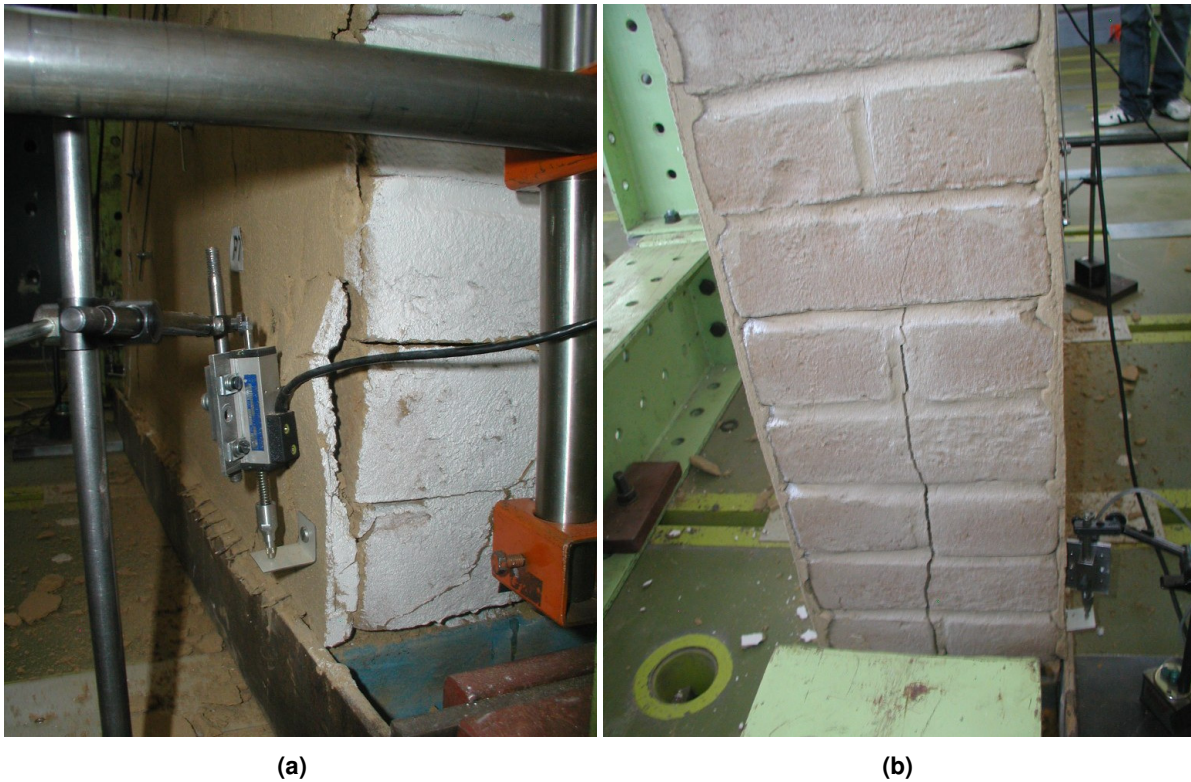


Figure 5.31. Damage at the base of the wall: detachment of the mortar layer (a) and large vertical crack in the wall thickness.

In the following the results of the tests presented in this section are reported in terms of cyclic curves horizontal force versus displacement of the wall top. In particular, in the graphs of Figure 5.32 the cyclic curves for each step of loading are presented, while in Figure 5.33 the global cyclic curve is shown.



Figure 5.32. Cyclic curves for different steps of loading – Retrofitted adobe wall.

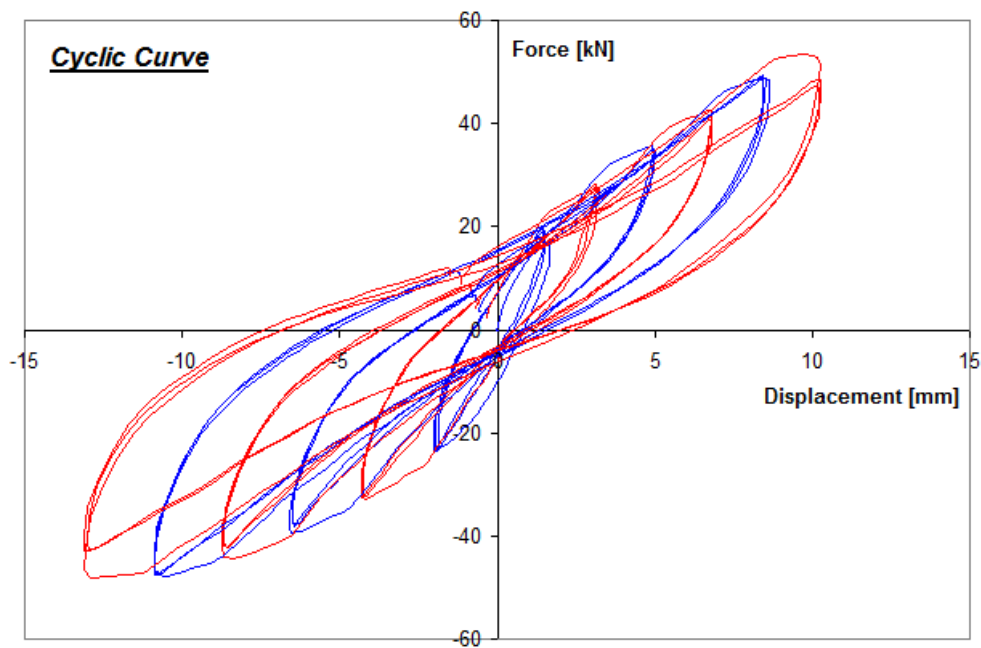


Figure 5.33. Cyclic curve for retrofitted adobe wall.

In Figure 5.34, the envelop curves obtained from the cyclic curves are plotted for both the extension side and the compression side of the cyclic curve.

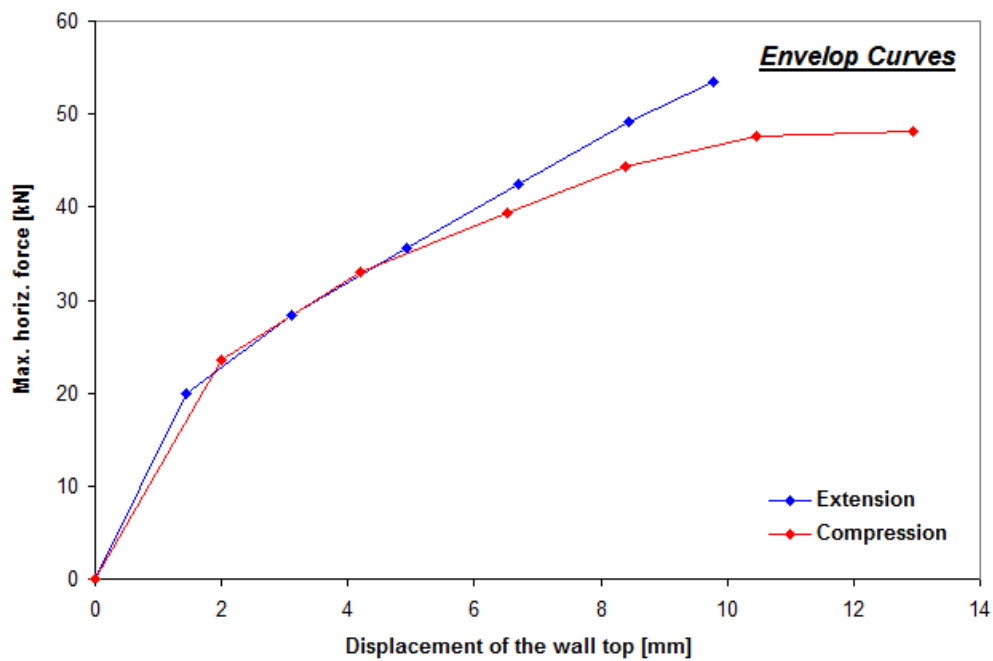


Figure 5.34. Envelop curves for retrofitted adobe wall.

Comparing the force-displacement curve of the retrofitted wall with the unreinforced adobe brick wall (Figure 5.35) it can be observed that the strengthening with mortar reinforced with geo-net

allow the specimen to reach a strength of about 70% of the original situation. However, the stiffness of the retrofitted wall is lower than the stiffness of the control wall, even after the intervention. Finally, in Figure 5.36, it is reported a comparison between the behaviour of two adobe brick walls reinforced with the same technique, represented by the application of geo-nets and plastering, in case of application on undamaged or damaged wall.

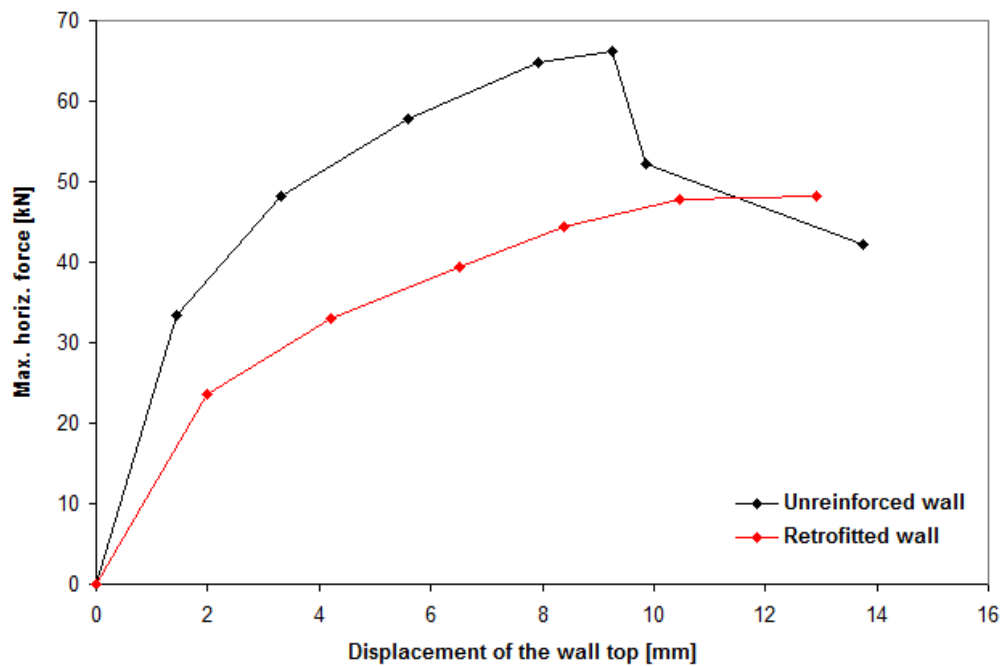


Figure 5.35. Behaviour of the retrofitted adobe wall to the unreinforced wall.

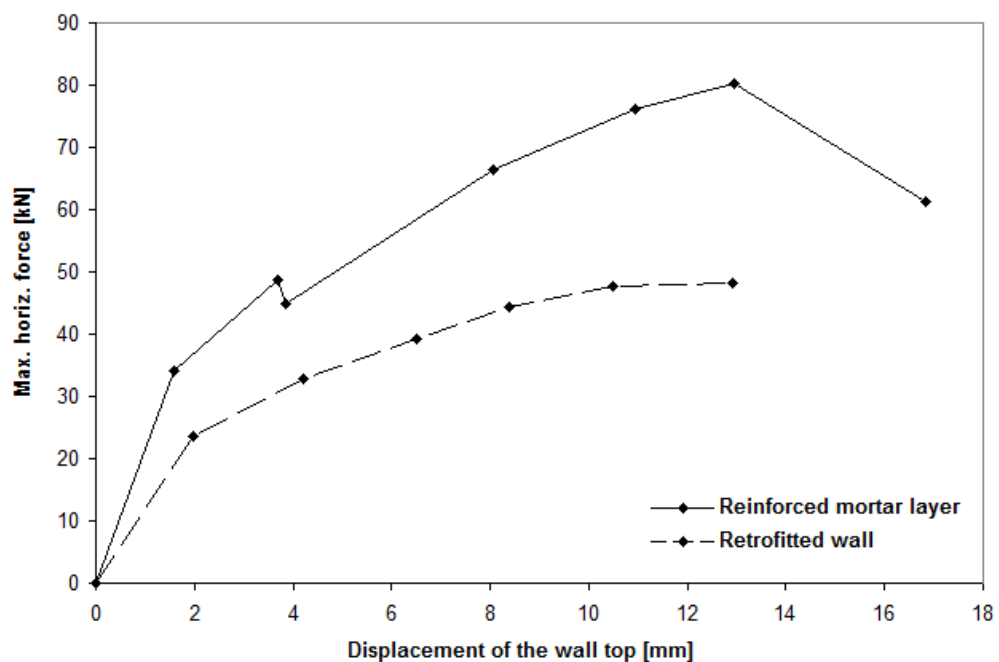


Figure 5.36. Comparison between undamaged wall strengthened with reinforced mortar layers and retrofitted wall.

6. NUMERICAL MODELLING OF REINFORCED MORTAR SPECIMENS AND MASONRY WALL

Mechanical tests on mortar elements reinforced with geo-nets have been carried out in order to characterize the behaviour of the strengthening system adopted to reinforce the masonry panels considered in this study. The description of the specimens' features in terms of dimensions and employed materials, and the experimental results obtained from the tests have been reported and discussed in Chapter 4. Moreover, in Chapter 5 the results obtained from the experimental campaign carried out on masonry walls strengthened with mortar layers reinforced with geo-nets are illustrated and discussed. The present chapter is intended to produce instruments for the validation of mechanical experiments on reinforced mortar specimens and masonry walls prototypes previously tested through the use of numerical modelling. In the following sections some theoretical aspects regarding the numerical models for materials and type of analysis carried out will be discussed. A general non-linear finite elements code has been used (DIANA 9.3) [59]. Furthermore, the models of the specimens for tensile test and shear test are described and the results of the numerical analyses are illustrated. The comparison with the experimental result can be used with the scope to calibrate some unknown parameters of the models, in order to be used for future analyses.

6.1 FINITE ELEMENT TECHNIQUES

6.1.1 General

The finite element method (FEM) is a numerical technique for finding approximate solutions of partial differential equations (PDE) as well as of integral equations. Finite element method is a way to simulate tests that had been done in the laboratory. This method is very powerful and it can be used to understand more about experiments. In a numerical analysis based on finite elements, a structure is divided into a large number of elements which are interconnected by nodes. These nodes are usually situated in the corners, but also may appear along the edges. Loads and supports are specified, and for a set of equilibrium and compatibility equations is set up, which can be solved numerically. The results are given at so called integration points, which do not coincide with the nodes.

6.1.2 Cracking models

The discrete crack concept is the most refined approach to model the crack formation in a material being based on modelling an interface element between two solid elements and capable to introduce a geometrical displacement discontinuity, but unfortunately this approach is not very computationally suitable to be applied in finite element method. From the point of view of numerical and computational implementation the smeared crack concept is certainly more viable, considering the cracked solid as a continuum and describing its behaviour in terms of stress-strain relation. Obviously, in the latter case it is evident that material is continuum by assumption only, being discontinuous the nature of phenomenon. Effort must be done to calibrate smeared crack model in order to average the real cracking process and to let it be able to reproduce all possible involved mechanisms.

A review of numerical models capable to reproduce cracking in quasi-brittle materials based on different cracking concepts is presented in (Rots and Blaauwendraad, 1989) [60]; a distinction is made in:

- discrete cracking concept, associated to the notion of a discontinuous,
- smeared cracking concept, associated to the notion of a continuum, based on (in function of the orientation of the smeared crack):
 - fixed single crack approach, if the orientation of the crack is kept constant;
 - fixed multi-directional crack approach, if the orientation of the crack is updated stepwise;
 - rotating crack approach, if the orientation of the crack is updated continuously.

6.1.2.1 Discrete crack concept

The firstly introduced, and most realistic, approach developed in order to model cracking of materials is the discrete crack concept, in which a given crack, or system of cracks, is reproduced by the possibility to generate a separation between elements of a finite element modelled body. Nevertheless, as already pointed out, this kind of approach is not simply implementable and easily manageable in finite element method, due to the existence of intrinsic limitations and complexities that can restrict its use.

In fact, a problematical aspect of discrete crack modelling is the necessity to allow the model not having fixed nodal connections, that may change during the loading process and update according to the evolution of cracking. The second fundamental drawback of the concept relies on the necessity to identify and preventively set down the possible crack path, since it is generally constrained to follow the element edges, although some attempts to define a few techniques in order to introduce the possibility for a crack to further develop through a finite element (Blaauwendraad, 1985) [61].

However, if the failure mechanism of a system can be recognized a-priori, the associated crack path can be identified and the orientation of potential cracks be set in the model. Fundamental

issue for the correct application of such modelling approach is the appropriate selection of the interface element simulating the geometry discontinuity, and its dummy stiffness. The dummy value of the initial stiffness is employed to simulate the uncracked state, rigidly connecting facing element nodes. Once a given condition is reached, such as maximum stress, the crack initiates and the element stiffness is changed. The crack tension stresses are generally described via a constitutive model, through which they are linked to the relative displacement across the crack by a factor representing phenomena like tension-softening and aggregate interlocking.

6.1.2.2 Smeared crack concept

The other possible approach that may be followed in the cracking behaviour description of brittle materials is based on the assumption for the medium to be continuous in spite the character of cracking phenomenon is not. The idea is to smear cracks that may initiate and propagate upon loading, their effect in the modification of geometrical and mechanical characteristics of element, in a continuum, in order to describe its behaviour in terms of stress-strain relations only, in the form firstly introduced by Rashid in 1968, (Rashid, 1968) [62].

Based on this approach, the application of smeared crack concept features passing from an initial isotropic behaviour to an orthotropic one upon cracking, without introduce modification in the finite element model mesh, or imposing limitations on the orientation of crack planes, as well as the material axes of orthotropy.

Due to the outlined aspects, and also considering the computational process, smeared crack concept seems to be a more easily viable path for description of crack formation in materials. Furthermore, such a concept may be much more powerful and more faithful to reality if applied in cases of distributed cracks and if the spacing between each crack is rather small compared to the representative dimensions of continuum.

Different approach can be followed in the framework of the application of smeared crack concept, but the main distinction can be made is between fixed and rotating crack, based on the assumption about the orientation of crack. The former approach is characterized by the assumption of fixed orientation for crack during the whole computational phase, while in the latter the orientation of crack is allowed to rotate according to principal strain axes rotation. In between the two previously described approach, the fixed multi-directional approach can also be introduced.

6.1.2.3 Fixed single crack approach

The fixed crack concept assumes the local crack axes to remain unaltered upon loading. The stress-strain law adopted in fixed smeared cracking is defined regarding to a system of fixed principal

axes of orthotropy, according to the direction normal to the crack (related to mode I) and two orthogonal direction tangential to the crack (related to mode II and mode III). The original formulation by (Rashid, 1968) [62] and some others developments in the early years, provided null normal and shear stresses along the crack, once it has formed. After, the initial isotropic stiffness moduli have been reintroduced taking into account some reduction, in order to do not definitively disregard the even slight capability of the material to transmit tension stresses normally and tangentially to the crack, and taking into account the higher numerical problems related to the sudden discontinuity which creates when switching from the initial isotropic linearly-elastic behaviour to an orthotropic behaviour with zero stiffness moduli. Such reduction factor are the so called 'shear stiffness reduction' or 'shear retention factor' β , when applied to the initial shear modulus G , and 'normal stiffness reduction factor' μ , when applied to the initial Young's modulus E .

Another important advance in the formulation of smeared crack model is achieved when the concept of strain-decomposition is introduced, taking into advantage the possibility to distinguish between the strain due to cracking and the strain of the solid part of material between cracks. The strain-decomposition is in a certain way closer to the discrete crack concept, in which an interface finite element is used to model the separation of the solid material.

6.1.2.4 Fixed multi-directional crack approach

The concept of strain decomposition originally introduced in fixed smeared crack model, has been considered again in order to further decompose crack strain and uncracked material strain. In particular, when referring to the crack strain the sub-decomposition allow to independently take into account the different contributions of a set of cracks simultaneously occurring at a given point. The state of cracking originating at a given point in the solid material is, thus, exemplified by multi-directional cracks, namely a set of fixed cracks each of them described by a local strain vector, a traction vector, and a transformation matrix.

The field of application of multi-directional crack approach includes axi-symmetric and plane-strain analysis, in the cases of biaxial or triaxial tension, where the separate behaviour of two or three expected orthogonal crack can be usefully modelled. Moreover, the utility of the use of multi-directional cracking can also be seen in tension-shear conditions, cases in which a crack generates in tension and then proceeds in tension-shear, producing a rotation of the principal stress axes with respect to the fixed crack axes.

In order to overcome the problem of difference between the system of principal axes and crack axes two possibility may be considered. The first one is an internal alternative within the multi-directional fixed crack approach, and allows the formation of a new crack when the angle of inclination between the existing crack and the current direction of principal stress exceeds a given threshold value. The other possibility is given by the application of the rotating crack approach.

6.1.2.5 Rotating crack approach

As previously stated, within the fixed crack approach a discrepancy between the principal stress directions and the crack axes. In the rotating crack approach, the axes of orthotropy, defined upon cracking, are allowed to co-rotate with the principal strain directions. This kind of approach needs the non-linear stress-strain relation to be specified for the principal directions only.

An important difference between multi-directional crack and rotating crack approaches is given by the fact that while the former controls the formation of subsequent cracks via the threshold angle, the rotating concept assumes the crack orientation to change continuously.

An advantage of rotating crack approach is that it can be based on the strain decomposition concept for both crack and uncracked material. The strain decomposition is also necessary when the model is to be combined with plasticity, creep or thermal loading.

The rotating crack approach does not preserve permanent memory of the damage orientation, while the fixed crack approach does. Due to this difference, the rotating crack concept does not allow to re-activate the defects during a subsequent loading process. Furthermore, the modality to take into account the shear effect is different between fixed and rotating cracking. Within the fixed crack approach the shear effect is taken into account using of a crack shear relation, making complicate the analysis because the axes of principal stress do not coincide with the axes of principal strain anymore. In rotating crack approach, instead, a unique shear term is defined, that is responsible for the coaxiality between principal stresses and strains, also if the possibility of incorporate different shear models is lost, and the crack always occur in a principal direction.

6.1.3 Solution procedures for non-linear systems

6.1.3.1 Iterative procedures

Unlike linear finite element analysis in which the relation between force vector and displacement vector can be explicitly expressed by a linear equation, for non-linear finite element analysis displacements at current stage often depend on the displacements at earlier stages. To achieve equilibrium between internal and external forces in non-linear equation, an incremental-iterative solution procedure should be preformed since the solution vector could not be calculated explicitly as we have in linear equilibrium. The non-linearity can be a result of non-linear elasticity, plasticity and path-dependent analysis which in the displacement is depend on load history.

The incremental-iterative solution procedures comprise of two parts: the increment part and the iteration part. The equilibrium is defined as the state in which the internal force vector is equal to the external force vector, satisfying boundary conditions:

$$\mathbf{f}_{\text{int}} = \mathbf{f}_{\text{ext}}$$

For each increment in non-linear analysis, correction iteration is necessary to keep the error in analysis in a certain acceptable level. The exact solution leads unbalanced or residual force which is generated in each iteration. The unbalanced force is the difference between external and internal loads or in other words, the difference between applied load and resisting load. The equation can be represented as follows:

$$\mathbf{g}(\Delta \mathbf{u}) = \mathbf{f}_{\text{ext}}(\Delta \mathbf{u}) - \mathbf{f}_{\text{int}}(\Delta \mathbf{u}) \leq \lambda$$

where:

\mathbf{g} = residual force;

λ = convergence rate.

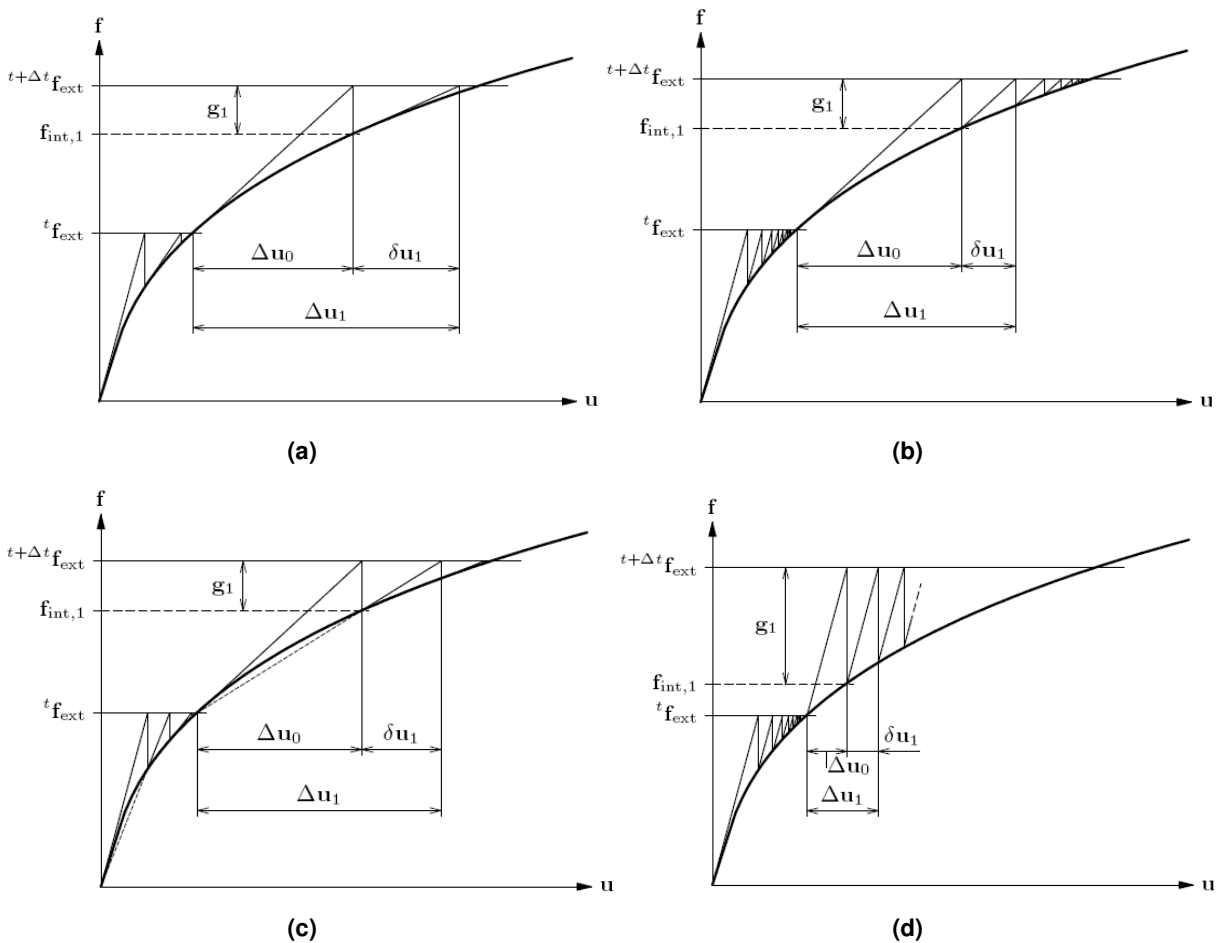


Figure 6.1. Different iterative methods: Regular Newton-Raphson iteration (b); Modified Newton-Raphson iteration (b); Quasi-Newton iteration (c); Linear Stiffness iteration (d).

Depending on how the stiffness matrix K is updated, iterative method can be classified in three broad categories with possible modification of each method (Figure 6.1): Tangent Stiffness Method (Newton-Raphson Methods: Regular N-R and Modified N-Raphson), Secant Stiffness Method (Quasi-Newton Method) and Linear and Constant Stiffness Methods.

The iterative solution requires an appropriate convergence criterion. If inappropriate criteria are used, the solution may be terminated before the adequate solution accuracy is reached or continue after the required accuracy has been reached.

6.1.3.2 Convergence criteria

In any iterative analysis the process is stopped after appropriate convergence is achieved. Three main criteria can be set to terminate the calculation. They are based on load norm, displacement norm and energy norm. The vector norms used for displacement and load norms are two vector norms (also called 2-norm) known as the Euclidean vector norms.

$$\text{Displacement norm ratio} = \frac{\sqrt{\delta \mathbf{u}_i^T \delta \mathbf{u}_i}}{\sqrt{\Delta \mathbf{u}_0^T \Delta \mathbf{u}_0}}$$

$$\text{Force norm ratio} = \frac{\sqrt{\mathbf{g}_i^T \mathbf{g}_i}}{\sqrt{\mathbf{g}_0^T \mathbf{g}_0}}$$

Proper tolerance should be employed in either case to satisfy desired accuracy. Depending on the type of analysis, proper criterion and its convergence. For instance if many displacement control points are used in analysis, displacement norm might be less useful. On the other hand for elasto-plastic problems with very small hardening rate when enters to the plastic zone, the out of balance load may be very small while the displacement may be much in error. In order to provide an indication of when both displacement and load are near their equilibrium, values, a third convergence criterion can be represented based on energy norm.

$$\text{Energy norm ratio} = \left| \frac{\delta \mathbf{u}_i^T (\mathbf{f}_{\text{int},i+1} + \mathbf{f}_{\text{int},i})}{\Delta \mathbf{u}_0^T (\mathbf{f}_{\text{int},1} + \mathbf{f}_{\text{int},0})} \right|$$

6.1.3.3 Incremental procedures

The incremental procedures can be basically of two types: load control and displacement control. These two methods can handle most incremental procedures depend on the required solution.

For pre-peak analysis, load control scheme can be the choice of solution while for analysis of pre- and post-peak regime, displacement control is the proper choice. The latter method can go beyond the peak and capture snap-through phenomenon especially for softening material. However in some cases such as snap-back even displacement control fails where alternative method called arc-length method can handle this phenomenon.

In the load control method, load steps are prescribed where the external load is increased at the start of the increment, by directly increasing the external force vector (Figure 6.2(a)). Alternatively in displacement control (Figure 6.2(b)) displacement is prescribed and corresponding load is calculated in each step. The solutions of both methods are based on generated residual force of each iteration.

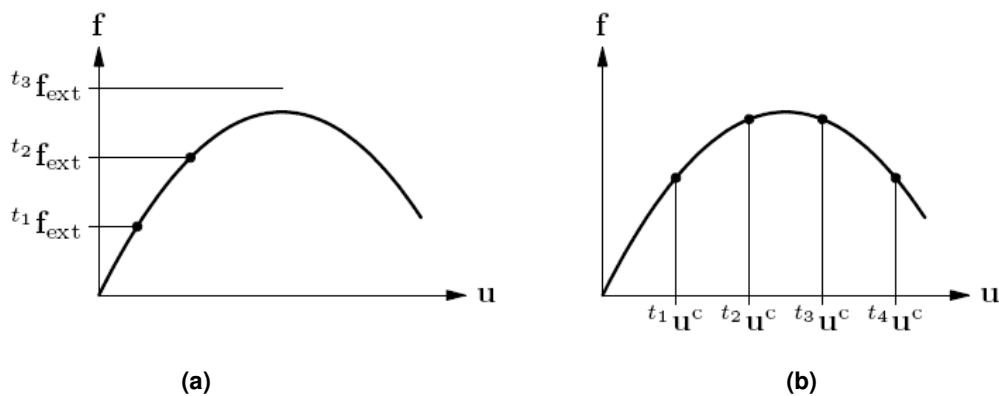


Figure 6.2. Possible incremental procedures: force controlled increment (a) and displacement controlled increment (b).

The arc-length method on the other hand uses an incremental method that can adopt the step size depending on the results in the current step. The initial choice of the step size for every increment is an important factor in the incremental-iterative process. This method, as can be seen in Figure 6.3, is capable to pass peak load even if snap back instability occurs in analysis.

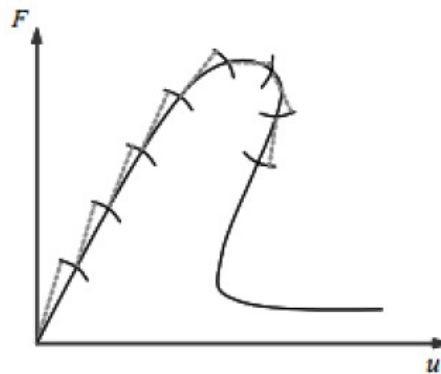


Figure 6.3. Arc-length method.

6.2 ADOPTED MATERIAL MODELS

The commonly used material model for the behavior of quasi-brittle material such as masonry uses a smeared cracking model for tension with a plasticity model for compression. In particular, the criterion showed in Figure 6.4 has been employed for the modeling of the material behaviour of both mortar and bricks.

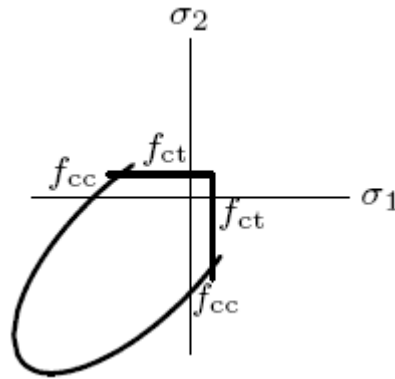


Figure 6.4. Material model adopted for mortar and bricks.

For compression a Drucker-Prager criterion has been chosen, which represent a yield condition in terms of a smooth approximation of the Mohr-Coulomb yield surface, which is a conical surface in the principal stress space, as is illustrated in Figure 6.5.

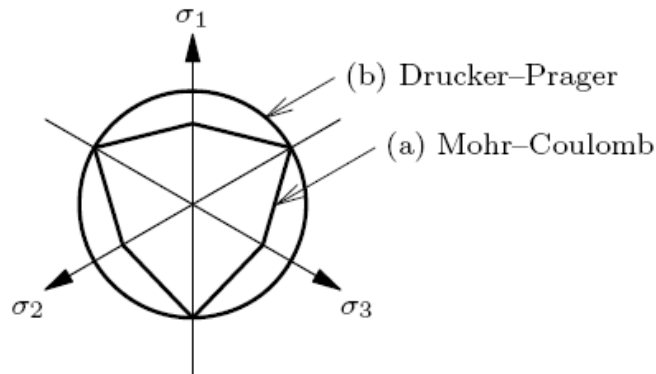


Figure 6.5. Mohr-Coulomb and Drucker-Prager yield conditions.

The formulation is given by:

$$f(\boldsymbol{\sigma}, \kappa) = \sqrt{\frac{1}{2} \boldsymbol{\sigma}^T \mathbf{P} \boldsymbol{\sigma}} + \alpha_f \boldsymbol{\pi}^T \boldsymbol{\sigma} - \beta \bar{c}(\kappa)$$

with $\bar{c}(\kappa)$ the cohesion as a function of the internal state variable κ . The projection matrix is equal to the projection matrix of the Von Mises yield condition. The scalar quantities α_f and β are given by:

$$\alpha_f = \frac{2 \sin \phi(\kappa)}{3 - \sin \phi(\kappa)} \quad \text{and} \quad \beta = \frac{6 \cos \phi_0}{3 - \sin \phi_0}$$

The angle of internal friction ϕ is also a function of the internal state variable. The initial angle of internal friction is given by ϕ_0 . The flow rule is given by a general non-associated flow rule, with the plastic potential given by:

$$g(\sigma, \kappa) = \sqrt{\frac{1}{2} \sigma^T \mathbf{P} \sigma} + \alpha_g \pi^T \sigma$$

with the scalar α_g defined by the dilatancy angle ψ :

$$\alpha_g = \frac{2 \sin \psi(\kappa)}{3 - \sin \psi(\kappa)}$$

For the tension side, a cut-off based on constant value of strength has been considered, as illustrated in Figure 6.6. Moreover, a tension softening based on (Cornelissen et al., 1986) [63] and (Hordijk, 1991) [64] has been employed (Figure 6.7), which proposed an expression for the softening behaviour of concrete which also results in a crack stress equal to zero at ultimate crack strain.

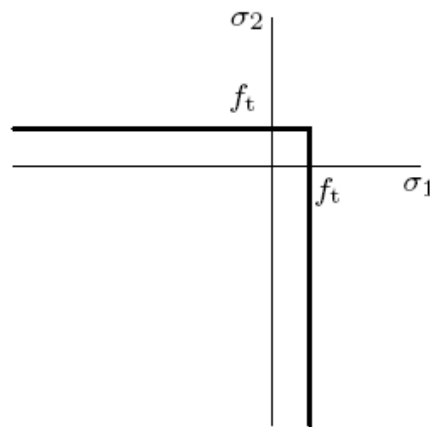


Figure 6.6. Tensile cut-off criterion.

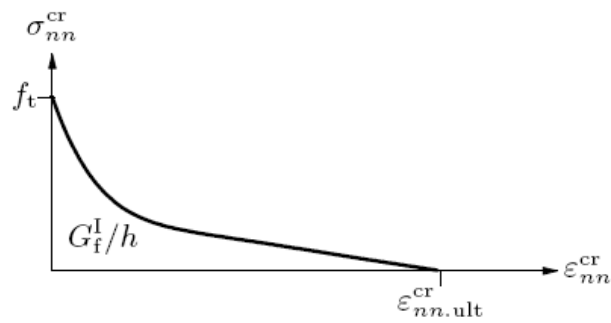


Figure 6.7. Non-linear tension softening according to Hordijk.

Regarding the shear behaviour, due to the cracking of the material the shear stiffness is usually reduced. This reduction is generally known as shear retention. In case of full shear retention the elastic shear modulus G is not reduced. In case of a reduced shear stiffness, the shear retention factor β is less or equal to one, but greater than zero. In this case a constant shear retention has been adopted, according to Figure 6.8.

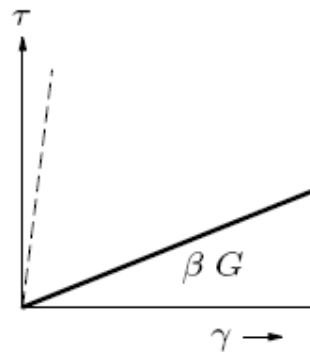


Figure 6.8. Constant shear retention.

For the frp reinforcement a linear-elastic law has been considered, with a brittle behaviour upon reaching failure. The reinforcement net has been modelled via discrete elements embedded in the mortar, respecting the actual position of the reinforcement lines.

6.3 MODELLING OF REINFORCED MORTAR SPECIMEN FOR TENSILE TEST

A three-dimensional model of the reinforced mortar specimen subjected to tensile loading has been built, using 3-D solid “brick” elements. In this case the mortar composing the structure is modelled with 20-noded elements and the geometrical features derives directly on the meshing characteristics. In particular, the thickness of the mortar specimens is equal to 20 mm and has not be given as an attached property of a shell elements but depends directly on the dimension of the solid elements.

The element used for this purpose is illustrated in Figure 6.9 and is defined by the coordinated of 20 nodes. The used element is an isoparametric element characterized by a quadratic interpolation of geometry and displacements.

The model is completed by the definition of a discrete reinforcement, modelling the actual position of the frp grid by means of single lines embedded in the solid elements representing the mortar. To each of the lines of reinforcement defined in the model, the actual cross-section has been assigned, according to the two orientations of the elements forming the grid. In particular, areas of 3.825 mm^2 and 4.95 mm^2 have been considered for the vertical and horizontal direction, respectively.

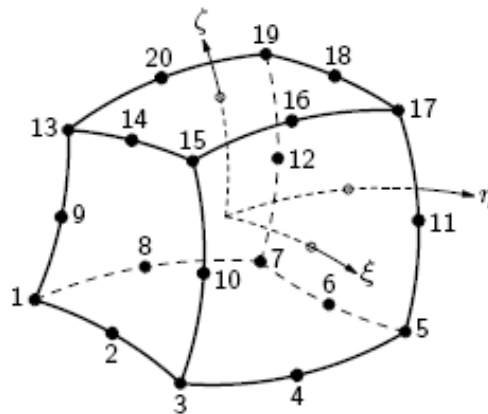


Figure 6.9. Finite Element (CHX60) used for 3-D model of mortar specimens.

In Figure 6.10 it is illustrated the geometry of the model with the indication of the internal embedded grid. The model has the same dimensions of the tested specimens, namely $82 \times 300 \times 20 \text{ mm}^3$. In the same picture, the imposed constraint condition is illustrated; in particular, on the two parallel faces of the model, on to which the tensile load is applied a rigid constraint in Z direction has been defined. Moreover, supports in X and Y directions have been also applied in order to eliminate possible rigid translation and/or rotations. Since the analysis carried out is a non-linear analysis, due to the high non-linearities of the material, it has been chosen to apply a load in terms of control of displacement on the two opposite faces of the model. The adopted mesh is illustrated in Figure 6.11 and it is made by 540 solid elements with a total of 2594 nodes.

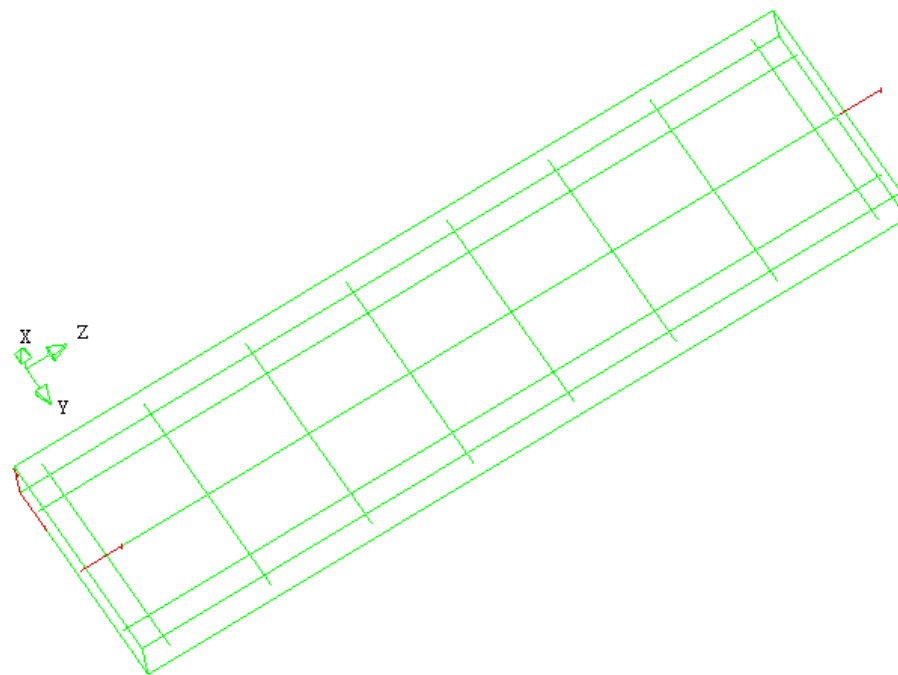


Figure 6.10. 3-D Finite Elements model of the specimen for tensile test.

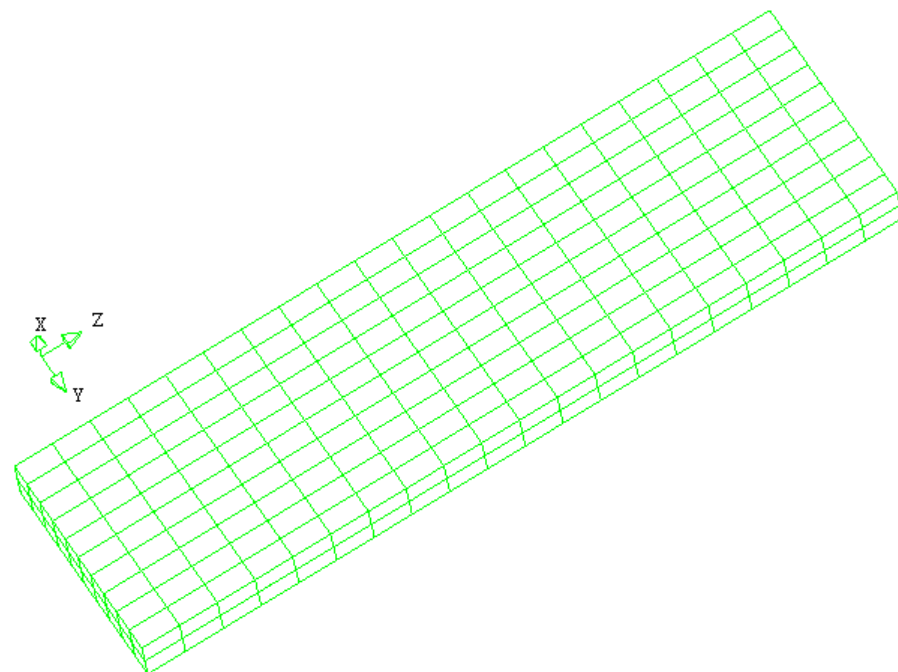


Figure 6.11. 3-D Finite Elements mesh (540 Elements x 2594 Nodes).

In Figure 6.12 it is reported the deformed shape obtained upon application of the tensile load in the longitudinal direction, for example referred to the step 50 of the non-linear analysis. In Figure 6.13 the crack strains in the integration points are illustrated. In particular, crack strains are visualized in the three-dimensional space as discs perpendicular to the strain direction. The cracks with light blue

colour are on the closing branch of the crack status, while the zones marked with red colour correspond to open cracks and clearly define the localization of cracking along discrete lines orthogonal to the application of the tensile load. Moreover, as it can be seen from next pictures, there is also an local effect on crack distribution due to the presence of the reinforcement grid with different stiffness. In a two-dimensional view, as the one shown in Figure 6.14 referred to the YZ face of the specimen, these disks show up as lines which clearly indicate the crack pattern. In the four pictures reported, the evolution of cracking upon loading can be observed.

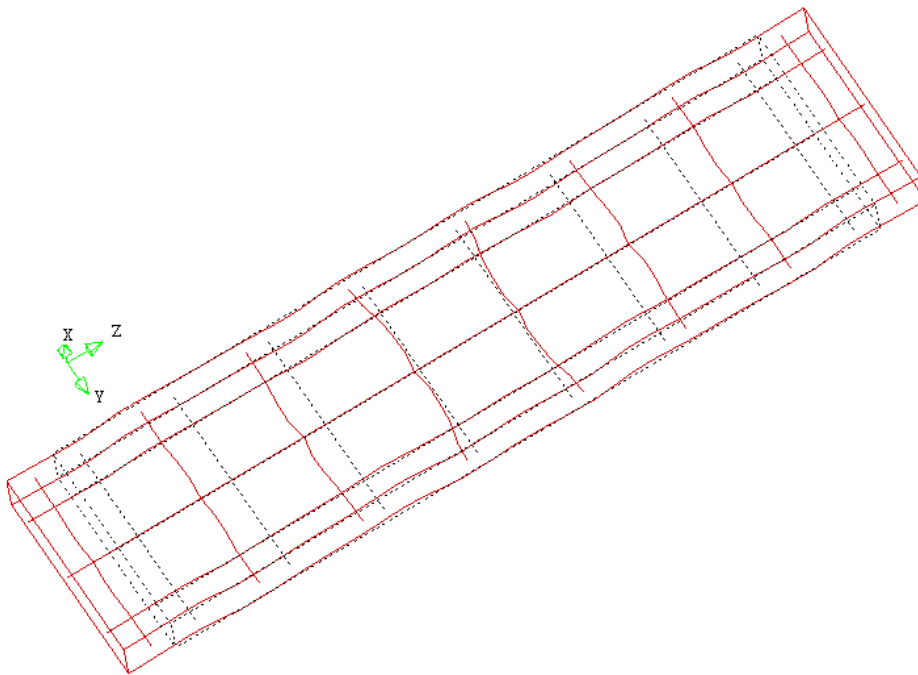


Figure 6.12. Deformed shape for Step 50.

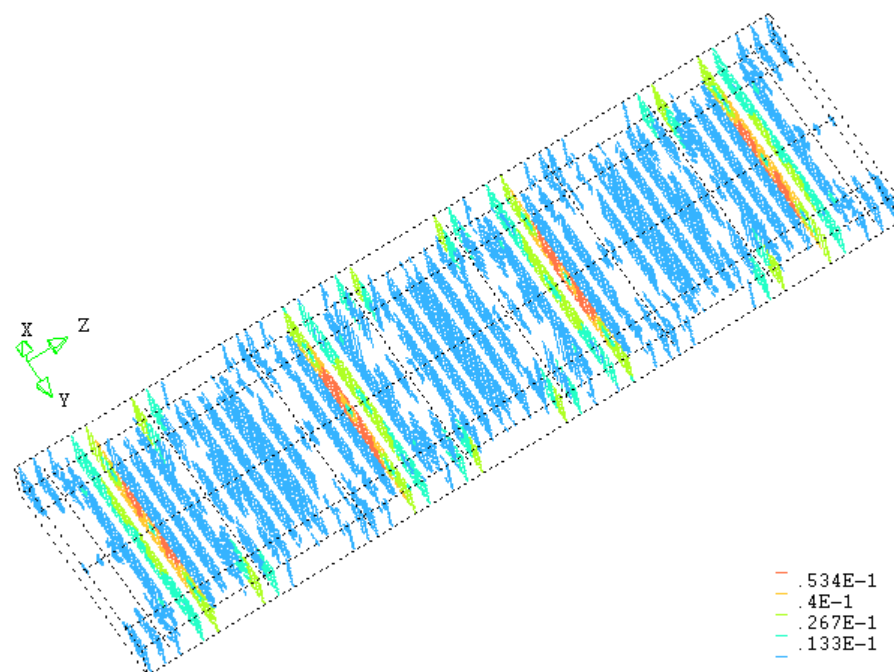


Figure 6.13. Cracking pattern at final stage of the non-linear analysis.

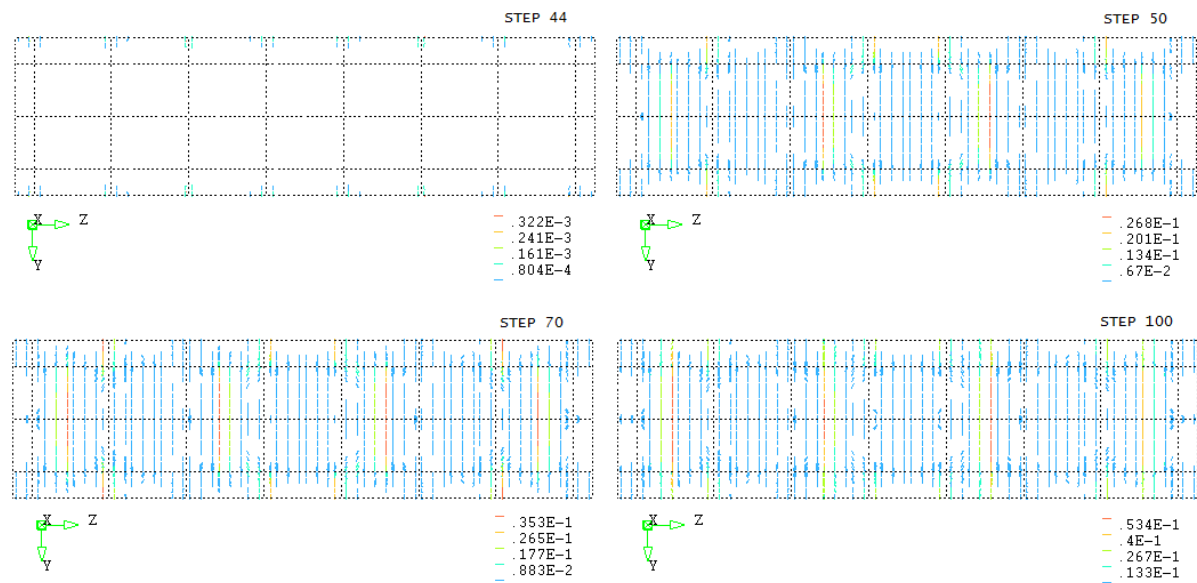


Figure 6.14. Evolution of cracking pattern for some significant steps of the analysis.

6.4 MODELLING OF REINFORCED MORTAR SPECIMEN FOR SHEAR TEST

A three-dimensional model of the reinforced mortar specimen subjected to shear loading has also been built, using 3-D solid “brick” elements already used for modelling the specimens for tensile tests and described in previous section. The thickness of the mortar specimens is also the same and

equal to 20 mm. Also in this case the grid reinforcement has been modelled by means of embedded discrete lines of reinforcement, according to the actual position in the mortar. The model has the same dimensions of the tested specimens, namely $85 \times 85 \times 20 \text{ mm}^3$. The adopted mesh is made by made by 200 solid elements with a total of 1265 nodes.

The analyses carried out is a non-linear analysis in control of displacement also in this case, and the applied load is again a displacement on the two opposite faces of the model.

For the modelling of the shear specimen different conditions have been considered by varying the imposed constraints. In particular in the first case, reported in Figure 6.15, the two vertical parallel faces of the specimen have been kept parallel via a rigid constraint in Y and Z direction, while the imposed displacement incremented during the analysis is in Z direction and applied with opposite sign on the same faces. In Figure 6.15(a) the deformed shape for this constraint condition can be seen, while in Figure 6.15(b) the correspondent crack pattern is reported. It is noted a certain redistribution of cracking in the mortar due to the presence of the reinforcement grid.

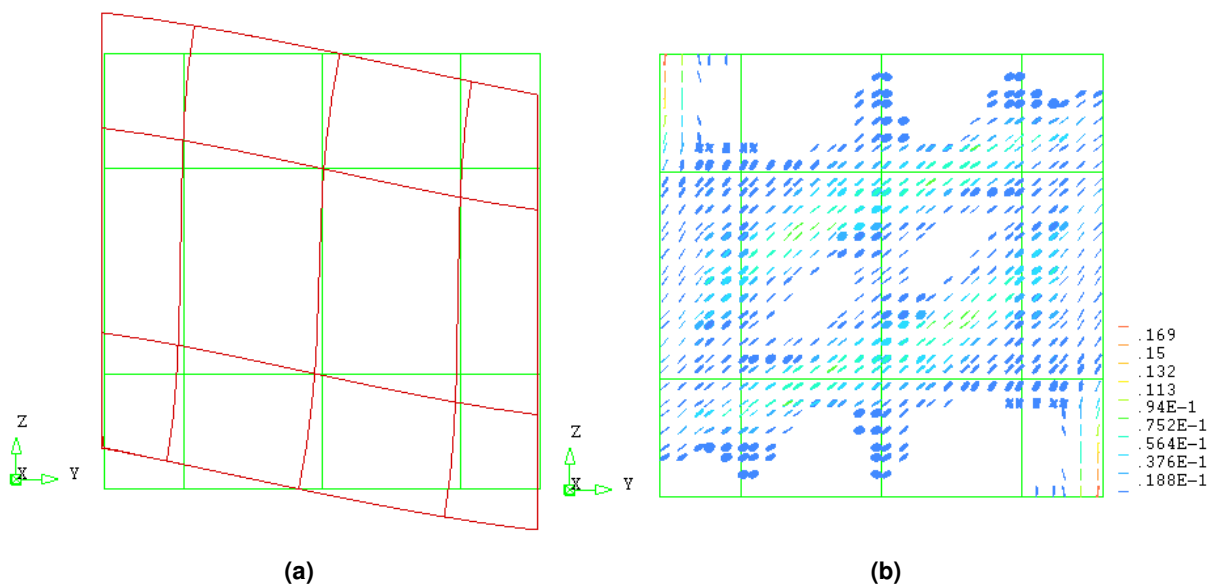


Figure 6.15. Constraint condition 1: deformed shape (a) and cracking pattern (b).

A second constraint condition considered is reported in Figure 6.16, in which for the right vertical face of the specimen is considered the same constraint of the previous case, due to symmetry conditions of the shear specimens that were tested. For the left face of the specimen the rigid constrain has been removed and supports in Y and Z direction have been added in order to simulate a hinge in the axis of the specimen. Thus, in this case that side is free to rotate and deform. In Figure 6.16(a) the deformed shape for this constraint condition is reported, while in Figure 6.16(b) the correspondent crack pattern is illustrated. The crack pattern is obviously different from the previous case due to a higher flexural effect in the specimen, with the formation of a well distinguishable vertical

crack in the right face of symmetry. Also in this case there is a certain redistribution of cracking in the mortar due to the presence of the reinforcement grid.

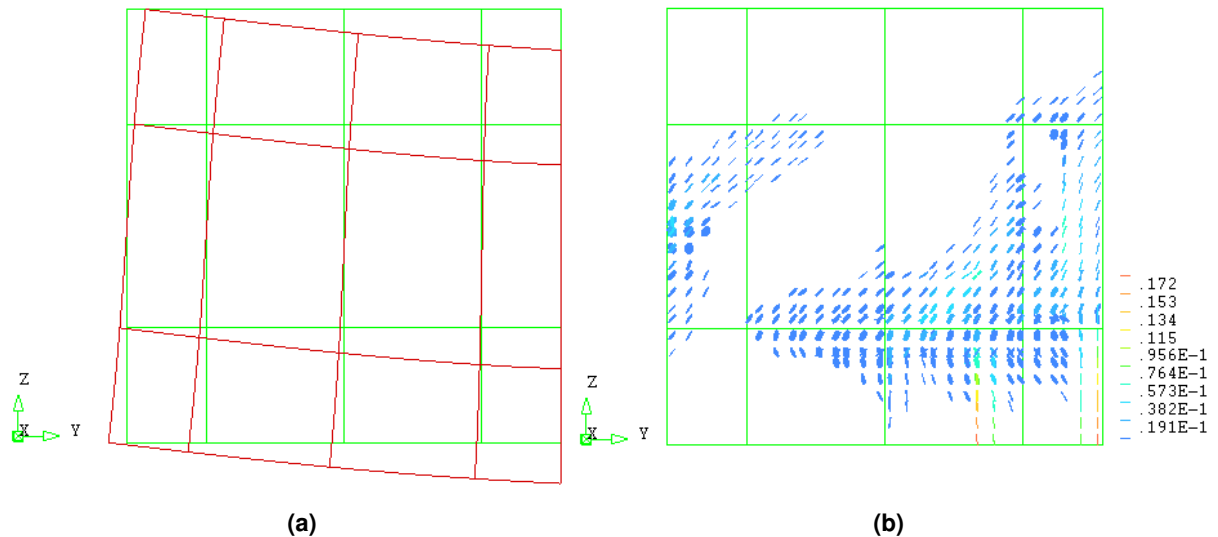


Figure 6.16. Constraint condition 2: deformed shape (a) and cracking pattern (b).

The last constraint condition is very similar to the second one, with the only difference that the point of rotation of the left face of the specimen has been moved on the lower edge, in order to simulate the support, according to the experimental set-up. In Figure 6.17(a) the deformed shape for this constraint condition is reported, while in Figure 6.17(b) the correspondent crack pattern is illustrated. In this case, beside the flexural vertical crack in correspondence to the symmetry plane, it can be noticed the formation of a strut defined by a compressed area in the specimen along the one diagonal direction, resulting in tension in the orthogonal direction.

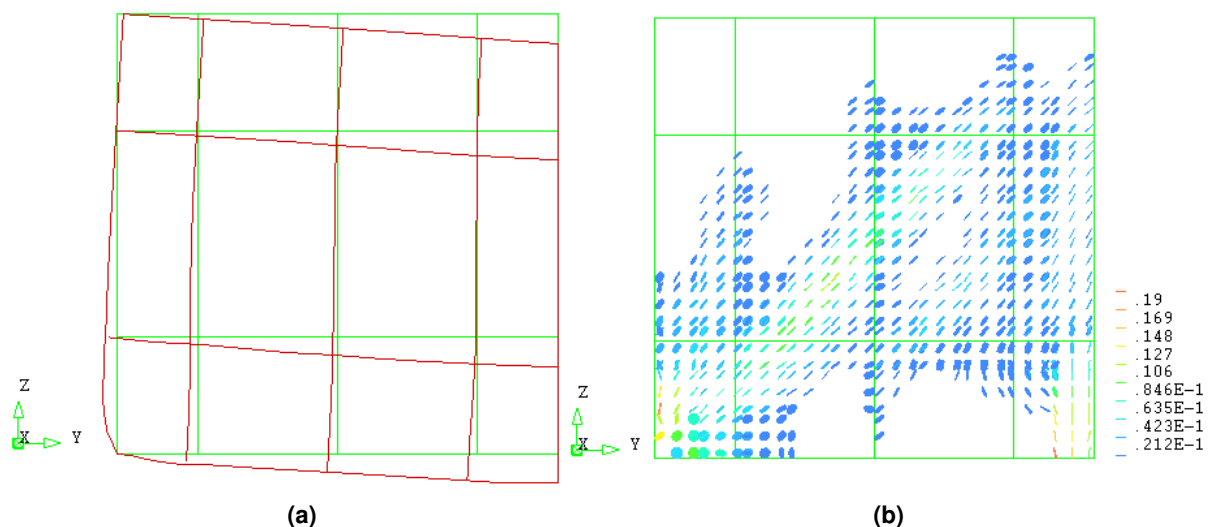


Figure 6.17. Constraint condition 3: deformed shape (a) and cracking pattern (b).

6.5 MODELLING OF MASONRY WALL

Finally, the three-dimensional finite element modelling of the masonry brick wall has been carried out. 3-D solid “brick” elements have been used, but in this case the structure is modelled with 8-noded elements and the geometrical features derives directly on the meshing characteristics. The element used for this purpose is illustrated in Figure 6.18 and is defined by the coordinated of 8 nodes. The used element is an isoparametric element characterized by a linear interpolation of geometry and displacements.

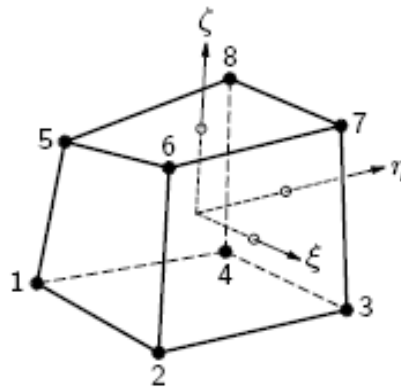


Figure 6.18. Finite Element (HX24L) used for 3-D model of masonry wall.

The model has been built considering the actual configuration in terms of bricks and mortar joints, resulting in the geometry reported in Figure 6.19(a). In particular, brick and mortar joints have been independently modelled, allowing the assignment of different material properties for both. The mesh (Figure 6.19(b)). has been defined on the basis of 4455 elements and 5712 nodes.

In Figure 6.20(a) the constraint applied on the wall is shown; in particular, the base has been considered fixed, while for all the nodes belonging to the top face of the wall a rigid constraint in the same direction of the applied horizontal load has been imposed. Finally, in Figure 6.20(b) the complete model, with the definition of different materials for bricks and joints is reported.

The model has been also tested under the application of a vertical prestressing load, kept constant during the analysis, and an horizontal load imposed on the top. The analysis carried out consisted in a non-linear analysis and the horizontal load incremented during the analysis is represented by an imposed displacement. The analysis is carried out in control if displacement, resulting in the non-linear curve reported in Figure 6.21.

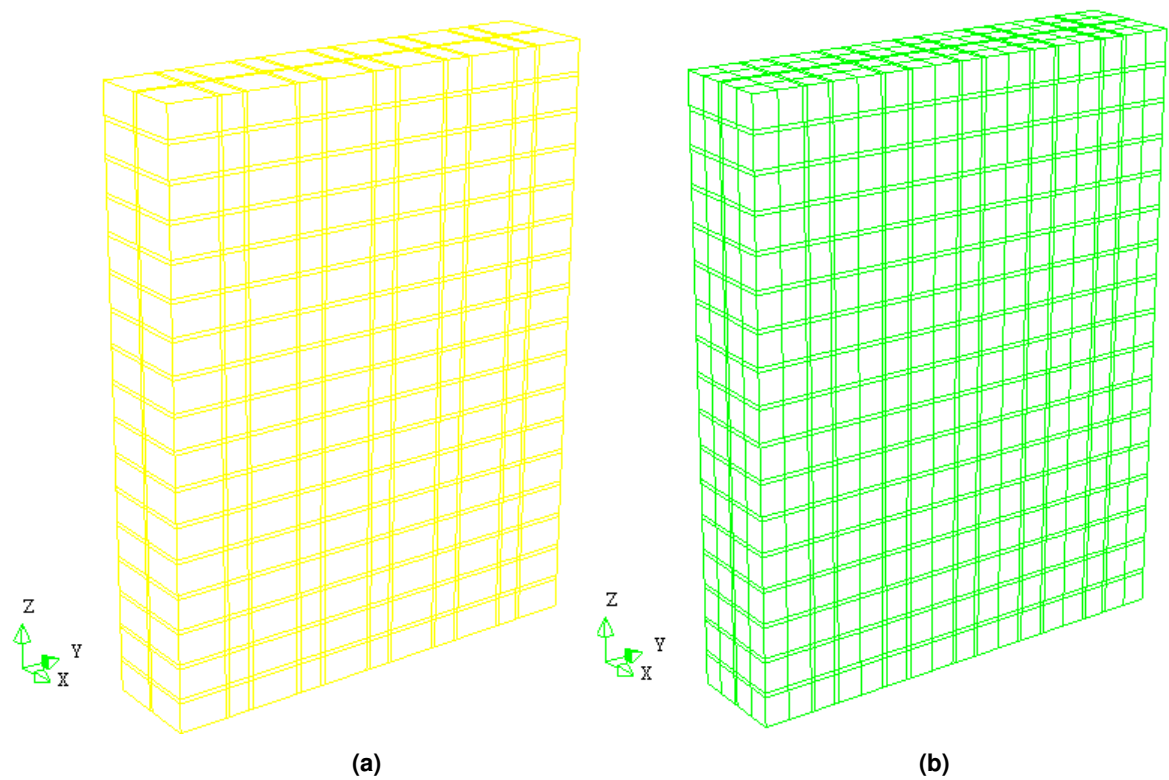


Figure 6.19. Masonry wall: definition of the geometry (a) and meshing (b).

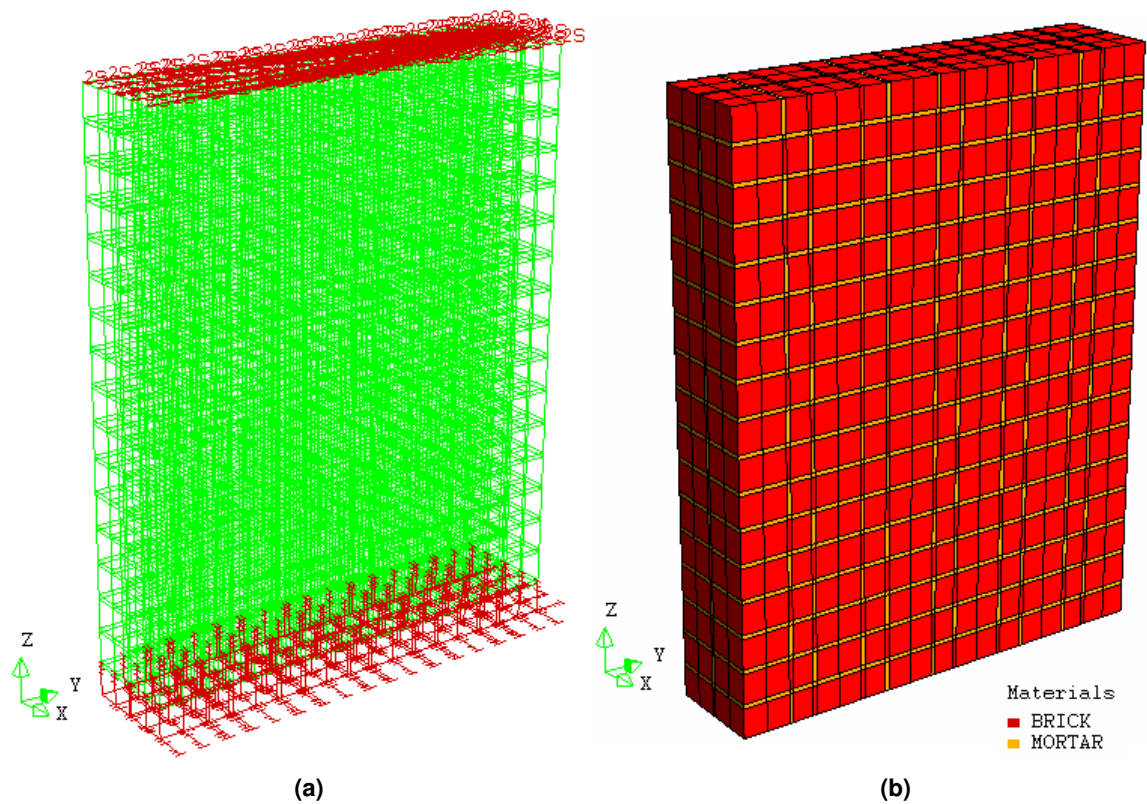


Figure 6.20. Constraint conditions (a) and assignment of materials (b).

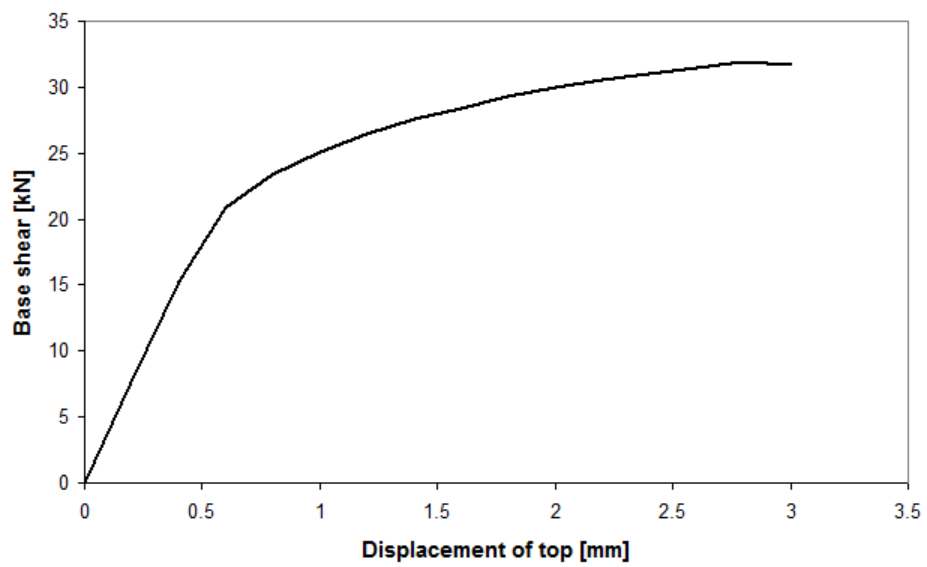


Figure 6.21. Example of non-linear curve obtained through a non-linear analysis for model testing.

7. DISCUSSION AND CONCLUSIONS

The present work was focused on the study of the structural behaviour of masonry walls strengthened by means of a recently introduced technique, which is based on the application on the wall surfaces of a layer of mortar reinforced with Fiber Reinforced Polymers (FRP) in form of grid.

First of all, the main issues concerning the reinforcing and strengthening of masonry walls, especially with regards to horizontal actions induced by earthquake, have been analyzed and some of the more common traditional techniques have been reviewed, particularly highlighting some of the disadvantages or drawback of each of them. Furthermore, a detailed bibliographic research has been carried out on the more recent strengthening techniques for masonry walls which make use of innovative materials, such as Fiber Reinforced Polymers. In particular, the literature review has been focused on the reinforcement of masonry walls by means of mortar layers reinforced with grids in FRP, considering the main developments in terms of both experimental and theoretical fields.

The considered strengthened technique is characterized by a number of advantages if compared to other possible FRP-based strengthening methods; particularly, a superior resistance to fire action has to be remarked, a good compatibility and bond with the substrate material, particularly in the case of masonry, vapour permeability. The main interest in the study of this strengthening technique is related to the promising possibility it offers in the upgrading in-plane shear behaviour of the system to which it is applied and one of the important issue to address is also the assessment of the effectiveness of the considered strengthening system in the improvement of the overall ductility of reinforced elements. Moreover, the choice of cementitious material for reinforcement layers is due to some advantages, mainly relate to its highly compatibility in terms of physical and mechanical properties with the tuff substrate. In addition, for strengthening of walls exposed to high temperature or environmental effects, the application of a thick layer of cementitious mortar substantially ensures a protection for the reinforcing grid and improves the long-term behaviour of the strengthening system.

A phase of the work consisted in the study of the reinforcing system in itself, on the basis of a series of experimental tests in order to characterize the mechanical behaviour of the mortar layer reinforced with the grid. In particular, different series of specimens have been prepared considering two different types of mortar: the for first group of specimens clay mortar with a low percentage of sand has been employed, while the second group has been realized with lime mortar with addition of Portland cement. For both types of mortar unreinforced and reinforced specimens have been prepared, in order to carry out tensile, compressive and shear tests on mortar only and on mortar with grid.

Besides the characterization tests on unreinforced and reinforced mortar specimens, an experimental campaign has been conducted on masonry wall prototypes strengthened with mortar layers reinforced with a polyethylene grid. The masonry walls that have been tested are represented by an unreinforced adobe brick wall used as a control specimen, an adobe brick wall strengthened with reinforced mortar layers and an adobe brick wall damaged during a previous experimental campaign and retrofitted with reinforced mortar layers. Moreover, in the present work, the results of a test carried out on an adobe brick wall strengthened with steel wire ropes have been also enclosed and illustrated. The masonry walls have been tested applying a vertical pre-stressing load kept constant during the experiment, and under cyclic horizontal loading with increasing amplitude of the imposed displacement.

It is observed that compared to the typical crack pattern usually found in plane masonry walls, with the formation of classical X-shaped main cracks, the case of the wall strengthened with reinforced mortar layer presents a more widespread and diffused crack pattern. The reinforced mortar layers reinforced with a frp grid has also the effect to redistribute the stresses originated upon loading and, thus, to spread the crack pattern over a wider area of the wall surface. The experimental tests evidenced also the necessity to study the interface behaviour between the external reinforcement and the masonry substrate to which it is applied represented by the wall in the evaluation of the effectiveness of this kind of reinforcement. Since the reinforced mortar layer applied on the wall surfaces is slightly thin and due to the different stiffness compared to the substrate, it can be subjected to out-of-plane forces that may cause its detachment. This effect has been registered also in the case of the retrofitted wall, localized particularly in the central area of the specimen

Comparing the behaviour of the reinforced wall with the control specimen, it has been observed that the application of the reinforced mortar layers onto the wall's surfaces allows the specimen to reach a higher value of strength, with an increment of about 20%, and produced an enhancement in terms of ductility. Considering the retrofitted wall the strengthening with reinforced plaster allow the specimen to reach a strength of about 70% of the original situation.

Finally, it has been seen that the wall reinforced with wire ropes behaves in a quite compact way, since the steel reinforcements play a very effective role in sewing up the cracks and keeping the masonry blocks together. The failure of the wall feature the formation of large damage in the wall at the level of the toe over the anchorage of the ropes. In this case, it is observed that the strengthening system is quite effective leading to an increment of strength of about 60%, and gives to the wall a higher capacity in terms of displacement.

Parallel to the experimental tests carried out in the framework of the present thesis, the numerical modelling of the specimens of reinforced mortar for mechanical characterization and the masonry wall has been carried out in order to produce an instrument to for validation of experimental evidences and to be used for prevision of behaviour of the whole strengthened system.

The reinforced mortar specimens has been modelled as three-dimensional, using 3-D solid "brick" elements. In this case the mortar composing the structure is modelled with 20-noded elements,

while the grid is modelled as a discrete reinforcement, according to its actual position, by means of single lines embedded in the solid elements. In both cases, for tensile and shear test specimens, the crack pattern given by the model has been studied. In particular, for the specimen subjected to tensile load the zones marked with corresponding to open cracks are clearly obtained, defining the localization of cracking along discrete lines orthogonal. Moreover, the effect of reinforcement has been also seen because of a local effect on crack redistribution. For the case of the shear specimens, in the model have been also considered different constraint configurations, since the test set-up was not yet defined. Finally, the three-dimensional finite element modelling of the masonry brick wall has been carried out, considering the actual configuration in terms of bricks and mortar joints. The model has been also tested under the application of a vertical pre-stressing load and an horizontal load imposed on the top. The experimental results obtained in this work, as well as the implementation of numerical models can become valuable reference for future experimental works or researches.

REFERENCES

- [1] ElGawady, E., Lestuzzi, P., Badoux, M. (2004). *A review of conventional seismic retrofitting techniques for URM*. 13th International Brick and Block Masonry Conference, Amsterdam, July 4-7, 2004.
- [2] Lourenço, P.B. (2004). *Current experimental and numerical issue in masonry research*. Congresso de sismologia e engenharia sísmica, Guimarães, 2004 – “Sísmica 2004 - “6º Congresso de Sismologia e Engenharia Sísmica”. Guimarães: Universidade do Minho, 2004, p. 119-136.
- [3] Seible, F., Kingsley, G.R. (1991). *Modeling of concrete and masonry structures subjected to seismic loading*. In: Donea J. & Jones P.M. (eds.). *Experimental and Numerical Methods in Earthquake Engineering*. Brussels: ECSC. 1991: 281–318.
- [4] Brencich, A., Gambarotta, L., Lagomarsino, S. (1998). *A macroelement approach to three-dimensional seismic analysis of masonry buildings*. 11th European Conference on Earthquake Engineering, 1998 Balkema, Rotterdam.
- [5] Cattari, S., Galasco, A., Lagomarsino, S., Penna, A. (2005). *Analisi non lineare di edifici in muratura con il programma Tremuri*. XIII Convegno ANIDIS – L’Ingegneria Sismica in Italia, Genova, 2005.
- [6] Hill, R. (1948). *A theory of the yielding and plastic flow of anisotropic metals*. Proc. Roy. Soc., (London) A, 193, p. 281-288.
- [7] Hoffman, O. (1967). *The brittle strength of orthotropic materials*. J. Composite Mat., 1, p. 200-206.
- [8] Tsai, S.W., Wu, E.M. (1971). *A general theory of strength of anisotropic materials*. J. Composite Mat., 5, p. 58-80.
- [9] De Borst, R., Feenstra, P.H. (1990). *Studies in anisotropic plasticity with reference to the Hill criterion*. Int. J. Numer. Methods Engrg., 29, p. 315-336.
- [10] Schellekens, J.C.J., De Borst, R. (1990). *The use of the Hoffman yield criterion in finite element analysis of anisotropic composites*. Comp. Struct., 37(6), p. 1087-1096.
- [11] Lourenço, P.B. (2000). *Anisotropic softening model for masonry plates and shells*. J. Struct. Engrg., 126(9), p. 1008–1016.
- [12] Sacco, E. (2009). *A nonlinear homogenization procedure for periodic masonry*. European Journal of Mechanics – A/Solid, Volume 28, Issue 2, March-April 2009, p. 209-222.

- [13] Avossa, A.M., Famigliuolo, P., Malangone P. (2009). *Prestazioni sismiche di edifici in muratura: impiego di un modello "concrete" modificato e analisi di confronto*. XIII Convegno ANIDIS – L'Ingegneria Sismica in Italia, Bologna, 2009.
- [14] Anthoine, A. (1997). *Homogenisation of periodic masonry: Plane stress, generalised plane strain or 3D modelling?* Comm. Num. Meth. Engrg., 13, p. 319–326.
- [15] Lourenço, P.B., Zucchini, A., Milani, G., Tralli, A. (2006). *Homogenization approaches for structural analysis of masonry buildings*. Structural Analysis of Historical Constructions, New Delhi 2006. P.B. Lourenço, P. Roca, C. Modena, S. Agrawal (Eds.).
- [16] Lourenço, P.B., Rots, J.G. (1997). *A multi-surface interface model for the analysis of masonry structures*. J. Engrg. Mech., 123(7), p. 660-668.
- [17] Lofti H.R., Shing, P.B. (1994). *Interface model applied to fracture of masonry structures*. J. Struct. Engrg., 120(1), p. 63-80.
- [18] Lemos, J.V. (1998). *Discrete element modeling of the seismic behavior of stone masonry arches*. In: Pande G et al. (ed) Comp. meth. in struc. masonry 4, E&FN Spon, 1998, p. 220–227.
- [19] Baggio, C., Trovalusci, P. (1998). *Limit analysis for no-tension and frictional three-dimensional discrete systems*. Mech. of Struct. and Machines, 26(3), p.287-304.
- [20] Orduña, A. (2003). *Seismic assessment of ancient masonry structures by rigid blocks limit analysis*. Ph.D. Thesis, University of Minho, Guimarães.
- [21] Lourenço, P.B. (1994). *Analysis of masonry structures with interface elements: Theory and applications*. Report 03-21-22-0-01, Delft University of Technology, Delft.
- [22] Triantafillou, T.C. (1998). *Composites: a new possibility for the shear strengthening of concrete, masonry and wood*. Composites Science and Technology 1998;58:1285–1295. Elsevier.
- [23] Croci, G., Ayala, D., Asdia, P. and Palombini, F. (1987). *Analysis on shear walls reinforced with fibres*. IABSE Symp. on Safety and Quality Assurance of Civil Engineering Structures, Tokyo, 1987.
- [24] Triantafillou, T.C. and Fardis, M.N. (1997). *Strengthening of historic masonry structures with composite materials*. Materials and Structures, 1997, 30, 486–496.
- [25] Triantafillou, T.C. and Fardis, M.N. (1993). *Advanced composites for strengthening historic structures*. IABSE Symp. on Structural Preservation of the Architectural Heritage, Rome, 1993, 541–548.
- [26] Schwegler, G. (1994). *Masonry construction strengthened with fiber composites in seismically endangered zones*. Proc. 10th Europ. Conf. on Earthquake Eng., Vienna, Austria, 1994.
- [27] Saadatmanesh, H. (1994). *Fiber composites for new and existing structures*. ACI Structural Journal, 1994, 91(3), 346–354.

- [28] Ehsani, M.R. (1995). *Strengthening of earthquake-damaged masonry structures with composite materials*. In Non-metallic (FRP) Reinforcement for Concrete Structures. Ed. L. Taerwe, 1995, 680–687.
- [29] Roca, P., Araiza, G. (2010). *Shear response of brick masonry small assemblage strengthened with bonded FRP laminates for in-plane reinforcement*. Construction and Building Materials 2010;24:1372–1384. Elsevier.
- [30] Valluzzi, M.R., Tinazzi, D., Modena, C. (2002). *Shear behavior of masonry panels strengthened with FRP laminates*. Construction and Building Materials 2002;16:409–416.
- [31] ElGawady, M.A., Lestuzzi, P., Badoux, M. (2005). *In-plane response of URM walls upgraded with FRP*. Journal of Composites for Construction 2005;9(6):524–535. ASCE.
- [32] Avramidou, N., Drdácáký, M.F., Procházka, P.P. (1999). *Strengthening against damage of brick walls by yarn composites*. Proc. “Inspection, Appraisal, Repairs & Maintenance of Buildings & Structures”, Melbourne, December 1999.
- [33] ElGawady, M.A., Lestuzzi, P., Badoux, M. (2007). *Static cyclic response of masonry walls retrofitted with fiber-reinforced polymers*. Journal of Composites for Construction 2007;11(1):50–61. ASCE.
- [34] Santa Maria, H., Alcaino, P., Luders, C. (2006). *Experimental response of masonry walls externally reinforced with carbon fiber fabrics*. In: Proceedings of the 8th US National Conference on Earthquake Engineering; 2006. Paper no. 1402.
- [35] Fam, A., Musiker, D., Kowalsky, M., Rizkalla, S. (2008). *In-plane testing of damaged masonry wall repaired with FRP*. Adv Compos Lett 2008;11(6):275–81.
- [36] Al-Salloum, Y.A., Almusallam, T.H. (2005). *Walls strengthened with epoxy-bonded GFRP sheets*. Journal of Composite Materials 2005;(39):1719–1745. SAGE.
- [37] Wang, Q., Chai, Z., Huang, Y., Zhang, Y. (2006). *Seismic shear capacity of brick masonry wall reinforced by GFRP*. Asian Journal of Civil Engineering (Building and Housing) 2006;7(6):563–580.
- [38] Stratford, T., Pascale, G., Manfroni, O., Bonfiglioli, B. (2004). *Shear strengthening masonry panels with sheet glass–fiber reinforced polymer*. Journal of Composites for Construction 2004;8(5):434–443. ASCE.
- [39] Marcari, G., Manfredi, G., Prota, A., Pecce, M. (2007). *In-plane shear performance of masonry panels strengthened with FRP*. Composites: Part B 2007;38:887–901. Elsevier.
- [40] Triantafillou, T.C. (1998). *Strengthening of masonry structures using epoxy-bonded FRP laminates*. Journal of Composites for Construction 1998;2(2):96–104. ASCE.
- [41] Luccioni, B., Rougier, V.C. (2010). *In-plane retrofitting of masonry panels with fibre reinforced composite materials*. Construction and Building Materials. Article in Press. Elsevier.
- [42] Chuang, S., Zhuge, Y., Wong, T., Peters, L. (2003). *Seismic retrofitting of unreinforced masonry walls by FRP strips*. In: Pacific conference on earthquake engineering; 2003.

- [43] Eshani, M.R., Saadatmanesh, H., Al-Saidy, A. (1997). *Shear behavior of URM retrofitted with FRP overlays*. Journal of Composites for Construction 1997;1(1):17–25. ASCE.
- [44] Haroun, M.A., Mosallam, A.S., Allam, K.H. (2003). *In-plane shear behaviour of masonry walls strengthened by FRP laminates*. In: 2nd International Workshop on Structural Composites for Infrastructure Applications, Cairo, 2003.
- [45] Aiello, M.A., Sciolti, S.M. (2006). *Bond analysis of masonry structures strengthened with CFRP sheets*. Construction and Building Materials 2006;20:90–100. Elsevier.
- [46] Liu, Y., Dawe, J., McInerney, J. (2005). Behaviour of GFRP sheets bonded to masonry walls. In: Proceedings of the international symposium on bond behaviour of FRP in structures (BBFS 2005), International Institute for FRP in Construction (IIFC), 2005. p. 473–80.
- [47] Willis, C.R., Yang, Q., Seracino, R., Griffith, M.C. (2009). *Bond behaviour of FRP-to-clay brick masonry joints*. Engineering Structures 2009;31:2580–2587. Elsevier.
- [48] Grande, E., Imbimbo, M., Sacco, E. (2010). *Bond behaviour of CFRP laminates glued on clay bricks: Experimental and numerical study*. Composites: Part B. Article in Press. Elsevier.
- [49] Papanicolaou, C.G., Triantafillou, T.C., Karlos, K., Papathanasiou, M. (2007). *Textile reinforced mortar (TRM) versus FRP as strengthening material of URM walls: in-plane cyclic loading*. Materials and Structures 2007;40(10):1081–1097. RILEM.
- [50] Papanicolaou, C.G., Triantafillou, T.C., Karlos, K., Papathanasiou, M. (2008). Textile reinforced mortar (TRM) versus FRP as strengthening material of URM walls: out-of-plane cyclic loading. Materials and Structures 2008;41(1):143–157. RILEM.
- [51] Papanicolaou, C.G., Triantafillou, T.C., Lekka, M. (2011). *Externally bonded grids as strengthening and seismic retrofitting materials of masonry panels*. Construction and Building Materials 2011;25:504–514. Elsevier.
- [52] Faella, C., Martinelli, E., Nigro, E., Paciello S. (2010). *Shear capacity of masonry walls externally strengthened by a cement-based composite material: An experimental campaign*. Construction and Building Materials 2010;24:84–93. Elsevier.
- [53] Prota, A., Marcari, G., Fabbrocino, G., Manfredi, G., Aldea, C. (2006). *Experimental in-plane behavior of tuff masonry strengthened with cementitious matrix-grid composites*. Journal of Composites for Construction 2006;10(3):223–233. ASCE.
- [54] Drdácáký, M.F. and Lesák, J. (2009). *Retrofitting severely damaged masonry with high performance FRP strips and with anchored PP net reinforced rendering - a comparison*. In ISCARSAH Symposium Mostar - 09 Mostar: Interproject d.o.o. Mostar, 2010. S. 91-97. ISBN 978-9958-9999-0-1.
- [55] Aldea, C.M., Mobasher, B., Jain, N. (2006). *Cement-Based Matrix-Grid System For Masonry Rehabilitation*. Textile Reinforced Concrete (TRC) - German/International Experience symposium sponsored by the ACI Committee 549, ACI Special Publications, ACI Special Publications, 2006.

- [56] Lignola, G.P., Prota, A., Manfredi, G. (2009). *Nonlinear Analyses of Tuff Masonry Walls Strengthened with Cementitious Matrix-Grid Composites*. Journal of Composites for Construction 2009;13(4):243–251. ASCE.
- [57] Lignola, G.P., Prota, A., Manfredi, G. (2007). *Numerical simulation of in-plane behavior of tuff masonry strengthened with cementitious matrix-grid composites*. Proc., 1st Asia-Pacific Conf. on FRP in Structures APFIS 2007, S.T. Smith, ed., International Institute for FRP in Construction (Hong Kong), 255–262.
- [58] Gabor, A., Bennani, A., Jaqueline, E., Lebon F. (2006). *Modelling approaches of the in-plane shear behaviour of unreinforced and FRP strengthened masonry panels*. Composite Structures 2006;74:277–288. Elsevier.
- [59] DIANA Finite Elements Analysis. (2008). *User's manual – Release 9.3*. Delft (The Netherlands). TNO Building and Construction Research.
- [60] Rots, J.G. and Blaauwendraad, J. (1989). *Crack models for concrete: discrete or smeared? Fixed, multi-directional or rotating?* Heron, Vol. 34, No. 1, 1989.
- [61] Blaauwendraad J. (1985). *Realisations and restrictions - Application of numerical models to concrete structures*. Finite element analysis of reinforced concrete structures, Proc. US-Japan Seminar, (Meyer c., Okamura H. Eds.), ASCE, 557-578 (1985).
- [62] Rashid Y.R. (1968). *Analysis of prestressed concrete pressure vessels*. Nuclear Engng. and Design 7(4),334-344 (1968).
- [63] Cornelissen, H.A.W., Hordijk, D.A., Reinhardt, H.W. (1986). *Experimental determination of crack softening characteristics of normal weight and lightweight concrete*. Heron 31, 2, 1986.
- [64] Hordijk, D.A. (1991). *Local Approach to Fatigue of Concrete*. PhD thesis, Delft University of Technology, 1991.

